Physical properties and isotopic characteristics of the winter water column and landfast sea-ice surrounding the Belcher Islands, southeast Hudson Bay

By

Eastwood, Rosemary Ann

A Thesis submitted to the Faculty of Graduate Studies of

The University of Manitoba

In partial fulfillment of the requirements of the degree of

MASTER OF SCIENCE

Department of Environment and Geography

University of Manitoba

Winnipeg

Abstract

The freshwater budget of Hudson Bay is governed by complex interactions between terrestrial, marine, and atmospheric systems. Inuit in Sanikiluaq have observed rapid freezing of flaw leads and polynyas around the Belcher Islands (southeast Hudson Bay) and have been seeking answers about what is contributing to this change. This study provides the first winter oceanographic observations of spatial and temporal distribution of freshwater in this region, using tandem measurements of salinity and $\delta^{18}O$ from water and ice core samples to decipher freshwater sources (river water, sea-ice melt). River water and sea-ice melt contribute to the fresh surface mixed layer mainly present along the eastside of the islands, and is likely preventing downward mobility of dense briny waters that is locally made and advected in. In addition, the river water inventory increases as winter progresses, an unexpected result since the natural cadence of river runoff is low during the winter months.

Acknowledgements

A special thanks to the local hunters who were willing to share their knowledge of their hunting grounds, safely navigate the researchers over sea-ice and through polar bear territory, and assist with field sampling. Nakurmiik Johnny Kudluarok, Josie Amitook, Johnassie Inuktaluk, Puasi Ippak, Lucassie Ippak, Johnassie Ippak, Jack Iqaluk, Johnny Takatak, Noah Arragutainaq, Davidee, Tamo, and to the wives. Support from the community of Sanikiluaq, Arctic Eider Society, and from the President of the HTA office Lucassie Arragutainaq was greatly appreciated.

Thanks to Nunavut General Monitoring Program funding to the Arctic Eider Society (Dr. Joel Heath) and ArcticNet for funding Dr. David Barber and, it was possible to launch this study in winter 2014. ArcticNet funding to Dr. Zou Zou Kuzyk (2015-2018) allowed completion of the project. Important contributors such as NSERC and its CERC program, and INAC's Northern Scientific Training Program (NSTP) also made our research possible. The Centre for Earth Observation Science, Arctic Science Partnership (ASP), and The University of Manitoba provided facilities, equipment, and instruments. Christine Michel and Andrea Niemi at Department of Fisheries and Oceans provided access to a salinometer.

Thanks Emme Wiley, Marcos Lemes, Ryan Galley, the administrative staff and other colleagues of CEOS for their support and assistance. To my office mates for being there through the thick and thin. To Michelle Kamula for being such a great team member in the field and in the lab.

Thank you Rob MacDonald for sharing your knowledge of Arctic freshwater systems and for the many inspiring conversations about the world of science.

Thank you Dr. Zou Zou Kuzyk for your support throughout this journey as your graduate student. You provided an environment full of encouragement for exploring the unknown. Thank you for your help with building my skills as a young scientist and expanding my mind to all the endless possibilities that come with seeking knowledge about the world we live in.

Dedication

To my family and friends.

Table of Contents

Table of Figures

Table of Copyright Figures

List of Tables

Chapter 1. Introduction

1.1 Overview of Arctic Ocean and Hudson Bay oceanography

1.1.1 Freshwater in the Arctic Ocean

The Arctic Ocean Estuary, a semi-closed ocean coastal zone that is inundated with river runoff, contributes to the physical and biochemical makeup of the Arctic Ocean and its surrounding seas (e.g. Beaufort Sea and Hudson Bay)(McClelland et al. 2012). It has been calculated that 11% of the world's river runoff flows into the Arctic Ocean, which is disproportionately high compared to the 1% of global seawater present in this polar system (Shiklomanov et al. 2000). The continental shelf that surrounds the Arctic Ocean is a transient domain where freshwater, mainly as river runoff, first enters the Arctic estuarine system. Seasonal variation of river runoff in this transient domain is governed by regional climatology, exhibiting low river runoff in winter and high in the summer, along with seasonal changes to nutrient and organic matter input into the Arctic estuarine system (Holmes et al. 2011; McClelland et al. 2012). Arctic estuaries are unique due to the sea-ice cycle, an additional complex mechanism that adds freshwater in the form of sea-ice melt during the late spring-early summer and adds brine into the surface waters as sea-ice grows during the winter, thereby impacting the positive and negative buoyancy of surrounding surface waters (Carmack et al. 2015).

The freshwater budget in the Arctic Ocean, a process by which the source, sink, and export of freshwater within a marine system are accounted for, is primarily comprised of freshwater input from 1) river water runoff discharged into the North Pacific and the Arctic Ocean, 2) freshwater removal and addition associated with the sea-ice formation and melt cycle, and 3) the contribution from precipitation-evaporation (P-E) that occurs above the Arctic Ocean

itself (Serreze et al. 2006). These types of freshwater inputs (+/-) impact the physical and structural properties of the Arctic Ocean, contributing to the chemical composition of the surface waters and stratification of the water column (Carmack 2000). With the warming climate of the Arctic and lower latitudes, more liquid freshwater will inundate Arctic estuarine systems in the future, less sea-ice will remain, and greater amounts of precipitation will lead to an overall larger freshwater budget (Carmack et al. 2016).

1.1.2 Freshwater in Hudson Bay

Hudson Bay is a marginal sea of the Arctic Ocean that also resembles an Arctic estuarine system by being seasonally inundated by river runoff, and undergoing a complete annual sea-ice cycle that contributes to changes in the surface water's buoyancy (Ingram and Prinsenberg 1998). The freshwater budget of Hudson Bay is presumed to be a balanced system that is mainly governed by river water arriving from the watershed, local sources of precipitation, and the sea-ice cycle (St-Laurent et al. 2011). The source seawater that flows into Hudson Bay from Foxe Basin also contains freshwater particularly as sea ice melt (Tan and Strain 1996). This overall balance is achieved by freshwater being exported from Hudson Bay to the North Atlantic through Hudson Strait.

Hudson Bay receives large volumes of river runoff (~700km^3yr^{-1}, Straneo and Saucier 2008) from its watershed that covers a significant portion of Canada and extends into the United States (Prinsenberg 1980). Within the last few decades, the regulation of river discharge for the purpose of producing hydro-electricity among other reasons has altered the natural cycle of many Hudson Bay rivers. Storage of water in reservoirs through spring and summer from release in winter has led to an increase in discharge to Hudson Bay over the period 1964-2008 (Dery et al. 2011). In addition to hydroelectric development, the recent trend in climate over Hudson Bay has

pushed sea-ice freeze-up later in the winter season while break-up is occurring earlier in the spring season reducing the overall duration of the sea-ice season in Hudson Bay (Hochheim et al. 2011; Hochheim and Barber 2014).

In the last few decades the local sea-ice surrounding the Belcher Islands in southeast Hudson Bay has become more inconsistent with regards to the traditional knowledge of this frozen environment possessed by Inuit hunters in Sanikiluaq (CARC 1997). The community of Sanikiluaq has been seeking answers about what factors are contributing to the changes they observe in their environment (c.f. Heath 2011). Very little is known scientifically about the oceanographic dynamics in this specific region, especially during the winter. Questions have arisen about whether increased amounts of river runoff in the winter season from controlled river systems may be contributing to rapid freezing of local flaw leads and polynyas (i.e. sea-ice openings). However, as stated above, there are many other environmental changes currently underway. In order to understand what external pressures are causing change in the local sea-ice surrounding the Belcher Islands, whether it may be anthropogenic changes to river systems, climate change, or a combination of both factors, an understanding of what the physical oceanographic conditions are like prior to and during the winter season surrounding the Belcher Islands is essential.

1.2 Thesis Overview

Chapter 1 sets the tone and structure of my thesis. A comprehensive literature review that expands upon the topics briefly discussed in this first chapter will be provided in Chapter 2 beginning with background on freshwater dynamics and sea-ice cover of the Arctic Ocean and its marginal seas, specifically Hudson Bay, and then leading into the motives and objectives for my research in the waters surrounding the Belcher Islands in southeast Hudson Bay. Discussing

Arctic Ocean dynamics first establishes the importance of studying freshwater in polar regions, provides context to the oceanographic dynamics observed in Hudson Bay, and is a reminder that even though my research only covers a small portion of this particular marginal sea, this study area is a part of and in some ways representative of an extensive system. Chapter 3 elaborates on the methodology required to study the winter dynamics and freshwater balance in my study area. Based on previous works in the Beaufort Sea and other locations. Field sampling and analytical methods of my research conclude the chapter. Chapter 4 and Chapter 5 state the results of my research and then discuss in details those results, placing a focus on the inventories of freshwater present in the water column during the winter campaigns of 2014-2015. Chapter 6 describes the conclusions, future applications, and potential implications of my findings.

Chapter 2. Literature Review

2.1 Freshwater dynamics in the Arctic Ocean

2.1.1 Arctic estuarine systems and their freshwater sources

Although almost the entire Arctic Ocean is influenced by estuarine gradients (McClelland et al. 2012), the 'Riverine Coastal Domain' is considered a transient region where freshwater-induced spatial gradients, among other complex mechanisms (e.g. seasonal cycle of sea-ice), ultimately govern the salinity flux (buoyancy) within the domain and offshore. This transient domain is present along Arctic marine coastal shelves where freshwater, mainly in the form of river water runoff, exits off the land and penetrates the saline waters of the marine environment (Carmack et al. 2015). The Arctic coastal shelf, where this event occurs, represents 25% of the world's continental shelf area (Lammers et al. 2001). As freshwater leaves the Arctic continental shelf area and enters one of the many basins that make up the Arctic Ocean (Figure 2.1), low density river water runoff is temporarily stored in the surface waters before the freshened coastal water masses are advected southwards towards the North Atlantic Ocean by surface currents (e.g. Beaufort Gyre, Canadian Archipelago) (Carmack 2000).

The salinity gradient which defines the 'Riverine Coastal Domain' in the Arctic Ocean is maintained mainly by the Ob, Yenisey, Lena and Mackenzie river systems (Aargaard and Carmack 1989) and low salinity Pacific waters that are freshened by Alaskan and Siberian runoff as they pass through the Bering Strait (see Ekwurzel et al. 2001). Due to the size of the Arctic basin, which covers 19 million km^2 (Shiklomanov et al. 2000) (Figure 2.1), the seasonal freshwater cycle is driven by the accumulation of snow on land and the vast expanse of river systems that discharge into the Arctic Ocean. Since precipitation exceeds evaporation in the northern latitudes, net-precipitation contributes to both the freshening of the Arctic Ocean surface waters and freshwater budget. Net precipitation has its own seasonal cycle contributing

to the freshening of the Arctic Ocean surface waters by 1) contributing precipitation directly over the ocean surface in the late summer early fall of the open water season, and 2) contributing to the spring freshest (Figure 2.2) by depositing snow on land during the winter season. Snow melt significantly increases input of river runoff into the surface waters of the Arctic Ocean in the spring season (Serreze et al. 2006). Snow-melt making up of 60% of river runoff inundating the Arctic shelves between April and July (Lammers et al. 2001; Serreze et al. 2006).

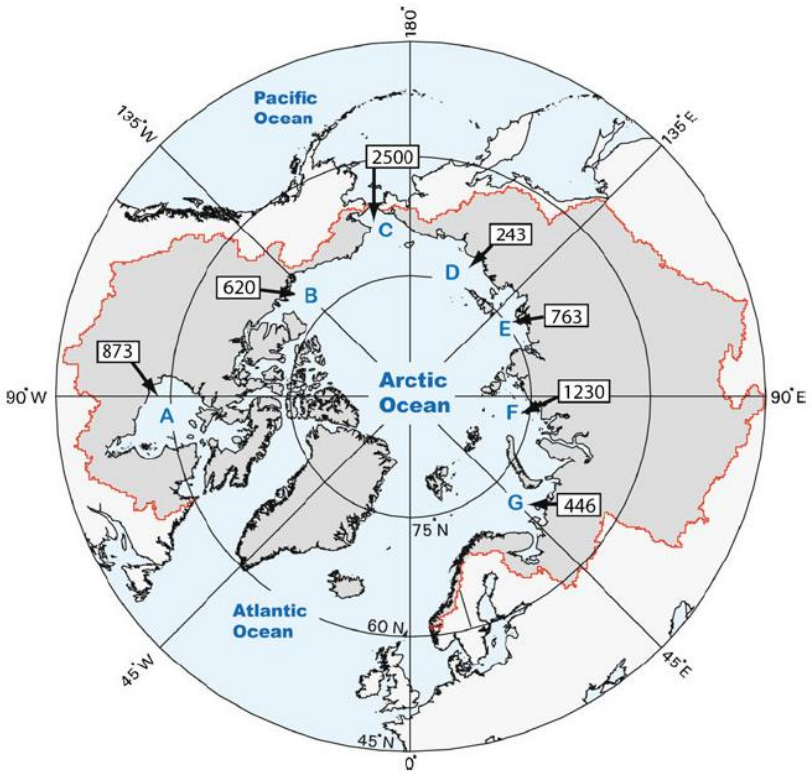

Figure 2.1. The pan-Arctic drainage basin and major freshwater inflows (km^3/year) to the Arctic Ocean and surrounding seas. Red line watershed boundary, A) Hudson Bay, B) Beaufort Sea, C) Chukchi Sea, D) East Siberian Sea, E) Laptev Sea, F) Kara Sea, G) Barents Sea. Inputs from land were calculated from the regional runoff estimates of Lammers et al. (2001). The 2,500 km^3/year input to the Chukchi Sea is the freshwater content of Bering Sea water flowing into the Arctic Ocean via Bering Strait based on a reference salinity of 34.8 (Serreze et al. 2006). Figure from McClelland et al. (2012) is adapted from McClelland et al. (2011), © Springlink, Estuaries and Coasts

Several studies have focused on the estimated annual river input and freshwater distribution into the Arctic Ocean through discontinuous and continuous monitoring of ~3500 hydrometric stations, even though one third of the river water input to the Arctic Ocean is still not monitored (Shiklomanov et al. 2000; Ekwurzel et al. 2001; Lammers et al. 2001; Serreze et al. 2006). Low salinity Pacific waters provide 2500 km^3/year of river runoff annually to the Arctic Ocean, which is by far the largest contribution of river runoff at one location (Figure 2.1). The Kara Sea (Ob and Yenisey Rivers) provides only 50% of river runoff compared to the amounts that the Pacific waters bring in. The Laptev Sea (Lena River) provides more river runoff than the Yenisey River discharges (Figure 2.2). The Mackenzie River in the Beaufort Sea releases a considerable amount of river runoff annually and has a similar annual mean hydrograph to the Ob River in the Kara Sea (Figure 2.2).

Within the annual freshwater budget of the Arctic Ocean there is a lot of complexity associated with the seasonality of various freshwater sources and sinks. Climate change and anthropogenic changes (hydroelectric development) have reduced the seasonality of annual discharge, increasing the presence of river discharge in the winter months, which complicates the freshwater budget of the Arctic and Pan Arctic system (see White et al. 2007). The seasonal hydrograph of each Arctic shelf and the volume of river runoff varies, due to the variations in precipitation relative to each basin and watershed (Serreze et al. 2006), however in general the natural peak of river runoff appears between May and July, promoting sea-ice break up, and is a cue to the transition into the warmer season (Figure 2.2).

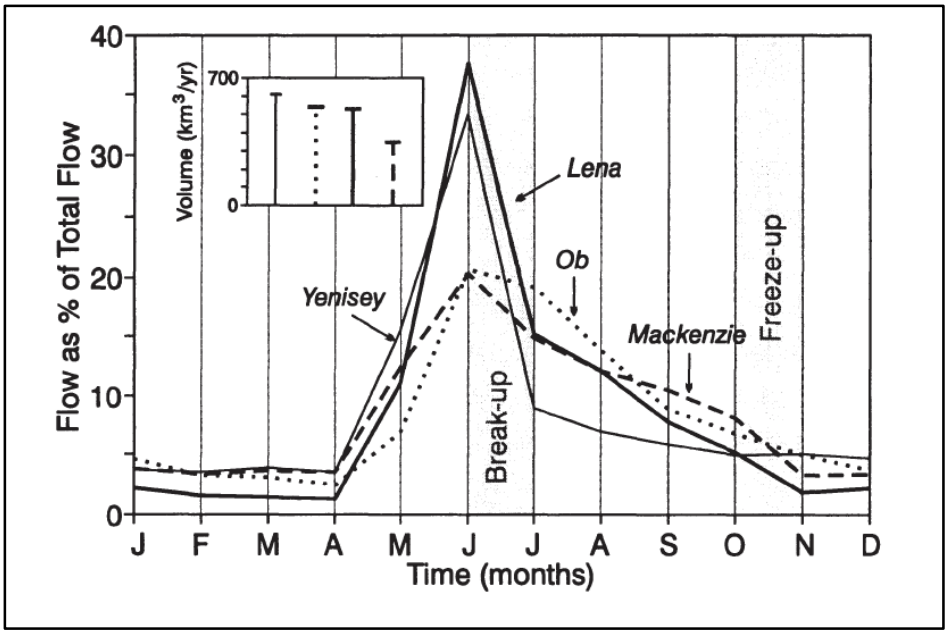

Figure 2.2. Average monthly flow of the four largest rivers in the Arctic (modified from Lawford 1994). Inset shows a histogram of the total volumetric flow for each of the rivers and the approximate dates of freeze-up and ice melt are given as vertical bands. Figure from Macdonald (2000), ©Springer Netherlands, The Freshwater Budget of the Arctic Ocean

During the summer season, an Arctic estuary functions in accordance with the widely used term "positive estuary", whereas during the winter, as the sea-ice grows, an Arctic estuary is strongly influenced by brine rejection into surface waters associated with sea-ice growth. This "negative estuary" process is an additional complex mechanism that alters the buoyancy of the surface waters in Arctic estuarine systems (Macdonald 2000). Indeed, Arctic estuarine systems are unique in that sea-ice cover is a dominant feature that plays a dual role in the freshwater budget, controlling spatial and temporal distribution of freshwater; specifically, freshwater is stored as sea-ice grows and freshwater is released as sea-ice melts (Macdonald 2000). The sea-ice cycle in Arctic estuaries promotes positive buoyancy in surface waters as sea-ice melt is added into the system, and promotes negative buoyancy as surface waters freeze and brine (dense saline water) is ejected as a part of the sea-ice growth process (Macdonald and Carmack

1991; Macdonald et al. 1995). Seasonal changes affect when positive and negative estuaries are present in the Arctic region. During the winter in particular, negative estuaries form in regions of open water, known as polynyas and flaw leads, where sea-ice is continuously or frequently forming, and consequently briny waters are continually or frequently rejected into the surface water as the sea-ice grows (Macdonald 2000). Examples of these recurrent sea-ice openings in the Arctic are the North Water polynya found in northern Baffin Bay, and the Cape Bathurst polynya in the Beaufort Sea which is connected to the Circumpolar Flaw Lead (Barber and Massom 2007).

Determining the freshwater budget of the Arctic Ocean is complex due to the seasonality of freshwater sources, and sinks that store and release freshwater throughout this polar system. As stated in Chapter 1, the freshwater budget in the Arctic Ocean consists primarily of 1) river water runoff discharged into the North Pacific and the Arctic Ocean , 2) freshwater addition and removal associated with sea-ice formation and melt cycle, and 3) the contribution of precipitation-evaporation (P-E) that occurs above the Arctic Ocean itself (Serreze et al. 2006). (Figure 2.1). This type of data collection is imperative to understanding the dynamics of the Arctic Ocean water column. Developing a freshwater budget provides insight as to where and how freshwater and sea-ice may be present, additionally to understanding changes due to environmental and anthropogenic impacts (Lammers et al. 2001).

2.1.2 Circulation, stratification and maintenance of the halocline

The maintenance of the halocline is critical to the Arctic Ocean as we know it. The cold well-mixed freshened surface layer insulates sea-ice from the warm dense saline Atlantic waters that circulate below the halocline (Ekwurzel et al. 2001). In addition, the surface layer of the Arctic Ocean is an important sink and temporary storage for incoming freshwater that circulates

through the Arctic Ocean (Aargaard and Carmack 1989). Incoming Arctic coastal, Pacific and Atlantic waters establish the salinity driven vertical gradient [layering] of the Arctic Ocean (Aagaard and Carmack 1994) aided in part by not having to overcome a temperature driven density gradient, a result of the small temperature margin of the Arctic Ocean and its surrounding marginal seas (Figure 2.3) (Aagaard et al. 1981). Horizontal and vertical boundaries naturally occur between water masses that arrive from different sources due to the unique physical and chemical composition each water mass possesses, meaning a difference in salinity and temperature resulting in a density gradient (Carmack 2000). The Arctic Ocean's well-developed halocline, which is the point in the water column where the salinity rapidly changes between the depths of 40 m to 250 m below the surface (Canadian basin waters less saline), is sustained by river runoff, sea-ice melt, and low salinity Pacific waters that accumulate on top of dense saline Atlantic waters (Figure 2.3a). Figure 2.3 (a) depicts the basic vertical profile of the water column relative to temperature and salinity (Aagaard et al. 1981). Even though the temperature profile remains close to freezing throughout the halocline, this portion of the water column is where the salinity increases, transitioning from low salinity surface water to deep saline waters. This process is in part due to the brine being released by sea-ice production over the shelves, specifically in flaw leads where high rates of ice growth occur (Figure 2.3b). The near-freezing dense briny waters sink below the low salinity surface layer and are advected away from their site of formation. This dense cold water mass then penetrates the interior Arctic Ocean water column at depth dictated by the density, thereby helping maintain the halocline of the water column. Warm saline Atlantic waters (Figure 2.3a) are isolated from the fresh cold surface waters and the overlying ice by the halocline, preventing the deep warm waters from melting the sea-ice on the surface. Within this broad conceptual model around the maintenance of the

halocline (i.e., Figure 2.3), there are many detailed processes that have been described in particular regions. For example, Dmitrenko et al. (2010) showed that supercooled briny waters formed by polynyas on the Laptev Sea, can be transported over the shelf by tidal processes and wind-forcing. Frazil ice grown in the polynyas was also found below the surface layer, implying that the brine produced in the polynyas sinks below the less saline surface waters.

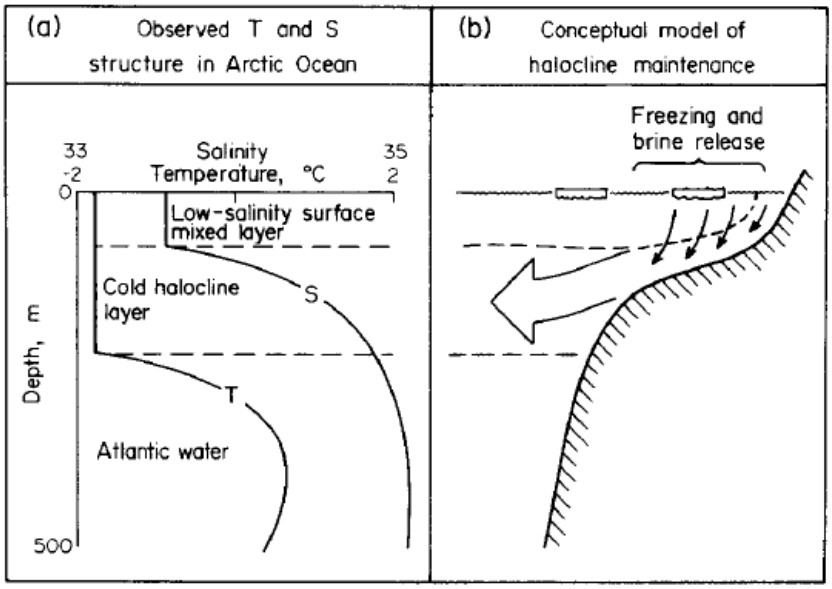

Figure 2.3. Schematic representation of the temperature and salinity structure in the upper Arctic Ocean and its maintenance. Figure from Aagaard et al. (1981), © Pergamon Press Ltd., Deep-Sea Research

In summary, the transition between the summer surface layer that is freshened by river runoff and sea-ice melt, and the winter surface layer salinized by the rejection of brine as sea-ice grows and the reduced presence of river off, contribute to the structure of the water column and the maintenance of the halocline throughout the Arctic Ocean (Carmack 2000). A particularly important process is the production of cold dense saline waters (brine) over the shelves, which is facilitated by the reduced presence of river runoff in winter (see chapter 3). The freshwater

budget is thus heavily influenced by the changes in salinity and temperature that occur on the surrounding shelves (Figure 2.3; Aagaard et al. 1981).

2.1.3 Seasonal cycle of sea-ice cover and sea-ice formation

The surface waters of the Arctic Ocean's coastal shelves and marginal seas undergo an annual seasonal transition from open water to extensive sea-ice cover. This process is an important component of the freshwater budget, contributing to the addition of sea-ice melt to the surface waters during the spring and summer, and brine as sea-ice grows during the winter (Figure 2.4). As the seasons transition from late fall to early winter, atmospheric temperatures cool the low salinity surface waters to their respective freezing points (i.e., seawater of a salinity 34 practical salinity units [psu] freezes at -1.86°C), promoting the growth of sea-ice. Temperature and salinity of the surface waters govern physical and chemical properties as sea-ice grows (Eicken 2008). As the winter progresses, sea-ice continues to grow from the ice-ocean interface, releasing latent heat (energy released during the phase change), and, through the ejection of excess salt, forming dense cold briny waters directly below the sea-ice (Leppäranta 1993). The schematic of thermodynamic sea-ice growth is shown in Figure 2.4. Exchange of heat occurs at the air-snow interface and the ice-ocean interface. As snow accumulates on top of the sea-ice, it acts as an insulator from the cold atmospheric temperatures and increases the reflection of incoming solar radiation (albedo effect), allowing for oceanic heat flux to impact the sea-ice temperature. With regards to the heat and salt flux occuring at the ice-ocean interface (Figure 2.4), the growth rate slows over time as the sea-ice thickens. The accumulation of snow also contributes to slower rates of sea-ice growth as the winter season progresses (Eicken 2008). Since some brine is captured in brine channels inside the ice during the sea-ice growth process,

liquid briny water also contributes to the heat transfer, and salinity gradient (see section 3.1.2.), in sea-ice (Lepäranta 1993).

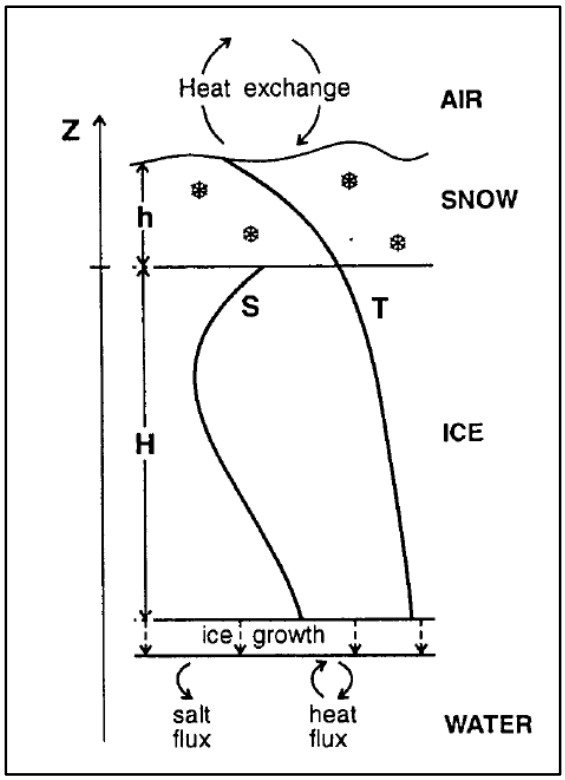

Figure 2.4. Schematic illustration of thermodynamic sea-ice growth. Figure from Leppäranta (1993) © Canadian Meteorological and Oceanographic Society, Atmosphere-Ocean

Throughout the polar regions, when the air temperature is below freezing, areas of open water that are partially or completely ice free, recur in the same geographic locations within the sea-ice cover. These sea-ice openings, which are known as recurrent polynyas and flaw leads, are important 'ice factories' that promote negative estuaries through the ejection of brine as sea-ice continuously forms. These regions of open water are also significant from a physical and biological standpoint (World Meteorological Organization (WMO), 1970 ; Smith et al. 1990; Stirling 1997; Maqueda and Biggs 2004). Polynyas are widespread in the Arctic and Canadian Archipelago during the winter months, and are important features of the local and regional "icescape" (Term developed by Barber and Massom 2007). The formation of recurrent polynyas

is reliant on several factors that include coastal and seafloor topography, direction and speed of wind, oceanic currents, and the transfer of heat and salt through air-ice-water interactions (Maqueda and Biggs 2004). Two categories of polynyas, latent heat and sensible heat, emerge from a combination of these factors. Latent heat polynyas remain open by wind and oceanic currents, and by the latent heat that is released from the fusion of continuous sea-ice growth (Smith et al. 1990). Sensible heat polynyas melt existing sea-ice cover and prevent the growth of sea-ice through the release of oceanic heat at the surface by processes of upwelling and vertical mixing (Smith et al. 1990; Barber and Massom 2007). Polynyas transform the properties of a water mass through processes of releasing heat at the surface, input of brine (salt), and input of freshwater as sea-ice melts in the spring and summer season (Maqueda et al. 2004).

2.2 Freshwater dynamics in Hudson Bay

2.2.1 Introduction to the Hudson Bay Complex

The Hudson Bay Complex (i.e. Hudson and James Bay) exists in both the Canadian Subarctic and Arctic that connects the Arctic Ocean to the North Atlantic Ocean (Figure 2.5). As Arctic surface waters pass through the Canadian Archipelago and Hudson Bay, the buoyancy fluxes are modified through sea-ice growth and melt processes and the addition of river runoff in this region (Ingram and Prinsenberg, 1998). The Hudson Bay Complex covers $1.3x10^6$ km^2, making it one of the largest inland seas in the world (Dionne 1980; Martini 1986). The average depth of Hudson Bay is less than 150 m (Ingram and Prinsenberg 1998) and it is roughly 925 km by 700 km wide (Prinsenberg 1987). James Bay is shallow with an average depth of 28 m, and has a surface area of roughly 150 km by 400 km (Prinsenberg 1980). The combined volume of freshwater added to Hudson Bay Complex is ~700 km^3yr^{-1} which exits Hudson Bay via Hudson Strait reaching the North Atlantic Ocean (Straneo and Saucier 2008).

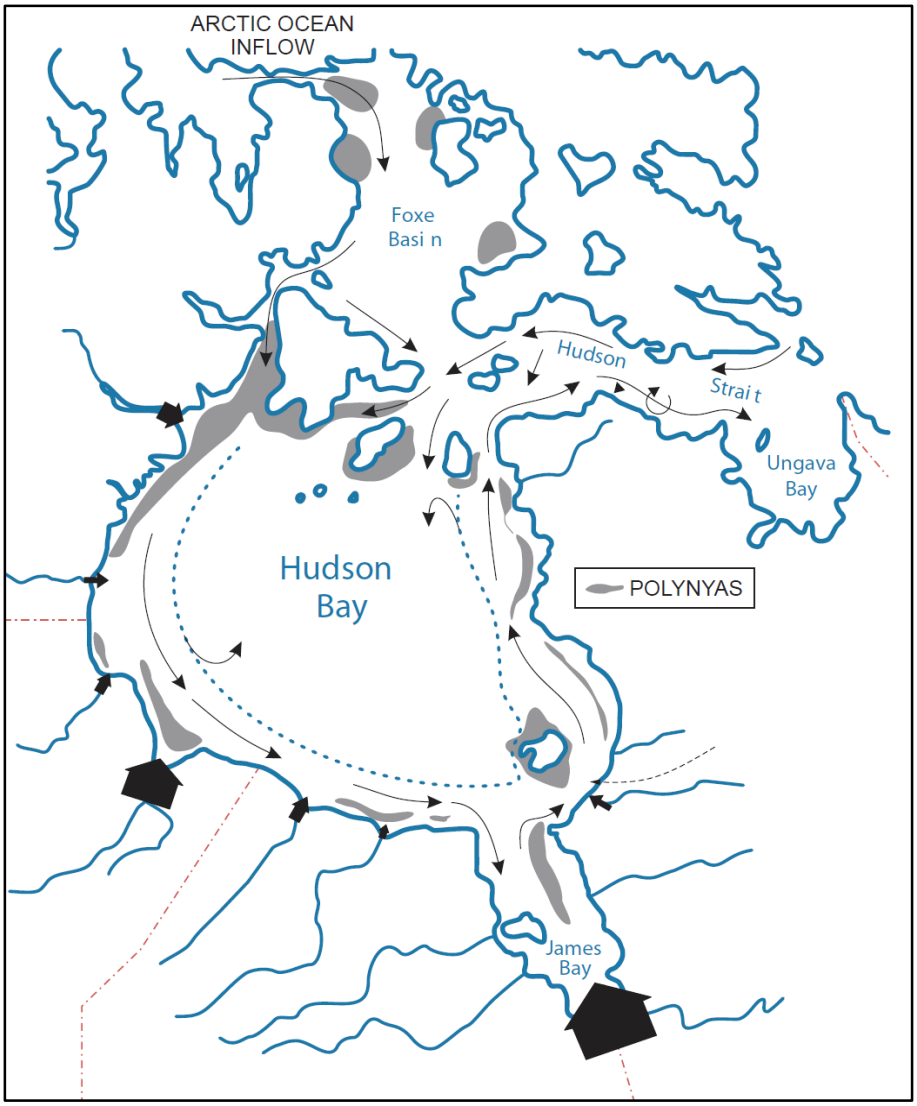

Figure 2.5. Hudson Bay System: circulation schematic and polynyas. Figure adapted from The Hudson Bay System: Macdonald and Kuzyk (2011) © Elsevier Ltd., Journal of Marine Systems

2.2.2 Circulation and Tides

The circulation of Hudson Bay Complex waters is cyclonic, creating a flow pattern from the northwestern opening of Hudson Bay, southward along the west coast towards James Bay, northward along the east coast of Hudson Bay, then exiting at the opening along the eastern shores of northern Quebec (Prinsenberg 1986; Wang et al. 1994; Ingram and Prinsenberg 1998). Several models have depicted in detail the surface circulation of the Hudson Bay Complex showing the pathway of the coastal and interior waters, providing detail to seasonal variations

that occur, and ultimately showing how fresh coastal waters are distributed through Hudson Bay Complex (e.g. Wang et al. 1994; Saucier et al. 2004; St-Laurent et al. 2011) . Bathymetry, wind patterns, and incoming freshwater (buoyancy flux) all influence the counterclockwise currents especially during open water conditions (e.g. Prisenberg 1986; Wang et al. 1994; Saucier et al. 2004). Pressure differences and prevailing wind stresses together establish a strong geostrophic coastal current in eastern Hudson Bay, in which freshened waters circulate (Saucier et al. 2004). Because the coastal boundary current of Hudson Bay retains incoming river water by being deflected to the right (Coriolis force), river water tends to have a transit time through Hudson Bay ranging from 0.8 years to 3.0 years (St-Laurent et al. 2011); indeed, freshened waters from southern Hudson Bay reach Hudson Strait in late fall and early winter (Saucier et al. 2004). The saline interior of Hudson Bay is mainly isolated from the fresh coastal boundary, with Ekman transport and eddies forcing a minor fraction of freshwater into the interior region (St-Laurent et al. 2011). This wind driven advection contributes to the recirculation of a minor portion of the fresh surface waters in Hudson Bay (St-Laurent et al. 2011).

Hudson Bay has a semidiurnal tide that affects water mass movement, such as river plumes (e.g. La Grande Rivière), and horizontal and vertical mixing of the water column. The presence of sea-ice in the winter months reduces tidal amplitude considerably compared to the open water period during the summer and fall months. During the winter period, the tidal height and tidal currents (in the interior Hudson Bay system) are subdued by the dampening effect of sea-ice cover, allowing river plumes to extend much further from the river mouth than in open water conditions (Prinsenberg and Freeman 1986). Note, however, that in shallow estuary areas, tidal velocity may be amplified in winter due to reduction of the cross-section of the channel by formation of the landfast ice cover (Wang et al. 2012).

Hudson Bay Complex waters exhibit spatial variations in temperature and salinity due to the seasonal fluctuations that influence river discharge, sea-ice melt, and sea-ice growth (brine rejection) (Prisenberg 1983). The broad oceanographic dynamics of the Hudson Bay Complex during the open water season exhibit two regions, a slowly circulating, saline interior region, and a low salinity, rapidly circulating, coastal boundary (St-Laurent et al. 2011). Eastern James Bay and southeast Hudson Bay have the least saline surface waters year-round, mainly due to river water and sea-ice melt processes, while the northern and western region of Hudson Bay have more saline waters due to brine production and a less pronounced presence of river water. The sea surface temperature margin is small (~ 0^0C ± 2^0C) across all seasons, except during the spring and summer when warm river waters inundate the coastal boundary along the southwestern coast and especially James Bay (Saucier et al. 2004). By late summer-fall, average temperatures in surface waters in southern Hudson Bay are much warmer than those in north and western Hudson Bay (8.33°C vs. 2.47°C; Lapoussiere et al. 2013).

2.2.3 Hudson Bay Complex water column structure

In addition to contributing to large-scale estuarine circulation, the role of river runoff and sea ice melt results in an overall strong stratification of the water column throughout Hudson Bay during the summer period (Anderson and Roff 1980a; Legendre et al. 1996; Roff and Legendre 1986; Lapoussière et al. 2013). This stratification impedes the renewal of nutrients in the surface layer (euphotic zone), and results in a simulated low annual primary production of ~ 40 g C/ m^2 yr for Hudson Bay (Ferland et al. 2011).

The (vertical) structure of the water column in Hudson Bay undergoes a significant transformation between summer and winter. Granskog et al. (2011) provide a detailed review of both the summer and winter water column stratification in regards to river runoff, sea-ice

production (brine), and sea-ice melt. Figure 2.6, reproduced from Granskog et al. (2011), shows the distribution of river runoff and sea-ice melt (in meters) during the summer and winter months (data collected in 2005), and shows how these inputs influence the vertical structure of the water column. Main differences between the two seasons include 1) runoff plays a dominant role in the stratification of the water column during the summer season preventing deep convection, and 2) the production of brine and reduced presence of river runoff promotes deep vertical mixing of the upper layer of the water column, as well as in places such as leads during the winter season. The stratification of the summer water column is displayed in Figure 2.6 beginning with the homogenized summer surface mixed layer (HSSML), well mixed to ~ 20 m; this region of the vertical water column is where, in summer, the river water (RW) and sea-ice melt (SIM) mainly reside. The summer surface mixed layer (SSML) lies between 30-60 m; RW dominates in this layer in the coastal boundary, while SIM is found in this layer in the interior region of Hudson Bay. As fall approaches, the SSML deepens due to tides, stronger winds and loss of buoyancy. As sea-ice begins to grow the dense surface waters lead to vertical convection (Saucier et al., 2004), creating the winter surface mixed layer (WSML) which mixes down to 50-124 m below the surface (Figure 2.6.b and d). The identity of deep waters is still being debated; however it has been suggested by Granskog et al. (2011) that deep waters are maintained by small areas of intense ice formation that produce enough dense briny waters to sink below the WSML. In addition, cold briny waters produced in polynyas in Foxe Basin and overflowing into northern Hudson Bay may supply a fraction of the deep waters in Hudson Bay (Defossez et al. 2008; Defossez et al. 2010).

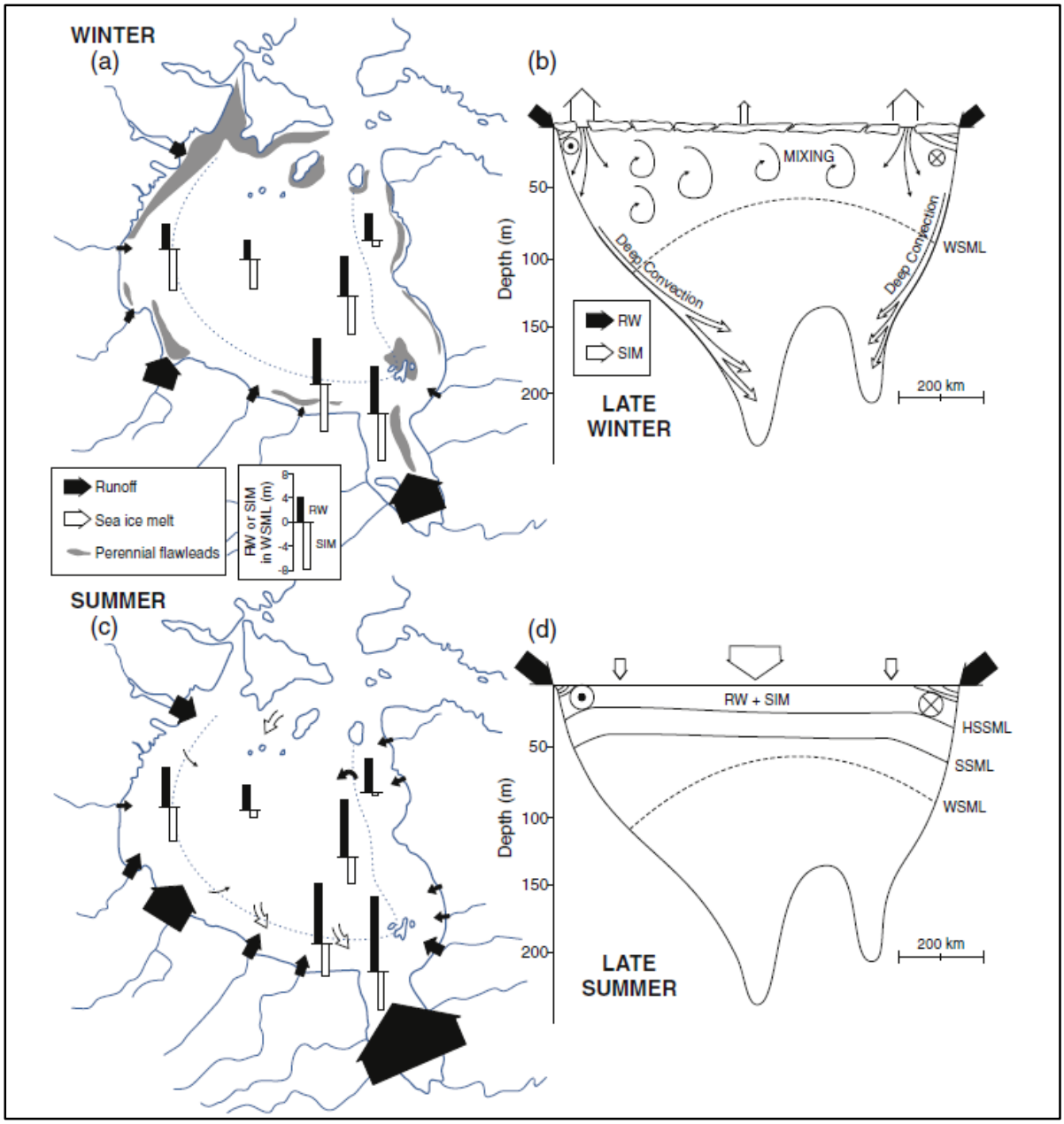

Figure 2.6. A conceptual diagram showing generally the contrast between freshwater input and storage in a, b winter and c, d summer. The bars denote the inventories (m) of RW and SIM down to the depth of the Winter Surface Mixed Layer at the end of (a) winter and (c) summer. The difference from winter to summer indicates seasonal inputs during summer. The dashed line in panels a and c indicates the approximate boundary between the interior domain and the coastal domain, which contains the coastal boundary current. Figure from Granskog et al. (2011). © Elsevier Ltd., Journal of Marine Systems

2.2.4 Freshwater Budget

The freshwater budget of Hudson Bay is governed by river water, local sources of precipitation (rain or snow), and the sea-ice cycle (presence and absence of sea-ice) (St-Laurent et al., 2011). An average of ~700 km^3/yr accounts for the annual river discharge of the basin with almost half (45%) of that amount coming through James Bay first (Prinsenberg 1994; Granskog et al. 2011). The Arctic Ocean supplies saline waters to Hudson Bay through Foxe Basin (Ingram and Prinsenberg 1998) and, to a lesser extent, Hudson Strait (Straneo and Saucier 2008). It has been estimated that sea-ice meltwater can contribute 0.82 m-1.15 m of freshwater to the Hudson Bay complex during the spring-summer melt (higher amount of meltwater in 2005, then in 2011; Landy et al. 2017). Annual precipitation (P) and evaporation (E), which contribute to the composition of the surface waters of Hudson and James Bay, have been difficult to estimate. However, compared to river water runoff and sea-ice melt, P-E contributes a small amount to the system's freshwater budget at ~220 km^3/yr (Straneo and Saucier 2008; St-Laurent et al. 2011).

2.2.5 Sea-ice Cover

From October to May, sea-ice cover is the dominant state of the surface of Hudson Bay (Maxwell 1986). Landfast ice covers the coastal zones and sheltered regions of Hudson and James Bay, while mobile ice covers the majority of Hudson Bay's interior (Prinsenberg 1987). In Hudson Bay, the northern portion and the northwestern coast are the first regions to freeze during the month of October, with freezing progressing southwards towards the Nelson Estuary and James Bay. The interior also freezes from north to south, leaving the southeastern region to freeze last during the month of December (Hochheim and Barber 2010). Areas of rapid sea-ice growth (i.e. flaw leads and polynyas) are prevalent in the northwestern entrance, along the coastal zones, eastern shore of James Bay, and around the Belcher Islands; as shown in gray areas of Figure 2.5 (Hochheim et al. 2011). The persistent latent heat northwestern polynya,

which opens due to westerly winds, has the highest sea-ice growth rates (2.4 cm/day in late December, 1-2 cm/day January-March) contributing to the ~ 2200 km^3 (maximum) of sea-ice produced during the winter months (modelled sea-ice growth for 1997 and 1998), which also contributes dense briny waters to the surface and/or subsurface waters of Hudson Bay (Saucier et al. 2004). This intense sea-ice production and advection of sea-ice into southern Hudson Bay contributes to the build-up of ridges and is more important than the local thermodynamic growth that forms this regions icescape during the winter season (Saucier et al. 2004). In the early spring (late April to early May) the intrusion of river runoff in James Bay triggers spring melt in the southern region (Saucier et al. 2004). By June the spring break-up is underway in James Bay and eastern Hudson Bay, as landfast sea-ice in the northwestern and northeastern region of Hudson Bay remains for another 3-4 weeks. The last remnants of sea-ice are present in southwest Hudson Bay in the month of July and by mid-August Hudson Bay is sea-ice free (Hochheim et al. 2011).

Since the 1980s, negative trends in sea-ice extent, defined as the length of time sea-ice is present in the system (presence/absence), have been documented for the Hudson Bay Complex. The trends have been linked to rising air temperatures, with every 1°C increase in temperature associated with a 0.7 week delay in freeze-up (Hochheim and Barber 2014). Between the years 1971 and 2003, sea-ice breakup in the southeastern Hudson Bay had moved earlier by a rate of 9.5 days/ decade (Gagnon and Gough, 2005). Spring sea-ice extent decreased -1.4% per year, with a 0.26 to 0.3°C increase in temperature (Hochheim et al. 2011).

2.2.6 River water runoff and hydro-regulation

River discharge contributes 0.9-1.0 m of freshwater to Hudson Bay water column annually (Dery et al. 2011; Granskog et al. 2011). However, as mentioned above, river discharge

impinges on southern Hudson Bay disproportionately with about 45% entering through James Bay. In general 15-20% of the water column in southeast Hudson Bay is river water (Granskog et al. 2011). Since the 1960s, no significant change to annual streamflow into the Hudson Bay system has been observed, however the distribution of discharge between seasons has shifted: an increased amount of river runoff is present during the winter season, whereas from spring to fall, stream flow has been reduced (Dery et al. 2011). This shift in river discharge is, in a large part, due to the construction of hydro-electric generating stations and reservoirs that, during the 1970s, altered river systems in northern Quebec (i.e. La Grande Rivère) and Manitoba (i.e. Nelson River). These systems altered the timing and output to address energy demands. Prior to development, the natural cycle of these river systems had two peak seasons and a low season, 1) the very pronounced peak of the spring freshet, as snow and ice melted, 2) the weaker fall peak, with increased precipitation prior to the onset of winter, and 3) the low discharge season, during the winter, when the entire region is in a frozen state (Prinsenberg 1980). Regulated river systems generally have an altered cycle. During the spring freshet and summer season, the water in the aforementioned regulated river systems is held in the reservoirs, lowering river discharge so it may be released at a controlled rate throughout the year maintaining a minimum constant production of energy. During the winter season in particular, when energy demands are high, the reserve of river water may be released, greatly increasing the amount of river discharge during the winter months, compared to the natural cycle (Dery et al. 2011).

The impacts of regulated river systems on local marine environments (estuaries) along the coast of Hudson and James Bay have been documented in a few instances (Prinsenberg 1983; Ingram and Larouche 1987; Kuzyk et al. 2008). However, the extent to which regulated river discharge influences the biochemical and physical composition of waters in the broader coastal

domains of Hudson Bay is still unclear. A growing concern is that modified timing of river discharge has an effect on the coastal marine environment of Hudson Bay, and potentially disrupts the formation of sea-ice (Dery et al. 2011). During the 1970s, before development, several studies tried to assess how hydro-electric development in the Hudson and James Bay watershed would alter the amount of river runoff along the coast, especially throughout the winter and early spring (Prinsenberg 1980). Prior to the completion of major hydro-developments, a baseline of the physical oceanography was established through the analysis of the freshwater content, salinity and temperature distributions, and physical processes of river plumes under sea-ice. Studies conducted before 1978 have been considered an appropriate depiction of Hudson and James Bays' "natural state" prior to modifications of river systems in the watershed (Messier et al. 1986).

La Grande Rivière, which discharges into northeast James Bay, was one of the major rivers that became heavily regulated through hydro-development. Several studies focused on the changes to the La Grande Rivière plume prior to and after development (e.g. El-Sabh and Koutitonsky 1977; Prinsenberg 1980; Freeman et al. 1982; Messier et al. 1986; Ingram and Larouche 1987). Ingram and Larouche (1987) observed that between the winters of 1980 and 1984, as winter discharge was increased from 1750 km^2 to 3000 km^2, the river plume expanded by about 20 km, making it detectable at distances of more than 70 km north of the river mouth. Messier et al. (1986) observed that the summer plume boundaries were decreased in size, reflecting reduced discharge; however, a more significant change was increase in the daily fluctuations in outflow. Regulation of the La Grande Rivière system can cause discharge to vary on an hourly basis (Dery et al. 2011). In part because of the reduced mixing under the ice and in part because of the increased winter discharge, river plumes moving under sea-ice in Hudson

Bay tend to be up to 40 times larger and 2-3 times deeper than plumes travelling in open water (Ingram and Larouche 1987; Ingram and Prinsenberg 1998).

The potential problem with an increased presence of river runoff in coastal Hudson Bay waters in winter is that it juxtaposes the opposing positive/negative estuarine processes in space and time. The presence of freshwater in flaw leads or polynyas in winter can significantly impact the buoyancy forcing of these 'ice factories'. Freshwater alters the rate of ice formation and its properties as well as the amount of brine rejected by growing ice. The process of deep water formation requires that the amount of brine rejected into surface waters be sufficient to overcome the buoyancy associated with any freshwater present in that layer (Granskog et al. 2011). Thus, the more freshwater in a polynya or flaw lead in winter, the more ice growth that is needed to sustain deep water formation or it may be shut down. Even at sites where salt input is not sufficient to make deep water, the presence of freshwater will tend to decrease the depth of winter mixing, thereby reducing the replenishment of nutrients from deep layers into surface layers and ultimately limiting biological production the following year. Because negative estuary processes are so sensitive to the sea ice and the ocean, including presence of freshwater, Arctic double estuaries are considered to be uniquely sensitive to environmental change (Macdonald 2000).

2.3 Belcher Islands, southeast Hudson Bay

The Belcher Islands, which are part of Nunavut, lie about 100 km west of the southeastern shoreline of Hudson Bay and ~120 km north of James Bay (Figure 2.7). The finger-like rock outcrops extend over an area of roughly 3000 km^2 (55.5^0N to 57.0^0N and 78.5^0W to 80^0W). The islands are separated by narrow channels and inlets with a north-south orientation (Figure 2.7). Water depths amongst the Belcher Islands vary mostly between 5 and 40 m but

exceed 80 m in places. The variably sloping shelf around the Belcher Islands covers approximately 10,000 km^2.

Although there are several small lakes on the Belcher Islands, there is little to no freshwater discharge to the ocean throughout the winter season (all the streams are frozen). This signifies that variation in the amounts of river water in the study area in winter is controlled by advection from other sources in Hudson/James Bay.

The Belcher Islands provide a barrier that deflects surface ocean currents, steering coastal water north along the Quebec shoreline, and interior water northward to the west of the Belchers as shown in Figure 2.5 (Wang et al. 1994; Saucier et al. 2014). As a result, in summer, the islands form a boundary between the fresh surface waters arriving from James Bay and further west, and the more saline interior surface waters of Hudson Bay (St-Laurent et al. 2011). In winter, the interior domain exhibits a strongly mixed layer down to 40-60 m promoted by the addition of brine from sea-ice production (Ingram and Prinsenberg 1991; Saucier et al. 2004; Granskog et al. 2011). The summer surface mixed layer present in southeast Hudson Bay during August 1975 and 1976 mixed down to 12-18 m where the halocline was then present until 40-50 m below the surface (El-Sabh and Koutitonsky 1977; Prinsenberg 1986; Ingram and Prinsenberg 1998).

Freeze up of the sea surface surrounding the Belcher Islands commences in late December but it takes ~1.5-2 months for the study area to become fully covered by ice (Figure 2.7 inset). The landfast ice forms first along the southwestern coasts of the Islands and later along the north-northeast coasts. Generally there is only a narrow margin (few kms) of landfast ice around the islands, particularly to the west, where there is a large recurrent flaw lead (Figure 2.7 inset). To the east of the islands, ice sometimes moves in and out during January before

consolidating in February or March and thereafter remaining in place until breakup. This ice surface can be rough but the landfast ice platform effectively extends eastward by ~20 km toward the end of winter. Occasionally, during the last 100 years, an 'ice bridge' has formed extending all the way across to the eastern coastline of southeast Hudson Bay; during the past few decades the ice bridge has not always formed, and when it has formed, the timing has varied (CARC 1997).

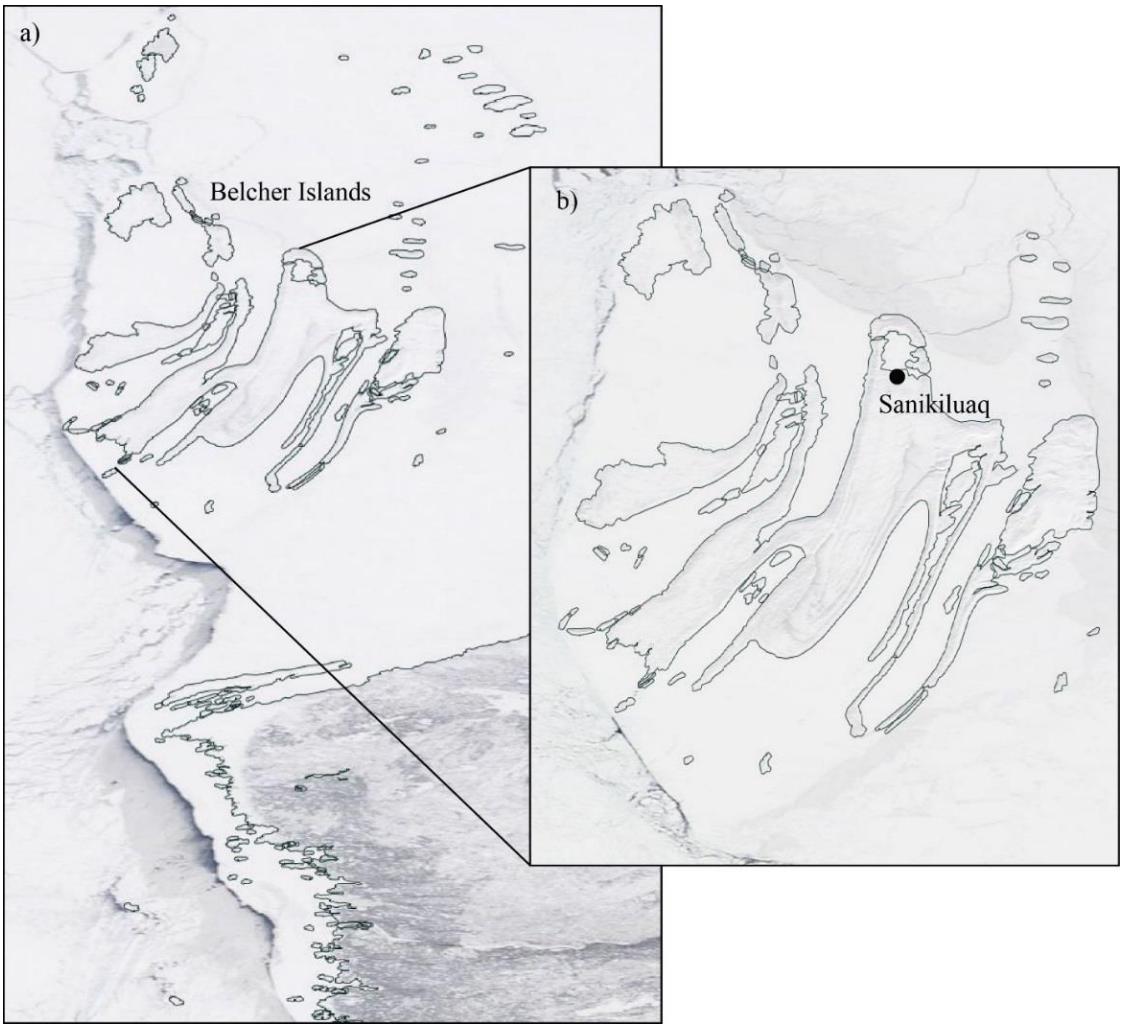

Figure 2.7. Icescape in February, 2015, a) showing the large NNW-SSE oriented flaw lead that extended from northeast James Bay into southeast Hudson Bay west of the Belcher Islands. b) A landfast ice platform is present around the Belcher Islands. Images are modified from EOSDIS February 14, 2015, (a) and February 8, 2015 (b).

Regional ice analysis charts of Hudson Bay (Environment Canada) show that, on average, the land fast ice is 30-70 cm thick by February around the Belcher Islands. Ice thickness increases to ~1 m by March. It should be noted that ice charts in the southern regions of Hudson Bay are available less frequently due to the lack of commercial/industrial marine activity in the region. In the channels amongst the Belcher Islands, there are numerous latent-heat polynyas (WMO 1970; Smith et al. 1990) kept open throughout winter due partly to strong tidal currents (Gilchrist and Robertson 2000). These polynyas and the associated system of flaw leads are biologically important (Stirling 1997), providing crucial winter habitat for eider duck populations, polar bears and seals (Gilchrist and Robertson 2000). Because the Inuit of Sanikiluaq (Figure 2.7) have relied for generations upon these polynyas as sites to obtain for country food, they have developed a deep knowledge of the seasonal patterns exhibited by the biota that populate these areas in winter.

Extensive ice cover remains around the Belcher Islands until break-up in June (Gagnon and Gough 2005, Hochheim et al. 2011). Between 1971 and 2009 the mean break up date was June 28 ± 11 days (sd) (Galbraith and Larouche 2011)).The temporal and spatial trends of Hudson Bay's sea-ice extent, relative to freeze up and break up dates described earlier, pertain to this region. Specifically, freeze-up is occurring later in the season and break-up earlier (CARC 1997).

Most of the past oceanographic work in southeast Hudson Bay has concentrated on the under-ice plume of the Great Whale River along the Quebec shoreline (Ingram 1981 ; Ingram and Larouche 1987; Ingram et al. 1996). Southeast Hudson Bay also has been included in large-scale studies of the distribution of freshwater components (river water and sea ice melt) in

Hudson Bay during the summer and fall periods (Granskog et al. 2007; 2011). However, there have been no previous studies in winter in southeast Hudson Bay that have included tracers capable of distinguishing between runoff and ice formation/melt. This gap needs to be addressed if we are to understand how much river runoff is present in winter and how it interacts with the ice cycle to modify water masses and circulation in this region.

2.4 Motivation and Objectives

2.4.1 Climate Change

In the past 40 years, global temperatures have been rising by ~ 0.3^{0}C per decade. Some northern regions of Canada have had increases in precipitation of almost 20% and there have been negative trends in ice extent (decreasing) by ~2.9% per decade, in addition to an overall 10% decrease in snow cover (Serreze et al. 2000). A contributing factor to the environmental changes noted above is that the annual increase in Arctic temperatures is twice that of the recorded annual global increase (AMAP 2012).

The Arctic climate balances the global climate system by influencing dispersal of energy (i.e. heat) through atmospheric-ocean circulation, and more importantly ice-albedo driven feedback (Stroeve and Maslowski 2008). Reduction in the amount of reflected light, due to less snow and sea-ice cover, increases the amount of energy being absorbed by the ocean surface and surrounding land, causing extensive change to energy retention in northern regions (Johannessen et al. 2004). Prolonged ice-free seasons will become more regular, forcing a surplus of energy (i.e., heat) to circulate through air-water masses moving towards more southerly latitudes in Hudson Bay, hence the fragility of high-latitude climates (Gagnon and Gough 2005).

2.4.2 Local changes to winter environment, Belcher Islands

Starting in the 1990s, rapid freezing of flaw leads and polynyas around the Belcher Islands began to close off the over-wintering habitat of the eider duck populations leading the

Inuit to question whether or not these changes were associated with coincident hydroelectric development of nearby rivers, especially those entering James Bay. This study was initiated to determine the sources and amounts of freshwater in this region during winter. Historically there have been few oceanographic observations in this region, and even fewer during winter. On the mainland, ~115 km to the east, the spreading of the Great Whale River plume under the sea ice has been studied by Ingram and colleagues (Ingram 1981; Ingram and Larouche 1987; Ingram et al. 1996). One other study collected profiles of temperature (T) and salinity (S) in waters adjacent to the Belchers in winter (Prinsenberg 1977). None of these studies collected samples that would permit the discrimination between ice melt and river water.

In this thesis, measurements of salinity and $\delta^{18}O$ from water samples and ice core samples are used as a two tracer system by which river water runoff and ice formation/melt can be distinguished. This data will be used to 1) determine the freshwater content of the water column (i.e. river water, sea-ice melt), 2) establish inventories of each freshwater type in the water column during the 2014-2015 fall and winter seasons, 3) describe the spatial variation in freshwater distribution around the Belcher Islands from early to late winter, and 4) infer temporal in river changes of the surface waters using the composition of sea-ice. Based on the results, I will adapt the currently accepted model of winter freshwater cycling and water mass evolution for the waters that surround the Belcher Islands. The data presented in this thesis is the first of its kind to be collected in this region during the winter season. The results offer a new perspective on the physical and chemical properties of the winter water column and landfast sea-ice, and is a first step towards addressing community concerns about freshwater and sea ice interactions in southeast Hudson Bay.

Chapter 3. Methodology

3.1 Freshwater tracers $\delta^{18}O$ and Salinity

3.1.1 The application of $\delta^{18}O$ in Arctic waters and sea-ice

Stable oxygen isotope composition of seawater ($^{18}O/\ ^{16}O$ ratio expressed as $\delta^{18}O$) has been widely applied in seasonally ice-covered oceans to establish the hydrological processes that affect the freshwater content of seawater (Östlund and Hut 1984; Gibson et al. 2005; McGuire and McDonnell 2008). Stable oxygen isotopes have been used as tracers of hydrological processes commencing with Craig's (1961) study investigating water transformations within the global hydrological cycle. Stable oxygen isotopic composition of water is commonly expressed as a difference between a sample and Vienna Standard Mean Ocean Water (VSMOW), which as a $\delta^{18}O$ of 0‰ (see equation 1).

$$\delta^{18}O\ (‰) = \left[\frac{\frac{^{18}O}{^{16}O}\ sample}{\frac{^{18}O}{^{16}O}VSMOW} - 1\right] \times 1000\,‰ \quad (1)$$

$\delta^{18}O$ provides evidence of the source of freshwater in the ocean, whether it may be seawater, river water, or precipitation (McGuire, and McDonnell 2008). Variations in isotope composition are produced by fractionation when water undergoes a phase change. For example, evaporation of water produces water vapour approximately 8‰ lighter (lower $\delta^{18}O$) than the water, and conversely, precipitation is approximately 8‰ heavier than the vapour it formed from. As water transports globally, it undergoes a number of E-P cycles, which lead to further depletions such that polar freshwater (e.g., rivers) may be 20-40 ‰ lighter than the original source of the water, such as surface ocean from more southern regions (Figure 3.1) (e.g., McGuire and McDonnell 2008; Friedman et al. 1964). Within a large water body, such as the

surface ocean, $\delta^{18}O$ is conservative making it possible to interpret change in $\delta^{18}O$ as a product of processes like mixing or sea-ice production. Therefore, river runoff (i.e., distilled water) can be detected in the Arctic marine coastal zone by a more negative $\delta^{18}O$ of the water mass (Macdonald et al. 1999).

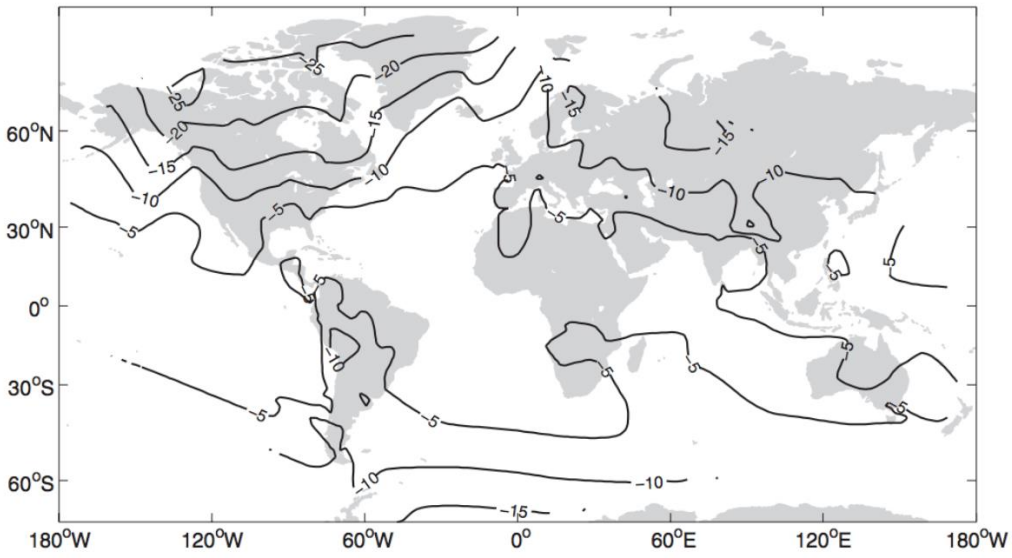

Figure 3.1. The global distribution of $\delta^{18}O$ in precipitation based on 389 WMO GNIP (Global Networks for Isotopes in Precipitation) stations between 1961 and 1999. Figure from McGuire and McDonnell (2008) © 2008 Blackwell Publishing, Stable Isotopes in the Watershed

Sea-ice reflects the isotopic composition of surface water it has grown from, but with an approximately 2‰ offset (sea-ice being isotopically heavier) due to the phase change (e.g., Macdonald et al. 2002). Fractionation may vary depending on freezing rate and amount of freshwater present (Eicken et al. 1998). In circumstances where ice forms in place and then accretes by growing thicker through the winter (e.g., landfast ice), a chronological record may be preserved within the growing ice of the isotopic composition of the water beneath it, but with a fractionation offset.

3.1.2 Salinity in Arctic waters and sea-ice

Salinity is defined as the ratio between the mass of seawater and the mass of dissolved substances in seawater, expressed as kg/kg or g/kg. The concentration of dissolved substances in seawater may vary depending on geographical location, but for the major ions, which are conservative, the ratios between them remain constant (see chapter 3, Talley et al. 2011). In the Arctic Ocean and its marginal seas, salinity governs the density of the water column, with temperature playing but a minor role (see Chapter 2 (Figure 2.3)). Salinity is reported in '*practical salinity units'*, and is referenced during conductivity measurements to commercial seawater standards (see chapter 3, Talley et al. 2011). To determine salinity through the measurement of conductivity relies on an accurate temperature reading to obtain a precise measurement (UNESCO 1983). Salinity in Arctic waters is altered mainly through the addition of freshwater from river runoff or precipitation and the removal of freshwater through evaporation. Salinity is most variable near the coast where it is largely affected by local river inputs. The formation and melting of sea-ice also alters the salinity in the water column, either through salt rejection as sea-ice forms or addition of brackish water as sea-ice melts (Carmack 2000). Sea-ice typically exhibits a bulk salinity of 6‰, however salinity is only partially retained as sea-ice forms on the surface waters (Nakawo and Sinha 1981). The combination of brine rejection, gravity drainage of brine from channels, and the formation of brine pockets within the ice results in a "C" shaped salinity profile in a column of ice (see Chapter 2, Figure 2.4; Eicken 2008).

3.1.3 The use of salinity-$\delta^{18}O$ tandem measurements in Arctic waters

Measurements of salinity together with $\delta^{18}O$ may be used in ice-covered oceans to distinguish river runoff (RW) from sea-ice melt or brine (+/- SIM). Östlund and Hut (1984) in their classic paper provided the algebraic methodology to use these two tracers (S, $\delta^{18}O$) to

determine the 'recipe' of seawater in terms of a mixed product of seawater, river water and sea-ice melt, expressing that recipe as fractional composition (Frw, Fsw, Fsim). To use this method requires the determination of the composition of the three components appropriate to the setting at hand. Östlund and Hut's (1984) equation and how it may be used for quantitative estimates of freshwater composition of samples will be explained in the analytical methods section. Figure 3.2 is a schematic diagram showing the general relationship observed between salinity (x-axis) and $\delta^{18}O$ (y-axis) when measured in Arctic estuarine waters. Samples with a high salinity and high $\delta^{18}O$ (less negative) predominantly contain seawater (SW), while samples with low salinity and low $\delta^{18}O$ contain significant fractions of meteoric water (MW, total of river water and precipitation combined). Samples that contain sea ice melt (SIM) will have a relatively low salinity and high $\delta^{18}O$. Finally, water samples containing brine rejected by the production of sea ice will have exceptionally high salinity and high $\delta^{18}O$. The mixing line on the figure shows the distribution of samples containing only SW and MW. Samples that lie either above or below the mixing line indicate, respectively, the addition of sea ice melt (+SIM) or brine (which is equivalent to -SIM).

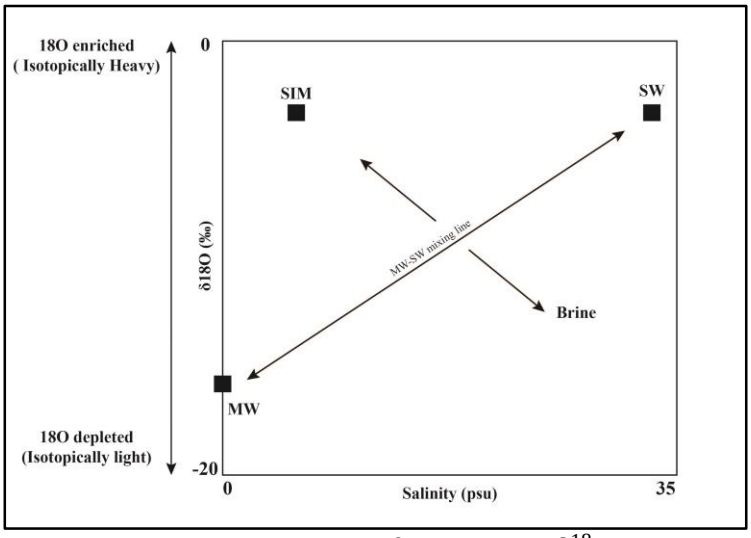

Figure 3.2. Schematic depicting the relationship of salinity vs. $\delta^{18}O$ and mixing between Sea-ice melt (SIM), Seawater (SW), and river water (RW) water masses

3.2. Methodology to study the spreading of freshwater plumes under landfast ice

Macdonald et al. (1995), developed the use of S- $\delta^{18}O$ measurements of water and ice in an estuarine system to understand the spreading of the Mackenzie Plume under the landfast ice in terms of quantities of water involved, their sources, and the progress of plume spreading throughout the winter commencing at freeze-up and ending in late spring prior to sea-ice breakup. Salinity and $\delta^{18}O$ measured in the water column and ice core samples were used to distinguish between Mackenzie River runoff, sea-ice melt, and brine. Inventories of RW and SIM in the water column, together with the inventories of growing ice, were used to produce freshwater balances for the system, and the changes in those balances between late fall and the subsequent late winter. By converting the $\delta^{18}O$ values in the landfast ice to implied RW content in the plume spreading under the ice, and by using a simple equation (Anderson 1961) to place a time frame on the landfast ice growth, Macdonald et al. (1995) were able to produce a reconstruction of the Mackenzie plume distribution under the landfast ice throughout winter. Eventually, this plume filled almost all of the inner shelf comprising landfast ice. This analysis presented the first use these freshwater tracers in an Arctic estuary over winter.

There are major differences in icescape and oceanography between the Beaufort study area and the Belcher Islands (Hudson Bay) study area, although both regions are affected strongly by RW and have large regions covered by landfast ice at the end of winter. Specifically, 1) the Belchers are located off the coast and are directly connected with Hudson Bay, not the Arctic Ocean; 2) the Belcher Islands themselves supply almost no RW – instead, RW is transported to the system by the coastal boundary current in Hudson Bay, which contains the outflow of many upstream rivers to the west and north; 3) many of the river systems that feed into the Hudson Bay study area are regulated for producing hydroelectricity, and; 4) the sea-ice immediately surrounding the Belcher Islands is predominantly continuous landfast ice without

the prominent stamukhi zones (rubble fields) prevalent in the flaw leads of the Arctic Ocean. The lack of stamukhi ice is important in that it permits fresh surface water to spread unimpeded without the 'inverted ice dams' associated with stamukhi (see Macdonald et al. 1995). Together, these differences mean that there is no traditional estuary associated with the Belchers; rather, the Belchers lie within the estuary produced by mainland rivers draining into coastal Hudson Bay. Furthermore, the remoteness of the Belcher Islands study area from any particular river mouth limits our ability to associate RW plumes observed within the study area with a specific source as could be done in the Mackenzie Estuary.

Nevertheless, the conceptual and methodological approach for investigating freshwater dynamics in an ice covered estuary developed by Macdonald et al. (1995) has found application in other settings (e.g. Alkire and Trefry 2006; Alkire et al. 2015; Eicken et al. 2005; Macdonald et al. 1999), and provides a suitable template for studying freshwater balances in the water around the Belchers during winter. The essential necessary components to conduct such a study include 1) Autumn water column data to determine system preconditioning, 2) general appreciation of the ice landscape, 3) measurements of two tracers (S and $\delta^{18}O$) in water and in sea ice to distinguish freshwater sources, and 4) sufficient resolution in water and ice core samples to determine freshwater budgets and the sources of change in these budgets during winter.

3.3. Field Sampling

Data for this study were collected during four field campaigns: 1) January15 to February 5, 2014; 2) October 27, 2014; 3) January 12 to 29, 2015; and 4) February 17 to March 14, 2015 (Table 3.1). Local Inuit hunters from Sanikiluaq, Arctic Eider Society (AES), and research partners from University of Manitoba contributed to the design of the project including the

selection of sampling locations. During the first campaign, sampling was conducted at eight stations distributed widely around the perimeter of the islands and at selected sites amongst the islands (SK 1, 2, 3, 4, 8, 9, 10 and 14; Figure 3.3). During the second campaign, four stations located along the east coast of the islands (SK 1, 3, 10 and 9) were resampled in open water conditions (Table 3.1). During the third field campaign, sampling was conducted at 12 'full' stations, where both CTD profiles and water samples were collected, and five additional stations where only CTD profiles were collected. During the fourth campaign, the 12 full stations were resampled and additional stations were visited for CTD profiles (n=12) and water sampling (n=4). The additional stations (T1A, T1B, T1C, A1-A4, and B1-B4) extended 5-20 km 'offshore', southeast and orthogonal to the Belcher Islands (Figure 3.3), where the ice platform had not been sufficiently consolidated to allow snowmobile travel during the previous campaign. Ice cores were obtained at a total of seven stations in Jan-Feb 2014 and 15 stations in Feb-Mar 2015. Daily observations of the weather were taken from Environment Canada Forecast, the monthly averages are presented in Appendix B.

Table 3.1. Summary of types of samples collected during the four campaigns starting January, 2014 and ending in March, 2015

Station	January 30 - February 5, 2014	October 27, 2014	January 12 - 29, 2015	February 17 - March 14, 2015
SK 1	W, CTD, IC	W	W, CTD	W, CTD, IC
SK 21			W, CTD	W, CTD, IC
SK 22				W, CTD, IC
SK 3	W, CTD, IC	W	W, CTD	W, CTD, IC
SK 23			W, CTD	W, CTD, IC
SK 10	W, CTD, IC	W	W, CTD	W, CTD, IC
SK 15			W, CTD	W, CTD, IC
SK 2	W, CTD, IC		W, CTD	W, CTD, IC
SK 9	W, CTD, IC	W	W, CTD	W, CTD, IC
T1C				W, CTD, IC
T1B				W, CTD, IC
T1A				W, CTD, IC
SK 12			W, CTD	W, CTD
SK 4	W, CTD		W, CTD	W, CTD, IC
SK 8	W, CTD, IC		W, CTD	W, IC
SK 14	W, CTD, IC		W, CTD	W, IC
A1				CTD
A2				CTD
A3				CTD
A4				CTD
B1				CTD
B2				CTD
B3				CTD
B4				CTD
SK 6			CTD	CTD
SK 13			CTD	CTD
SK 17			CTD	CTD
SK 20			CTD	
SK 25			CTD	CTD

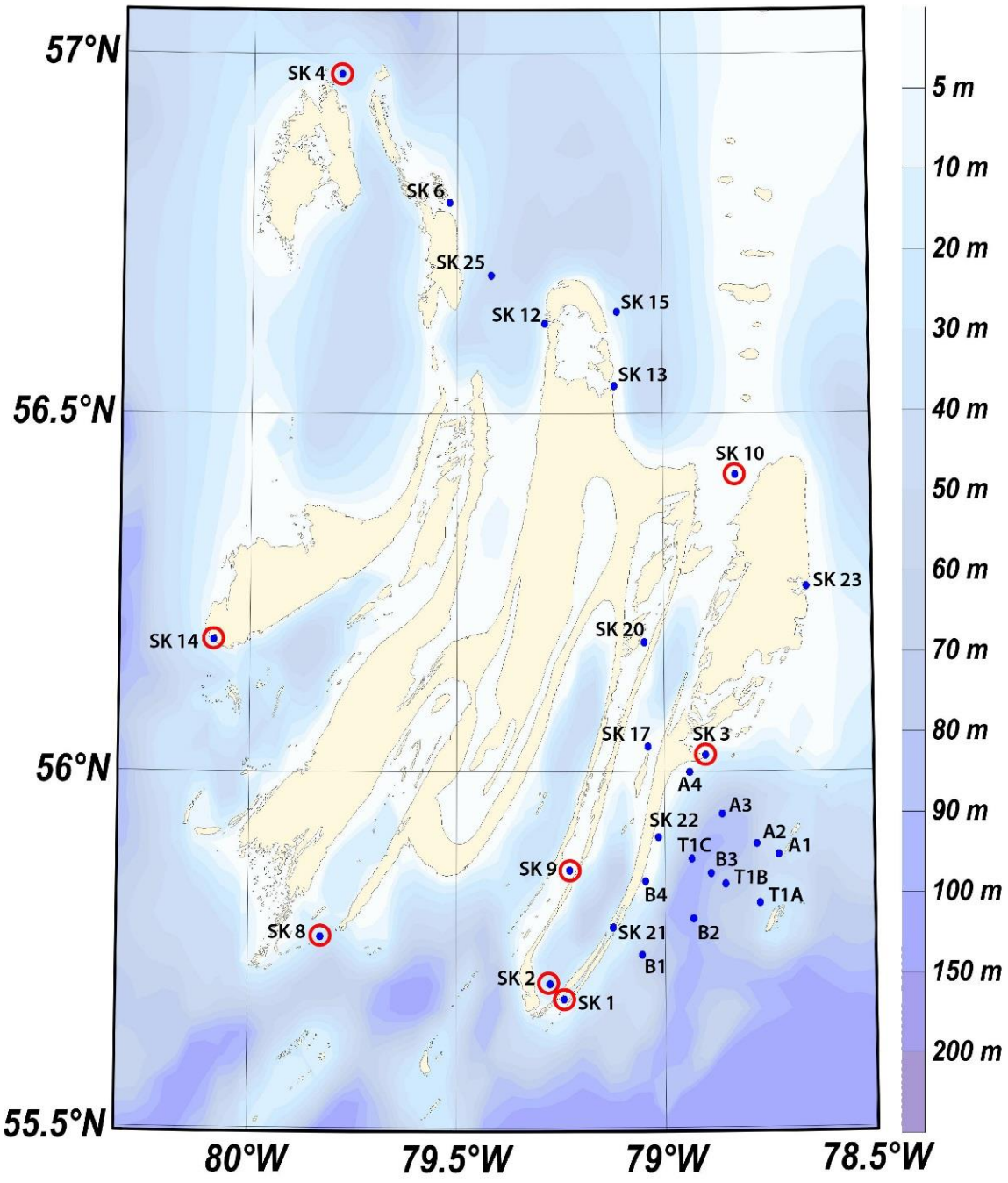

Figure 3.3. Belcher Islands study area and sampling stations. Blue points indicate stations sampled in 2015 and the red circled points indicate stations also sampled in January-February, 2014

Temperature and salinity profiles of the water column were collected at each sampling station using a Castaway Conductivity Temperature Depth (CTD) sensor during the 2015 field season (temperature accuracy ±0.05ºC, conductivity accuracy of 0.005 mS/cm and pressure

(depth) accuracy of ±0.25%) and an RBR CTD sensor during the 2014 field season (temperature accuracy ±0.002ºC, conductivity accuracy of 0.001 mS/cm and pressure (depth) accuracy of ±0.05%). A Kemmerer (1.0 L) water sampler was deployed to designated depths in the water column (measured from the ice bottom), and then brought to the surface to fill dry 1 L Nalgene bottles. Sampling depths were chosen to focus on the top 20 m of the water column (1, 5, 10, 20 m), and a sample also obtained ~5 m above the sea bed (Table 3.2). In winter, the 1 L water samples were stored in an insulated cooler that contained hot water bottles to prevent the samples from freezing during transport back to town. In a field lab established in the HTA/AES office, the bulk samples were redistributed into120 mL Boston rounds and 20 mL borosilicate vials (rinsing three times before filling), for salinity and oxygen isotope analysis respectively, then capped and sealed with parafilm to prevent evaporation and stored at 4^0C. Just prior to analysis, subsamples for oxygen isotope analysis were pipetted from the 20 mL vials into sealable 2 mL vials.

Ice cores were collected in January-February, 2014 and again in February-March, 2015 (Table 3.2). A Mark II Kovac ice coring system was used to retrieve an ice core (9 cm diameter; maximum of 1 m in length), which was then sectioned by sawing into 5 cm lengths with care to avoid contamination by snow. Individual core sections were placed in sealable plastic bags, stored in a cooler and kept frozen until further processing. At the University of Manitoba CEOS laboratories, each ice core section was placed in a new plastic bag, vaccum sealed, then left at room temperature (21ºC) for a full 24 hrs to melt. The melted ice samples were then redistributed into bottles and vials in the same manner as the water samples (120 mL Boston round bottles for salinity analysis and 2 mL vials for oxygen isotope analysis), sealed, and stored at 4^0C.

Table 3.2. Ice and snow properties for all stations sampled during the 2014 and 2015 winter campaigns, and the depths sampled in the water column

Year	Station	Latitude [degrees_north]	Longitude [degrees_east]	Bottom Depth [m]	Freeze-up date	First Sampling Date	First Ice Thickness [cm]	First Snow Thickness [cm]	Final Sampling date	Final Ice Thickness [cm]	Final Snow Thickness [cm]	Water sampling Depths [m]
2014	SK 1	55.6808	-79.2426	65	16-Dec-13	21-Jan-14	50					0, 1, 5, 10, 20, 60
2014	SK 2	55.7024	-79.2763	>65	16-Dec-13	21-Jan-14	50					1, 5, 10, 20, 60
2014	SK 3	56.0231	-78.9010	32	23-Dec-13	22-Jan-14	23					1, 2, 5, 10, 20, 32
2014	SK 4	56.9719	-79.7839	52		25-Jan-14						1, 2, 5, 10, 20, 50
2014	SK 6	56.7938	-79.5187	7		25-Jan-14						
2014	SK 8	55.7689	-79.8276	13	21-Dec-13	8-Feb-14						1, 5, 10, 13
2014	SK 9	55.8620	-79.2285	>50	14-Dec-13	14-Feb-14	77					1, 2, 5, 10, 20, 60
2014	SK 10	56.4150	-78.8246	28	3-Dec-13	14-Feb-14	75					1, 2, 5, 10, 28
2014	SK 12	56.6260	-79.2870	>50		15-Feb-14						
2014	SK 13	56.5390	-79.1180	>50		16-Feb-14						
2014	SK 14	56.1847	-80.0881	>50	3-Dec-13	19-Feb-14	82					0,2,5,10,20,60
2014	SK 1	55.6808	-79.2426	65		27-Oct-14						
2014	SK 3	56.0231	-78.9010	38		27-Oct-14						
2014	SK 9	55.8620	-79.2285	60		27-Oct-14						
2014	SK 10	56.4150	-78.8246	27		27-Oct-14						
2015	SK 1	55.6808	-79.2426	57	10-Dec-14	14-Jan-15	39	2.5	14-Mar-15	87	10	1, 5, 10,20
2015	SK 2	55.7024	-79.2763	>80	17-Dec-14	26-Jan-15	50	5	12-Mar-15	89	5	1,5,10,20,60
2015	SK 3	56.0231	-78.9010	48	10-Dec-14	15-Jan-15	50	2.5	11-Mar-15	109	5	1,5,10,20,32
2015	SK 4	56.9719	-79.7839	42	10-Dec-14	20-Jan-15	55	1.25	6-Mar-15	104	3	1,5,10,20,40
2015	SK 6	56.7938	-79.5187	19		20-Jan-15	52	4	13-Mar-15			
2015	SK 8	55.7689	-79.8276	8	10-Dec-14	17-Jan-15	30	2.5	7-Mar-15	80	5	1,5,8
2015	SK 9	55.8620	-79.2285	>80	8-Dec-14	29-Jan-15	72	16	12-Mar-15	97	5	1,5,10,20,60
2015	SK 10	56.4150	-78.8246	13	16-Dec-14	29-Jan-15	51	2.5	1-Mar-15	89	2.5	1,5,10
2015	SK 12	56.6260	-79.2870	28		24-Jan-15	90	5	13-Mar-15	104	5	1,5,10,15
2015	SK 13	56.5390	-79.1180	40		25-Jan-15	40	1	1-Mar-15	32	15	
2015	SK 14	56.1847	-80.0881	25	5-Dec-14	21-Jan-15	44	5	8-Mar-15	78	5	1,5,10,20
2015	SK 15	56.6420	-79.1110	19	16-Dec-14	25-Jan-15	39	0	1-Mar-15	93	2	1,5,10,20
2015	SK 17	56.0348	-79.0400	60		26-Jan-15	64	5	28-Feb-15	100	5	
2015	SK 20	56.1812	-79.0479	12		29-Jan-15	59	20				
2015	SK 21	55.7815	-79.1249	22	10-Dec-14	26-Jan-15	58	7	14-Mar-15			
2015	SK 22	55.9079	-79.0154	>80	10-Dec-14		100	5	26-Feb-15			
2015	SK 23	56.2585	-78.6547	30	5-Jan-15	28-Jan-15	44	5	11-Mar-15	96		1,5,10,(30)
2015	SK 25	56.6930	-79.4170	50	16-Jan-15	23-Jan-15	28	0	13-Mar-15	94	3	1,5,10,20,50
2015	T1A	55.8155	-78.7728	54	16-Jan-15		98	0.5	20-Feb-15			1,5,10,20,60
2015	T1B	55.8424	-78.8555	>80	16-Jan-15		110	5	22-Feb-15			1,5,10,20,60
2015	T1C	55.8775	-78.9359	>80			86	5	22-Feb-15			
2015	A1	55.8838	-78.7270	74			87	4	17-Feb-15			
2015	A2	55.8986	-78.7798	58				4	17-Feb-15			
2015	A3	55.9407	-78.8621	74			70	4	17-Feb-15			
2015	A4	55.9996	-78.9396	74			74	4	17-Feb-15			
2015	B1	55.7431	-79.0557	80			71	5	18-Feb-15			
2015	B2	55.7936	-78.9324	72			85	7	18-Feb-15			
2015	B3	55.8574	-78.8893	>80			86	7	18-Feb-15			
2015	B4	55.8463	-79.0471	>80			76	7	18-Feb-15			

3.4. Analytical Methods

3.4.1 Salinity

The salinities of seawater and melted ice samples were measured with a Guideline Portasal (model 8410A) in the laboratory of Dr. C. Michel at the Freshwater Institute, Department of Fisheries and Oceans in Winnipeg, Manitoba. The salinometer was calibrated with 34.8 ppt OSIL standard seawater before and after each day of analysis (~30 samples). A standard deviation of 0.0002 for at least two conductivity readings from a sample was considered

to reflect accurate measurement. The practical salinity unit (psu) was then recorded. Over a single month, between June and July 2015, an overall accuracy of ±0.001 between standard seawater measurements was obtained. A precision of ±0.02 was achieved for sample duplicates (n=42) throughout the month of analysis.

3.4.2 $\delta^{18}O$ of water samples and melted ice

Just prior to analysis, subsamples for oxygen isotope analysis were pipetted from 20 mL vials into sealable 2 mL vials. The oxygen isotopic composition was measured by a Picarro Cavity Ring-Down Spectroscopy High Precision Isotopic Water Analyzer (CRDS model L2130-i) at the University of Manitoba (U of M). Three reference standards, Standard Light Antarctic Precipitation (-55.50 ‰), an in-house artificial seawater standard created at the University of Manitoba Sea Ice Research Facility (SERF) (-16.50‰), and Vienna Standard Mean Ocean water (V-SMOW) (0‰), were run before and after each set of 10 samples to recalibrate the instrument, reduce drift, and maintain precision. Six measurements were made in total for each 2 mL sample and the latter three values used to calculate the average $\delta^{18}O$ (‰) for that sample. Although the analysis of seawater causes a salt build-up inside the instrument (cf.,Walker et al. 2016), proper maintenance and routine flushing was practiced to ensure there was no influence on the quality or integrity of the measurements. Over the course of several months, between June and August 2015, the overall precision obtained for duplicate samples and standards was ±0.10‰ (n=53). This precision is similar to that reported in previous studies of coastal Hudson Bay waters (Kuzyk et al. 2008; Granskog et al. 2011). The average difference for a set of 20 samples analyzed both at the U of M and the lab used in previous studies (G.G. Hatch Isotope Laboratory, University of Ottawa) was 0.29‰. The U of M results showed a slight positive bias, which implies that the data used in this study will slightly underestimate the fractional contribution of river water relative to previous work.

3.4.3 Water mass analysis

As in all seas where sea-ice may be formed in winter or melted in summer, the freshwater in the ocean surrounding the Belcher Islands is affected by runoff (RW) and sea-ice formation/ melting (SIM). Mixing these two freshwater components with ocean-sourced salt water (SW) produces a three-component system. Two conservative tracers and the conservation rule allow unique algebraic solutions for any mixture of three distinct water types.

Here, the two conservative tracers, $\delta^{18}O$ and salinity, were applied to estimate the amounts of each water type (RW, SIM, SW) in a sample using the following simultaneous equations (Östlund and Hut 1984):

(2) $Fsw + Frw + Fsim = 1$

(3) $FswSsw + FrwSrw + FsimSsim = Sobs$

(4) $Fsw\delta^{18}Osw + Frw\delta^{18}Orw + Fsim\delta^{18}Osim = \delta^{18}Oobs$

where F refers to the fraction of each water type that is denoted in the subscript (RW, SIM, SW), S and $\delta^{18}O$ refer to the salinity and $\delta^{18}O$ end-members for each respective water type, and S_{obs} and $\delta^{18}O_{obs}$ refer to the values from the sample of interest. The three component system (Fsw, Frw, Fsim) was solved quantitatively for each seawater sample using these equations after assigning appropriate properties to the three end-members (see discussion section).

3.4.4 Interpreting $\delta^{18}O$ records in the ice

The chemical properties of sea ice reflect the properties of the surface waters from which the ice was grown. In the case of salt (salinity), which is rejected into the brine, the sea ice contains a poor, non-conservative record; however, in the case of $\delta^{18}O$, which is captured within the frozen water, the record is conservative and reflects the sea water beneath the growing sea ice with a fractionation offset. Therefore, following Macdonald et al. (1995, 1999), we have used

$\delta^{18}O$ profiles in the ice cores collected in 2015 to infer changes in the meteoric water content of surface waters throughout the period of ice growth.

There were two steps required to use the records in the ice cores: 1) convert depth in the ice core into a time scale and 2) apply a fractionation correction to convert the $\delta^{18}O$ value in the core to the corresponding $\delta^{18}O$ value in the water from which it originated. The time scale for each core is constrained by two known dates. The date of freeze-up was estimated from satellite imagery (EODIS Worldview) of the study region. At most stations, freeze-up fell within the second week of December (December 5-17, 2014, Table 3.2). Off the southeast coast, landfast ice began to form in December; however a permanent platform did not persist until after January 5-16, 2015. The second known date is the time of ice core collection, which coincides with the bottom most layer of the ice. The cores were collected while winter conditions prevailed and before spring thaw commenced according to the freezing-degree day record at Sanikiluaq (Figure 3.4).

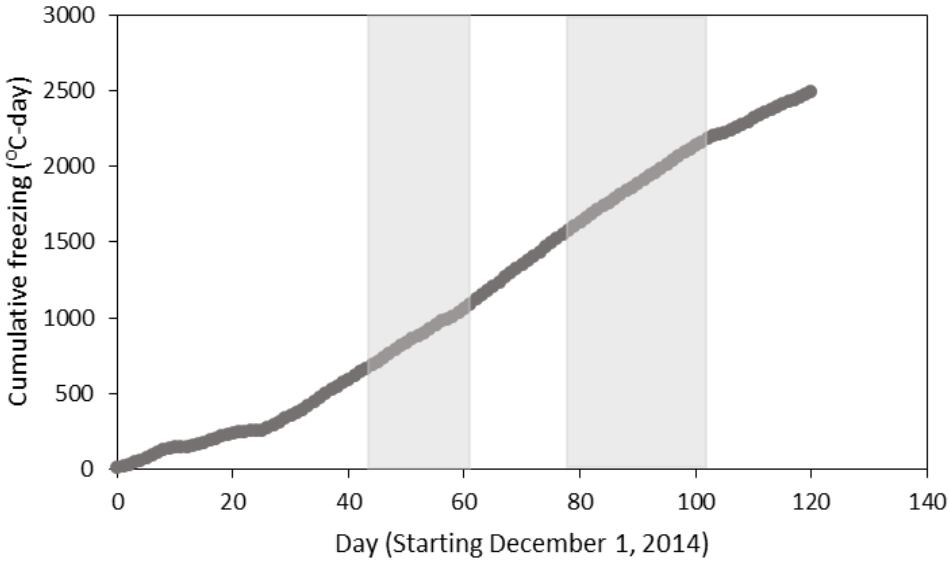

Figure 3.4. Cumulative freezing degree days (^{0}C) starting on December 1, 2014 and ending March 31, 2015, at Sanikiluaq (NU). First Campaign in 2015 occurred between January 14-31

and second campaign occurred between February 17, 2015 and March 14, 2015 (highlighted in grey)

The start of freezing and the date at the bottom of the ice were then used to relate depth in the core to time using the Anderson equation (1961):

$$H = d\sqrt{t} \quad (5)$$

This empirical equation models ice growth as a function of the square root of time. Knowing the length of the core (H), and total days of growth (t), a constant (d) is determined to assign a date to each section of the core. For the midpoint of each 5 cm core section, we then applied *d* to calculate the time elapsed since freeze up. Adding the time elapsed to the estimated date of freeze up for that core allowed a date to be assigned to that particular section. In this way a time scale was assigned section by section to the entire core.

We have evaluated the uncertainty in this method of dating the cores by comparing the ice thicknesses predicted using the Anderson equation with ice thicknesses that were measured at various stations 35-53 days into the period of ice growth. The predicted ice thicknesses exceeded the observed thicknesses by, on average, 16 (±3) cm (n=10). This disagreement between predicted and observed thicknesses implies that the dates assigned to sections in the middle of the cores are too early by as much as 1-2 weeks. If snow cover were included in the sea-ice growth model, it would tend to decrease predicted ice thicknesses and thus bring the predicted thicknesses closer to the observations. When ice thickness observations were made in January, 2015, about 5±5 cm of snow had accumulated on the ice at the sampling stations. Unfortunately, continuous measurements of snow by which we could improve the model are not available. When considering the timescales attributed to the ice cores, a possible error of 1-2 weeks should thus be kept in mind.

Chapter 4. Results

4.1 Spatial and temporal variations in salinity and temperature

Salinity and temperature profiles of the winter water column recorded during January-February, 2014 (Figure 4.1), January, 2015 (Figure 4.2), and February-March, 2015 (Figure 4.2) were compiled by campaign to show the physical variability of the winter water column during each time period. The salinity of the entire water column ranged from ~ 26 to 30, while the temperature ranged from ~ -1.55 to -0.5 °C (see Figures 4.1 and 4.2). Salinities recorded at stations SK 1 and SK 3, located in the southeastern section of the study area, have been highlighted to distinguish the lower salinity limit present in the surface waters, accompanied by a stratified water column (see Figures 4.1 and 4.2). Low saline (26.4±0.6) surface waters were present during each winter campaign, specifically in the southeastern region of the study area, and with the opportunity to expand sampling off the southeastern coast during February-March, 2015 (Figure 4.2), the low saline surface mixed layer of the top 20 m remained a prominent feature in the water column. This top 20 m feature is a dominant feature in all three winter campaigns, and has been considered the general halocline mark in our study area. The temperature above the halocline was near the freezing point, and exhibited a stratified profile in relation to its salinity profile counterpart (e.g. Figure 4.2, February-March, 2015). Remnant heat (~ -0.5^{0}C) was present below the surface mixed layer in all three campaigns (Figures 4.1 and 4.2), and remains in the lower portions of the water column throughout the winter season when comparing January, 2015 temperature profiles to February-March, 2015 (Figures 4.2) . The upper salinity limit of the study area (29±0.8) shown in Figure 4.1 and 4.2 is found in predominantly well mixed profiles with little to no stratification, and defines the water column for stations mainly on the northwestern side of the islands (e.g. SK 14 and SK 4).

To determine whether there was a spatial and temporal variability in the salinity and temperature profiles shown in Figures 4.1 and 4.2, a sectional view of the study area extending around the Belcher Islands beginning in the northwest (station SK 12), extending down the west side of the islands, then across the south side, and finally up the east side to the northeast corner (station SK 15) was used to look at the study area as a whole (Figure 4.3). Two trends emerged from the three winter campaigns when looking at the spatial variability in the salinity profiles. The east-southeast section of the study area had a water column that was strongly stratified with a fresh surface mixed layer within the top 20 m of the water column, whereas along the west-northwest section of the study area the salinity profile was well mixed and more saline than the east-southeast surface waters. From here on, we have designated these as two domains; the coastal domain and interior domain (dashed line, Figure 4.3), in reference to the fresh coastal corridor and saline interior waters that make up Hudson Bay (St-Laurent et al. 2011).

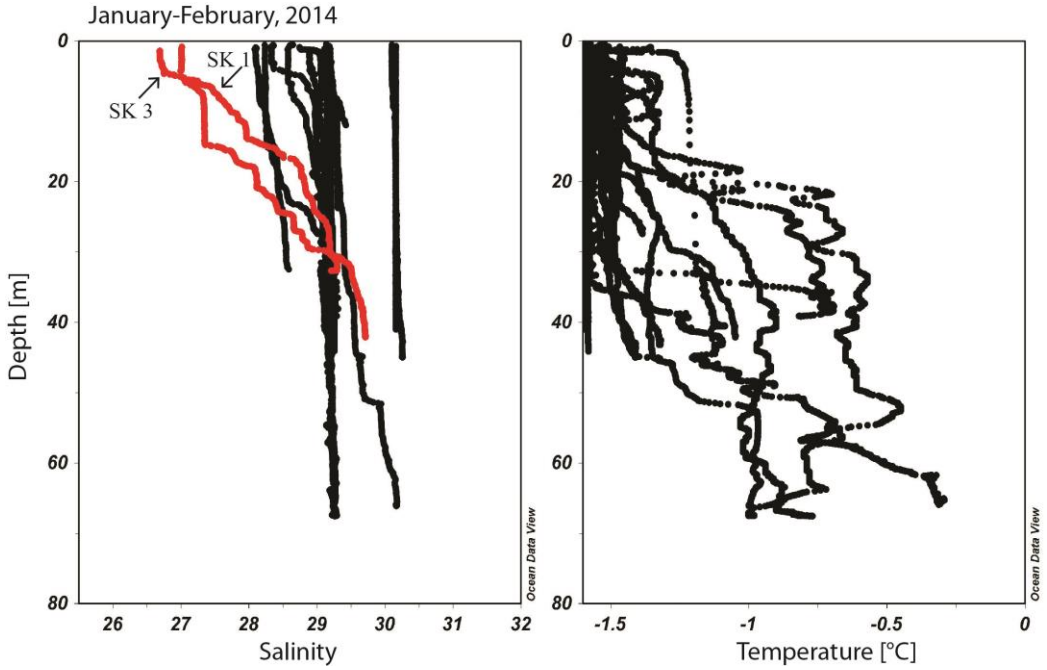

Figure 4.1. Salinity and temperature profiles for January-February, 2014. Stations SK 1 and SK 3 are highlighted to identify profiles with low salinity surface waters

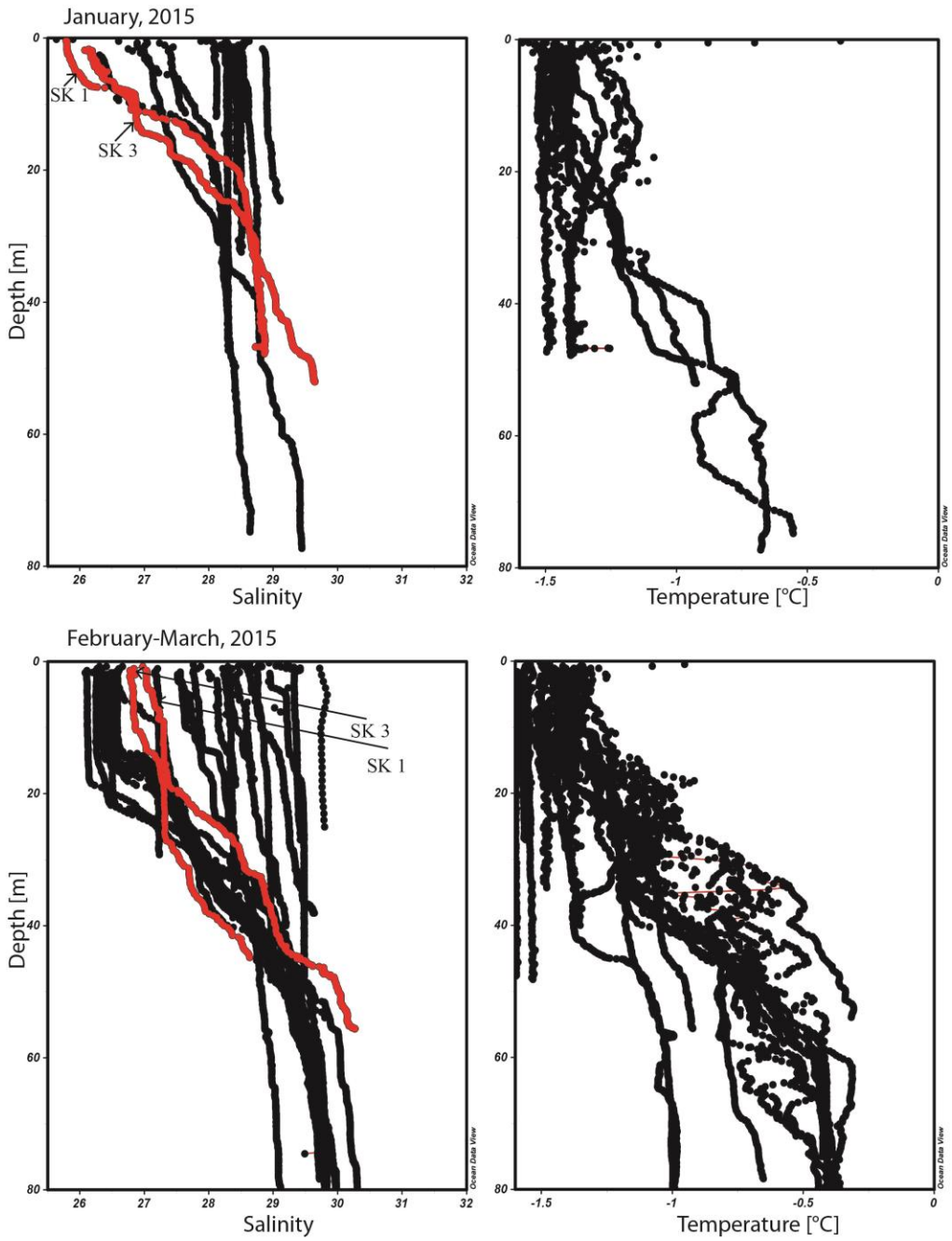

Figure 4.2. Salinity and temperature profiles for January, 2015 and February-March, 2015. Stations SK 1 and SK 3 are highlighted to identify profiles that have low salinity surface waters. February-March, 2015 salinity plot displays profiles that are less saline than highlighted stations. These stations are located in the southeast corner of study area near stations SK 1 and SK 3

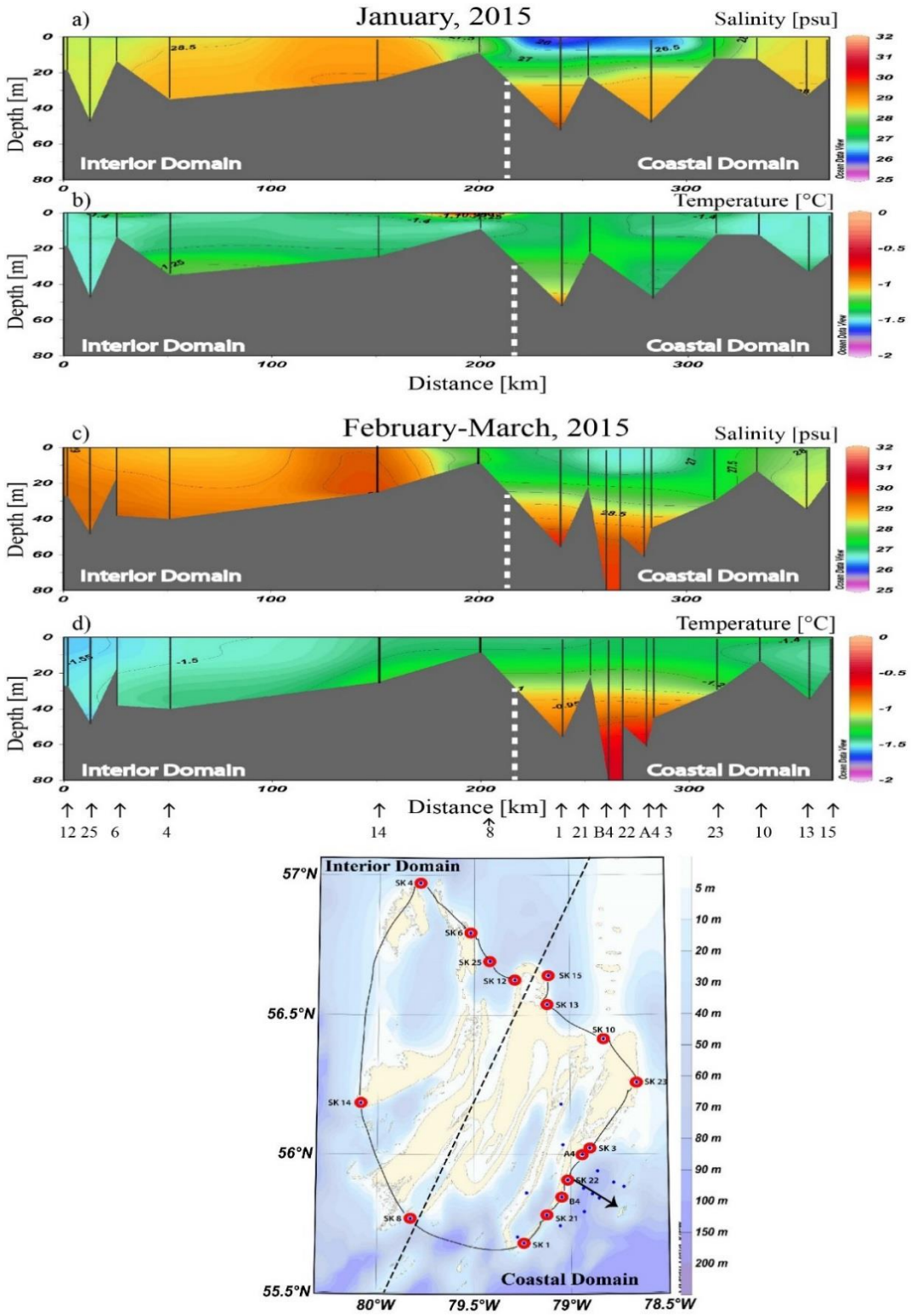

Figure 4.3. Sectional view of salinity (a,c) and temperature (b,d) distributions using a section that extends around the Belcher Islands beginning in the northwest (station SK 12), extending down the west side of the islands, then across the south side, and finally up the east (arrow indicates the orthogonal transect, see Figure 4.4)

In January, 2015 (Figure 4.3a), the strong component of freshwater was concentrated along the southeast portion of the coastal domain, beginning southwest of SK 1 and moving northwards towards SK 23 along the east coast of the Belchers. The low salinity surface mixed layer (~26) present above the halocline can be clearly seen in the sectional view, including the near freezing temperatures of the water. In February-March, 2015 (Figure 4.3b), the low salinity surface mixed layer expanded vertically and laterally in the water column, reaching below 20 m at some stations (e.g. SK 1 see Figure 4.2, February-March, 2015). The salinity of the water below the halocline was generally 29.3 ±0.6, with temperatures near -0.5°C, implying that remnant heat from summer waters was captured in the lower portions of the coastal domain's water column. In the interior domain, between January (Figure 4.3a) and Feb-March, 2015 (Figure 4.3b), the water column exhibited a well-mixed salinity profile that slightly increased in average salinity 29.0±0.2 from early to 29.3±0.3 in later winter and remained near freezing ~1.55 to – 1.4°C. The most saline, well mixed profile was present at the westerly station SK 14 with a maximum salinity of 30.1.

The salinity and temperature spatial variability along the orthogonal transect (SK22, T1C, T1B, T1A, see map Figure 4.3), was consistently strongly stratified up to 20 km away from the coast during February-March, 2015 (Figure 4.4). The top 15-20 m of the water column was a cool fresh surface mixed layer that had a low salinity of 26-26.5 and a temperature near freezing. This freshwater lay on top of a strong halocline that separated the surface mixed layer from the deep saline (>29.5), warm waters (-0.4°C) below.

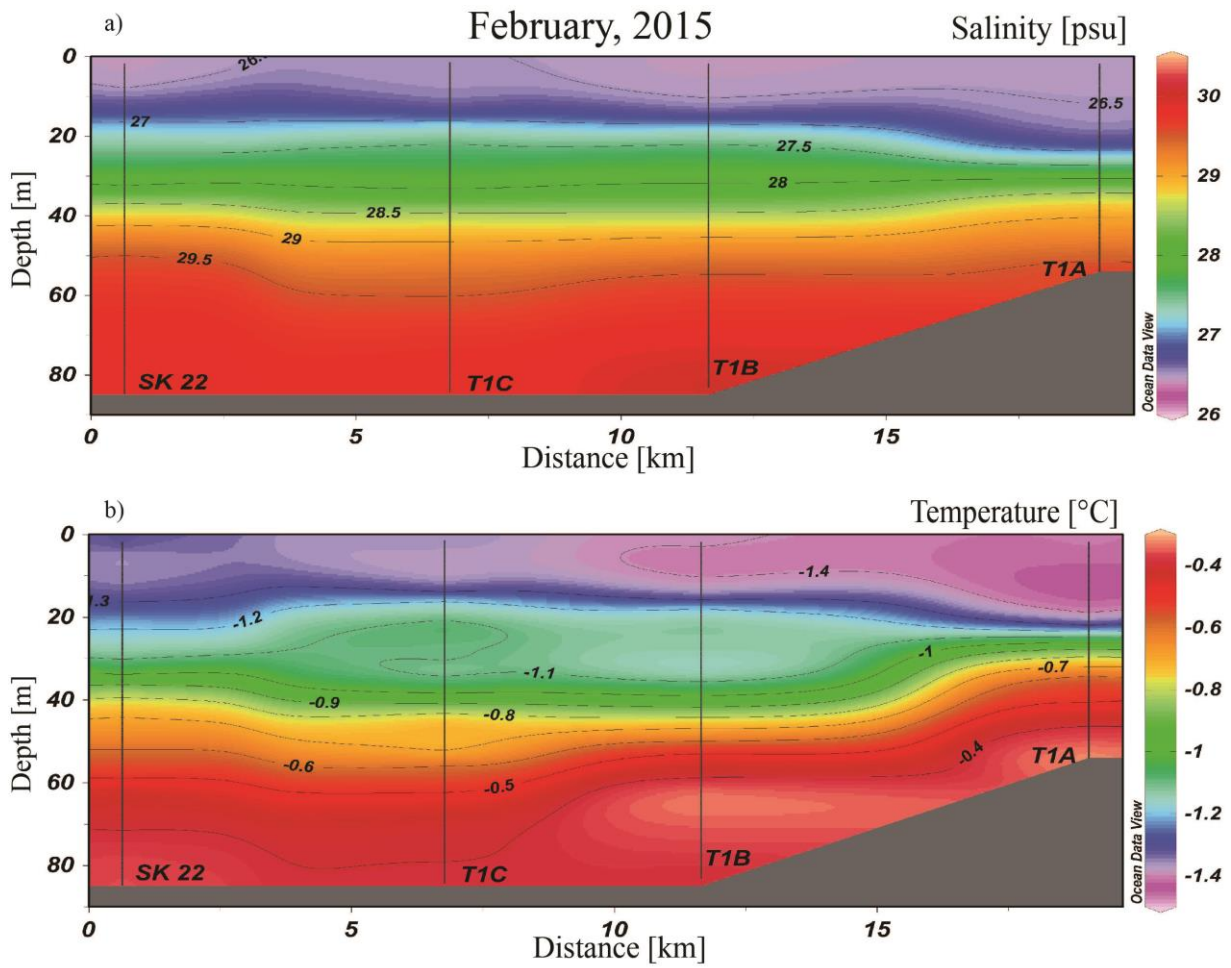

Figure 4.4. Salinity and temperature distribution along an orthogonal section extending from the southeast coast of the Belcher Islands eastward ~ 20 km toward mainland Hudson Bay. Data were obtained in February-March, 2015

A comparison of coastal domain properties in January, 2015, (Figure 4.3) with those during the preceding fall season (October, 2014; data not shown) reveals that surface salinity decreased between fall and winter (from ~27.2 to 26.5), while deep water salinity increased (from 28.7 to 29.8). October data are not available for stations in the interior domain. However, in October, 2005, the salinity in the surface mixed layer west of the Belchers (station BI-2) averaged 27.5 (ArcticNet/Amundsen cruise AN02; unpublished). Assuming a similar salinity in nearshore waters in October, 2014, implies an increase in salinity from fall to winter (from 27.5 to ~29.2).

4.2 Oxygen isotope ratios ($\delta^{18}O$) in seawater, river water, and sea ice

When $\delta^{18}O$ data from the various freshwater sources (river water, sea-ice melt) and seawater samples from our study area were plotted against salinity, a large S-$\delta^{18}O$ field was produced spanning a salinity range of 0 to 33 and $\delta^{18}O$ range of -19.5‰ to 0‰ (Figure 4.5; Appendix A). The mixing line shown implies a connection between the S-$\delta^{18}O$ properties of river water and seawater (Figure 4.5). Previously reported $\delta^{18}O$ values for rivers discharging into western Hudson Bay and James Bay, 'upstream' from the Belcher Islands study area, vary from -19.5‰ to -10.3‰ (Granskog et al. 2011; see Table 4.1). Specifically, river discharge from La Grande Complex in January, 2015, had a $\delta^{18}O$ value of -13.28‰ (Table 4.1). Our own water samples collected between 2014-2015 lie within range of the previously established $\delta^{18}O$ values in southeast Hudson Bay during the open water season (-5.7‰ to -2.3‰ from 2005-2010 ArcticNet/Amundsen cruises; see Figure 4.5a). During our four campaigns the water samples exhibited a $\delta^{18}O$ range of -5.2‰ to -2.3‰ (Figure 4.5b). Seasonal shifts in $\delta^{18}O$-S water properties separated each campaign into overlapping clusters of data where the first campaign in October, 2014 generally set the upper $\delta^{18}O$ limit for our dataset (less negative), while the second campaign spanning January-February, 2014, set the lower $\delta^{18}O$ limit (Figure 4.5b). The winter campaigns in 2015 lay in-between the limits, displaying a slight shift to more negative $\delta^{18}O$ values from January, 2015 to February-March, 2015.

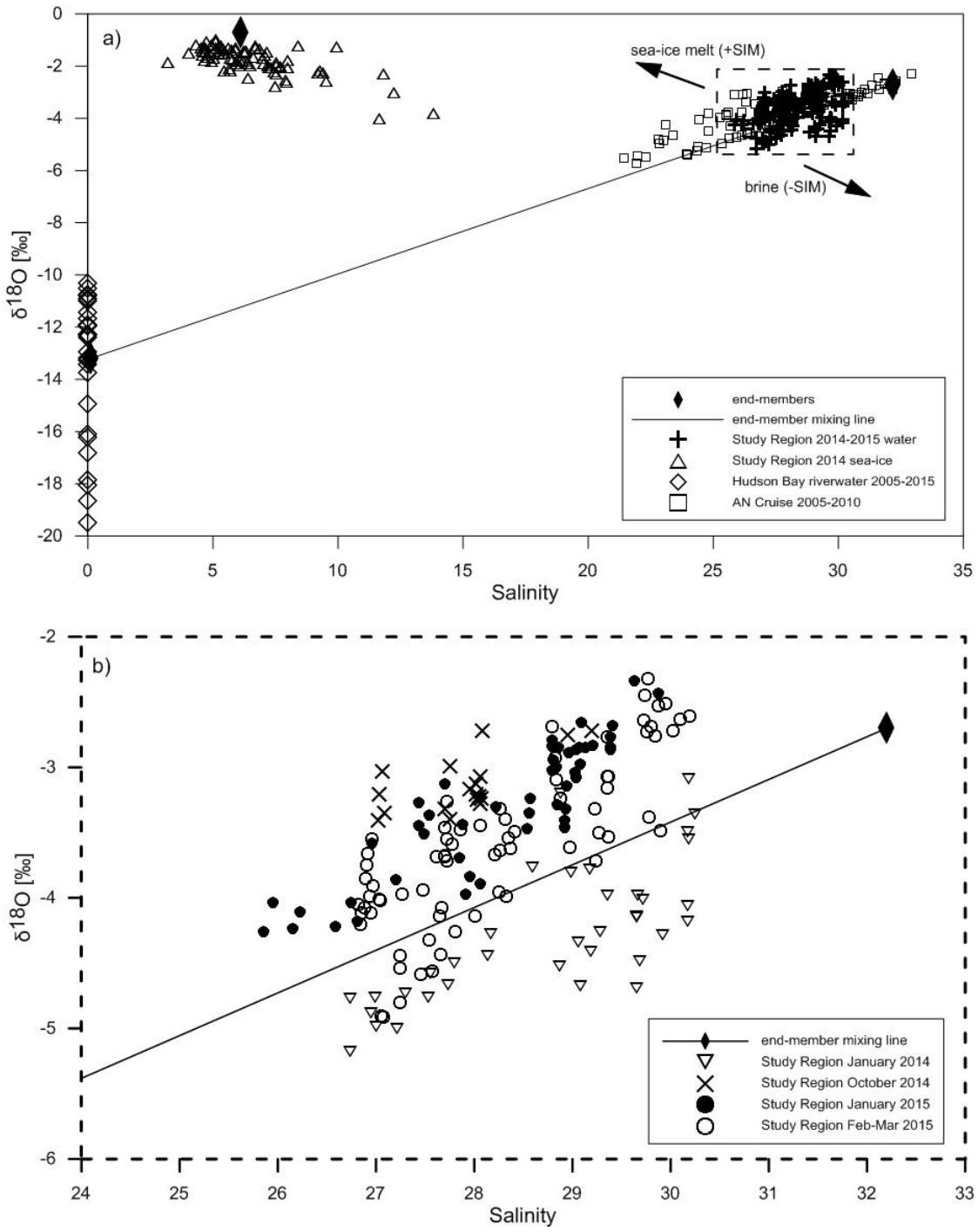

Figure 4.5. Plots of $\delta^{18}O$ versus salinity for the study region. a) Hudson Bay water (study region water samples + and ArctiNet/Amundsen (AN) cruises 2005-2010 □), river samples (◇), and melted sea-ice samples (○). End-members assigned for local seawater, river runoff, and sea-ice (Table 5.1) are shown as (◆). The line indicates the mixing line between river runoff and seawater end-member values. b) Seawater samples from this study re-plotted to highlight the changes in properties between January-February, 2014 (+), October, 2014 (×), January, 2015 (●) and February-March, 2015 (□). Values above the mixing line indicate the presence of sea-ice melt (+SIM), while values below the mixing line indicate the presence of brine (-SIM)

Table 4.1. Mean annual flow and $\delta^{18}O$ values for rivers upstream of the study region, organized by territory, province and drainage region. The mean annual flow data are from Dery et al. (2011) and Stadnyk et al. (2017), the La Grande $\delta^{18}O$ data are from this study (winter 2015), and the remaining $\delta^{18}O$ data are from Granskog et al. (2011) and/or 2005-2010 ArcticNet/Amundsen cruises (unpublished)

River	Mean Flow [km³/yr]	δ18O [‰]
Nunavut (NW)		
Chesterfield Inlet	41.1	-17.85
Wilson	2.60	-14.39
Ferguson	2.56	-16.22
Tha-anne	6.94	-16.82
Thlewiaza	6.90	-16.08
Manitoba (SW)		
Churchill	19.4	-15.51 (3.08)[a]
Nelson	92.6	-11.06 (0.70)[b]
Hayes	19.4	-12.27 (0.64)[c]
Ontario (SW)		
Severn	21.6	-11.01
Winisk	15.3	-11.22 (0.65)[d]
Quebec (JB)		
La Grande	80.5	-13.28
Total	308.9	
Weighted Mean		-13.21

a_Standard deviation of 7 measurements, b_Standard deviation of 6 measurements, c_Standard deviation of 4 measurements, d_Standard deviation of 2 measurements

The salinity and $\delta^{18}O$ values observed in our melted sea-ice samples collected during the first campaign (January-February, 2014) varied from 4 to 14 and -4.0‰ to -1.0‰ (Figure 4.5a). The $\delta^{18}O$ values of the melted sea-ice samples from the final campaign (February-March, 2015), varied from ~ -3.5‰ to -0.5‰ (Figure 4.6). The individual vertical profiles of $\delta^{18}O$ in each ice core shown reflects the composition of the surface water from which the sea-ice grew. In the top 10-15 cm of each ice core the $\delta^{18}O$ value was suspect because of possible incorporation of snow during the freezing process. Snow at the latitude of the Belcher Islands has an extremely low $\delta^{18}O$ value (~ -25‰ at 54-56°N along Nelson River basin; Smith et al, 2015). Below this surface layer, the $\delta^{18}O$ values in the upper portion of the ice core are a reflection of surface waters in the early portion of the sea-ice growth cycle (first freeze-up date December 10, 2014). Whereas the

ice toward the bottom of the core reflects surface water properties just before the collection date (last collection date March 14, 2015). Disregarding the first 10-15 cm of each ice core, the average $\delta^{18}O$ value present in the ice cores collected from the coastal domain was -1.9 ± 0.5‰, whereas ice cores from the interior domain had an average $\delta^{18}O$ value of -1.1 ± 0.3‰ (Figure 4.6). Ice cores collected from the coastal domain contained more negative $\delta^{18}O$, indicating that fresher waters were present in the surface water. Lack of consistency of the profiles indicates a spatial dependence of where the freshwater is present in the coastal domain. The $\delta^{18}O$ profiles of the ice cores from the interior domain were less negative, overlapped one another, and showed little fluctuation in the presence of fresher waters in the domain.

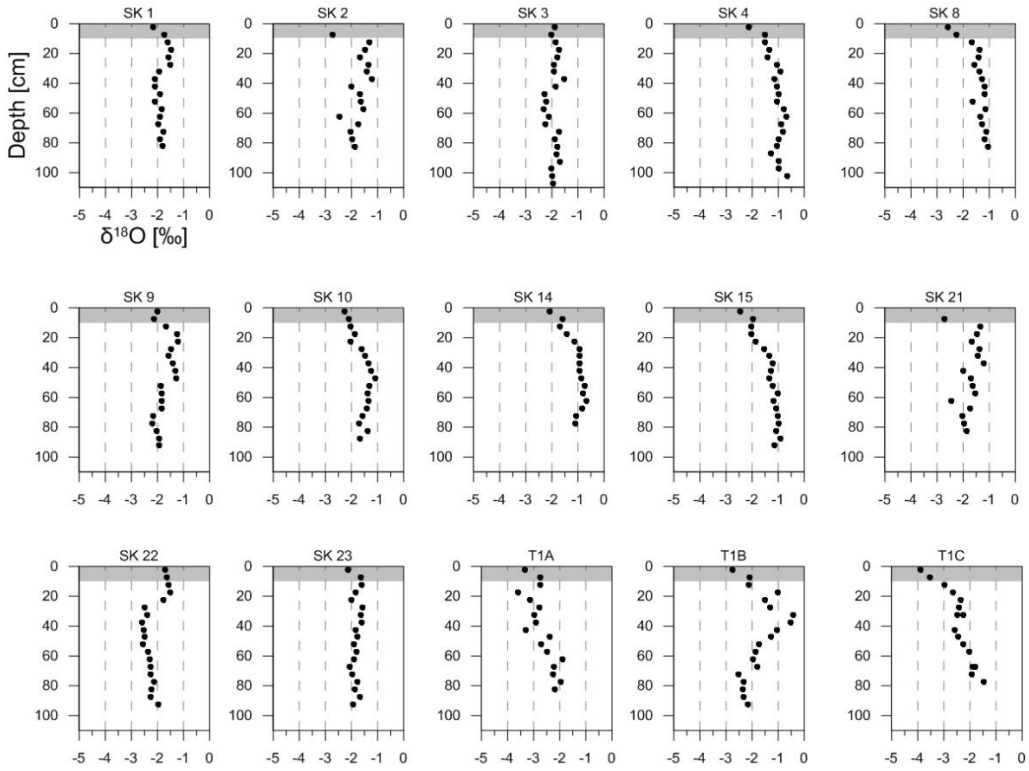

Figure 4.6. Individual vertical profiles of $\delta^{18}O$ in ice cores that were collected during the 2015 winter field season shown in the sectional view (see map Figure 4.3). Increasing depth in the ice reflects ice accumulated later in the year such that change in ice composition with depth reflects change over time in the composition of surface water from which the ice was grown. The top of the core (0 cm) represents the start of ice formation at the site; the bottom of the core reflects the last few days up until the ice core was collected. Low $\delta^{18}O$ values in the top ~10cm are likely due to contamination by snow and have been excluded from the figure

Chapter 5. Discussion

The distribution of salinity as measured in winter, 2015, in sections circumscribing the Belchers (Figure 4.3 a, c) shows stronger stratification to the east of the islands (Hudson Bay coastal domain) than in the west (interior domain). Furthermore, the fresh water in the coastal domain is organized as a lobe of fresh water apparently constrained by the SE coast of the Belchers. This lobe is sharply defined in January, but appears to have expanded in area and depth by late February. The 20 km section out from the coast, collected in February, 2015, (Figure 4.4 a,b; inset Figure 4.3) shows that the freshwater at the SE corner of the Belchers extends well into the strait between the Belcher Islands and the mainland to the southeast. Beneath this freshwater lens in the coastal domain, the water is noticeably warmer and well above its freezing point, especially in late February-March, 2015 (Figure 4.3 b,d; Figure 4.4). The warming that has occurred between the sections measured in January and late February, 2015, sections can only have occurred through advection of warm sea water, which has been protected from cooling by the strong surface stratification. In the interior ocean, where stratification is weaker, we see evidence of widespread cooling, especially in the northern stations, during the same time period. Broadly speaking, the separation between fresher, well-stratified water to the east of the Belchers and more saline, less-stratified water to the west of Belchers makes sense because the Belchers lie at the outer boundary of the coastal current (Figure 2.5), which transports most of the runoff around the margin of Hudson Bay and out into Hudson Strait. The distinction in freshness, stratification and temperature between waters in the coastal corridor and waters in the interior of Hudson Bay previously observed during summer is maintained through winter (St-Laurent et al. 2011). Although the CTD data give a definitive image of freshwater content and distribution along the sections, and its effect on heat distribution in the late-winter water column, the data do not explain the roles played by sea ice

formation/melting and runoff in producing the distributions. The distinction between the two processes is crucial if wanting to understand how sea ice and runoff interact in this region and how these two sources of freshwater manipulation might affect the maintenance of the many polynyas that form around the Belcher Islands during winter.

The spread in salinity and $\delta^{18}O$ measured in the water samples (Figure 4.5) shows that both sea-ice melt (SIM) and river water (RW) are important additions to sea water (SW) in the water column. At bottom left of Figure 4.5a, river water, which has been distilled through atmospheric processes, exhibits low $\delta^{18}O$ values ranging from -10‰ to -20‰. At top right, the oval cluster of points comprises the data for water samples collected around the Belchers during our study and prior to it. Broadly speaking, these data cluster around a major axis of variance (the line in Figure 4.5), which is produced by mixing saline, isotopically heavy ocean water with isotopically light RW. As found in numerous other studies where sea ice is a seasonal feature, there is large component of variance *across* this line. This second source of variance is produced by the formation of sea-ice in winter, which expels brine into the water to drive data points downward with points below the line showing an excess of brine. In summer, melting sea ice (SIM) adds water of low salinity and relatively high $\delta^{18}O$, as shown by the composition of sea ice (cluster of points at the top left in Figure 4.5a). The addition of SIM drives points upward: points above the line contain SIM, points below the line contain brine.

A crucial step to calculate freshwater components is the assignment of end-member properties ($\delta^{18}O$, S) for the three water-mass components that make up surface water (RW, SIM, SW). Geographic settings vary widely in water masses and sources and, therefore, so do the end-member values chosen for various studies. Taking into consideration the data set collected

in this study, including river, sea-ice and water samples, and previous water-column sampling in Hudson Bay (e.g. Granskog et al. 2009, 2011), we have chosen the values listed in Table 5.1.

Table 5.1. Specified end-members for southeast Hudson Bay provide reference for identifying the parcels of water that are present in the local system

Local end-members for SEHB		
	Salinity	$\delta^{18}O$ (‰)
Runoff (RW)	0.1 ± 0.1	-13.2 ± 1.3
Sea-ice melt (SIM)	6.1 ± 1.4	-0.7 ± 0.1
Seawater (SW)	32.2 ± 0.1	-2.7 ± 0.1
Fractionation		2.0

For the RW endmember, we used the flow-weighted average $\delta^{18}O$ for measurements available for rivers upstream (to the west and north) of the Belcher Islands (Table 4.1). Net precipitation (P-E) also may add (or subtract) distilled (isotopically light) freshwater to the sea surface. For the southern Hudson Bay region, precipitation has been measured or estimated at -12‰ to -15‰ (Gibson et al. 2005; Delavau et al. 2011). In view of the likely small and uncertain contribution of P-E relative to the riverine yield for Hudson Bay (~80cm; Prinsenberg 1977) and its similarity in isotopic composition to RW, we will henceforth consider RW to include both meteoric sources, the bulk of which will be river runoff. An uncertainty of ±1.3‰ (SD) assigned to the end-member value in Table 5.1 includes variation associated with $\delta^{18}O$ in river water and in the mean flows of the rivers. Small and unregulated rivers have an inherently larger uncertainty because of pronounced seasonal variability in $\delta^{18}O$ (cf., Kuzyk et al. 2008), but individually they contribute less to the total inflow. Large regulated river systems with lakes and reservoirs such as the Nelson River have a consistent flow rate with a relatively small standard deviation (~6%). For the Nelson River, seasonal variability in $\delta^{18}O$ value is also low. Based on a

large dataset (n=344) obtained from upstream sites on the Nelson River, Smith et al. (2015) estimated the coefficient of variation as ± 4% of the average $\delta^{18}O$ value (-10.64‰).

The sea water end member (SW) is based on the S-$\delta^{18}O$ data collected in this study together with data collected during AN 2005-2010 cruises (Granskog et al., 2011; unpublished) at stations closest to those in the study region. The values of 32.2 ± 0.1 and -2.7±0.1‰ lie to the right of our data set (Figure 4.5a) and on the apparent mixing line from the AN Cruises.

For the sea-ice end member (SIM), we use a $\delta^{18}O$ value (-0.7‰) consistent with the SW end member. When sea ice forms from seawater, there is a fractionation of 2‰-3‰ such that sea ice is isotopically heavier (Macdonald et al. 2002; Eicken et al. 1998; Crabeck et al. 2014). For the Belcher Island data set, tandem measurements of ice and seawater below the ice imply an average fractionation of 2‰ ± 0.5‰, which falls within the range of 2-2.2‰ estimated by Kuzyk et al. (2011) and Granskog et al. (2011) for other locations in Hudson Bay. Salt is not conservative in sea ice, and tends to vary over time and with depth in ice cores (e.g., Leppäranta 1993**)**. Based on the ice cores collected in February-March, 2015, we use an average salt content of 6.1 ± 1.4.

5.1 Distributions of river water in winter, 2015

The partitioning of the water samples into the RW and SIM components provides evidence that the bulk of freshwater observed in January to March, 2015, at the SE corner of the Belchers was, indeed, due predominantly to runoff (Figure 5.1 a,b). As suggested by the salinity section (Figure 4.3), the runoff was constrained mostly to the coastal domain and predominantly within the lobe (plume) abutting the SE shore of the Belchers. This RW plume widened and deepened between January and late February. The inventories of RW in the top 20 m, shown as bars across the top of the sections (and see Table 5.2), indicate that in January there was a

relatively small inventory of RW in the interior surface water (~0.5 m), compared to the >2 m found in the lobe.

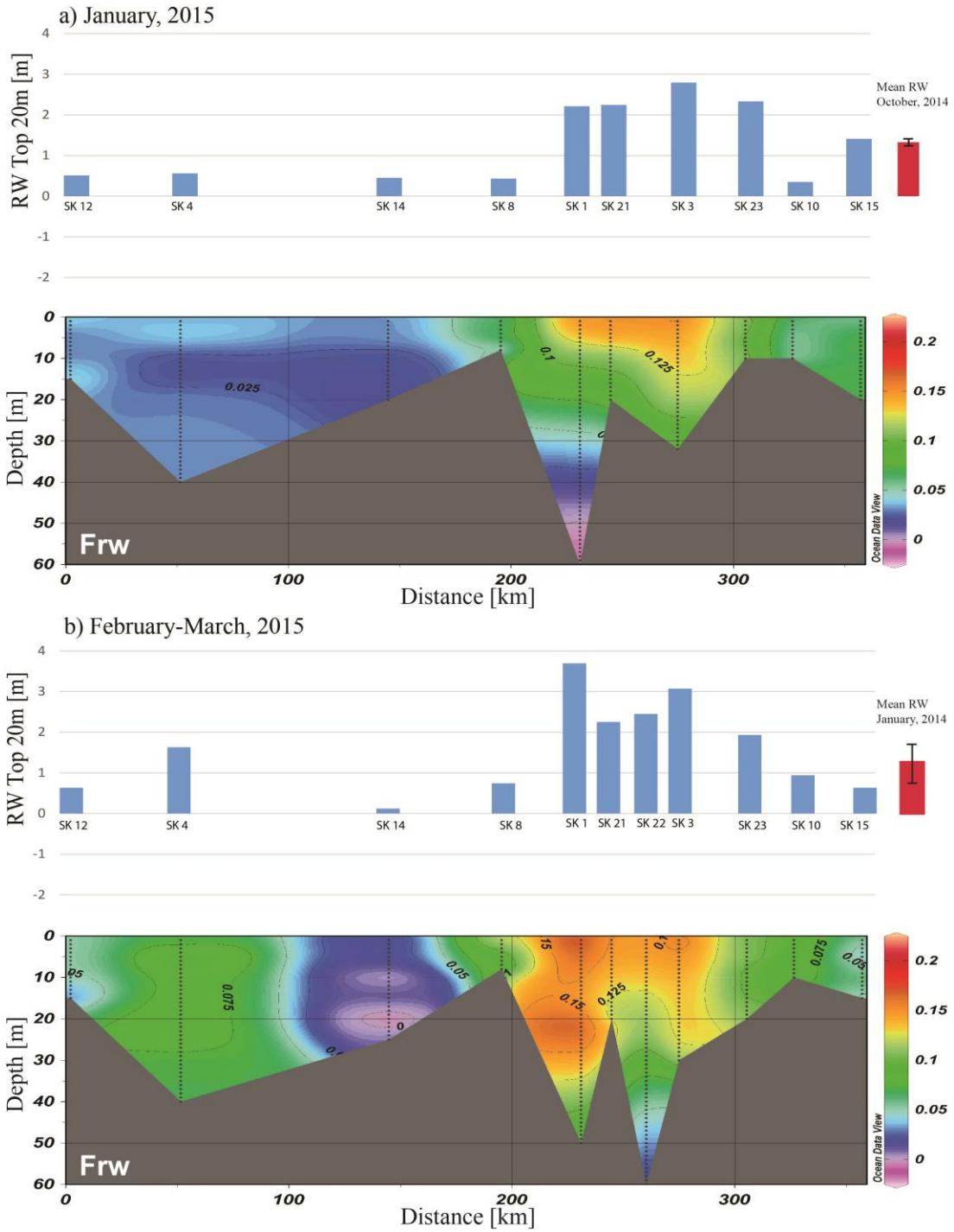

Figure 5.1. Fraction of river water (Frw) present in the water column along the section view (see map Figure 4.3) of the study region in January, 2015 (a) and February-March, 2015 (b). Above the sections, bars show the RW inventory in the top 20 m of the water column, including the mean RW present in the top 20 m in October, 2014 (a) and January, 2015 (b)

Table 5.2. Inventories of RW and SIM in the top 20m of the water column

		Top 20m of Water Column							
		January-February, 2014		October, 2014		January, 2015		February-March, 2015	
Stations	Depth [m]	RW	SIM	RW	SIM	RW	SIM	RW	SIM
Coastal Domain									
SK 1*	57	3.9	-0.91	1.35	1.71	2.21	1.51	3.69	-0.79
SK 21*	22	-	-	-	-	2.24	0.73	2.25	0.75
SK 22*	>80	-	-	-	-	-	-	2.45	0.73
SK 3*	48	2.85	-0.15	1.22	1.67	2.79	0.8	3.07	-0.21
SK 23*	30	-	-	-	-	2.33	0.33	1.93	1.07
SK 10*	13	2.78	-0.79	1.36	1.67	0.35	0.78	0.94	0.33
SK 15*	19	-	-	-	-	1.41	0.78	0.63	1.16
SK 2	>80	3.07	-0.47	-	-	1.52	1.24	2.81	-0.09
SK 9	>80	-	-	1.46	2.15	1.38	1.72	1.79	1.04
T1C	>80	-	-	-	-	-	-	2.3	1.19
T1B	>80	-	-	-	-	-	-	2.72	0.68
T1A	54	-	-	-	-	-	-	2.14	1.4
Interior Domain									
SK 12*	28	-	-	-	-	0.51	1.33	0.63	0.86
SK 4*	42	3.07	-1.07	-	-	0.56	1.71	1.63	0.23
SK 14*	25	1.95	-0.76	-	-	0.45	1.6	0.12	1.71
SK 8*	8	1.86	-0.74	-	-	0.43	0.53	0.74	0.23
Coastal		3.18	-0.62	1.35	1.8	1.80	0.92	2.14	0.43
(SD)		(0.6)	(0.4)	(0.1)	(0.2)	(1)	(0.3)	(1.1)	(0.7)
Interior		2.29	-0.86	-	-	0.49	1.29	0.78	0.76
(SD)		(0.7)	(0.2)			(0.1)	(0.5)	(0.6)	(0.7)
P-value		>0.05	>0.05	-	-	0.02	>0.05	0.01	>0.05

By late February, the RW inventory had generally increased in the lobe within the coastal domain, but had also built up in the interior domain at SK 4, where >1 m of RW was added to the top 20m after January. The addition of RW at SK 4 clearly extends deeply into the water column (Figure 5.1b), with the total RW inventory increasing by over 4 m (Table 5.3). These inventories underscore the far stronger stratification due to RW in the coastal domain compared to the interior domain, but also show that RW may transport into the interior episodically during

winter. Interestingly, the sparser data set collected in January to February, 2014, indicates that there was more RW in the interior domain in winter, 2014 than in winter, 2015, but the inventories were generally less than those in the coastal domain. The inventories of RW for the entire water column, which varied in depth among stations (Table 5.3), shows over +7 m storage within the lobe (SK 1, SK 2).

Table 5.3. Inventories of RW and SIM in the entire water column

		Total Water Column							
		January-February, 2014		October, 2014		January, 2015		February-March, 2015	
Stations	Depth [m]	RW	SIM	RW	SIM	RW	SIM	RW	SIM
Coastal Domain									
SK 1*	57	9.74	-3.06	2.99	5.40	3.02	5.76	7.75	-1.58
SK 21*	22	-	-	-	-	2.24	0.73	2.25	0.75
SK 22*	>80	-	-	-	-	-	-	4.35	3.22
SK 3*	48	3.71	0.41	1.66	2.72	3.92	1.38	4.50	-0.31
SK 23*	30	-	-	-	-	1.17	0.18	1.93	1.07
SK 10*	13	3.67	-0.96	1.90	2.27	0.35	0.78	0.94	0.33
SK 15*	19	-	-	-	-	1.41	0.78	0.63	1.16
SK 2	>80	7.56	-0.85	-	-	3.72	3.70	6.97	0.26
SK 9	>80	-	-	2.91	6.52	2.45	5.28	3.50	3.64
T1C	>80	-	-	-	-	-	-	3.59	4.67
T1B	>80	-	-	-	-	-	-	4.77	3.16
T1A	54	-	-	-	-	-	-	3.60	3.96
Interior Domain									
SK 12*	28	-	-	-	-	0.51	1.33	0.63	0.86
SK 4*	42	7.38	-3.62	-	-	1.12	3.33	3.10	0.42
SK 14*	8	1.86	-0.74	-	-	0.43	0.53	0.74	0.27
SK 8*	25	5.48	-2.06	-	-	0.45	1.60	0.13	1.23
Coastal		5.71	-1.2	2.18	3.46	2.21	1.63	3.19	0.66
(SD)		(3.5)	(1.8)	(0.7)	(1.7)	(1.2)	(2.1)	(2.5)	(1.5)
Interior		4.91	-2.14	-	-	0.63	1.70	1.15	0.70
(SD)		(2.8)	(1.4)			(0.3)	(1.2)	(1.3)	(0.4)
P-value		>0.05	>0.05	-	-	0.03	>0.05	0.04	>0.05

The appearance and increase through winter of the RW component, especially within the coastal domain, runs counter to the normal winter hydrographs for undeveloped rivers in Hudson

Bay. Rivers exhibit their lowest flows in winter with declining flows continuing from December through to April (Dery et al. 2005) and many small rivers freeze entirely. The temperature records during winter, 2015 (see Figure 3.4), indicate no periods of thaw that could have produced melt water in the small rivers at that time. Thus, counter to what would be expected for a system in which greatest river inflows occur during spring freshet (May-June), the amount of RW around the Belcher Islands increased from fall through to late winter with the most dramatic increase in the coastal domain.

5.2 Distributions of SIM in winter, 2015

In the coastal domain in October, 2014, the average SIM inventory in the top 20 m for all stations was +1.80 m (Table 5.2). This large inventory derives from the sea ice that has melted through summer and, given the smaller thickness of sea ice produced locally in winter (< 1 m), likely reflects excess SIM due to sea ice and SIM transported by winds into the region from the north. In January, 2015, the top 20 m of the water column contained an average +0.99 m SIM (Figure 5.2a; Table 5.2), which indicates a loss of ~0.81 m of SIM inventory. This change would be equivalent to the brine released by the formation of ~0.89 m of sea-ice (correcting for the density of ice). Given that the average observed ice thickness during the January sampling period was 0.5±0.11 m (Appendix A), and deducting the 10% RW in the ice implied by $\delta^{18}O$ values (Table 5.4), the 0.45 m of sea ice produced locally after October can explain only about half of the brine that has been added to the top 20 m of the water column during this time period (Figure 5.2a).

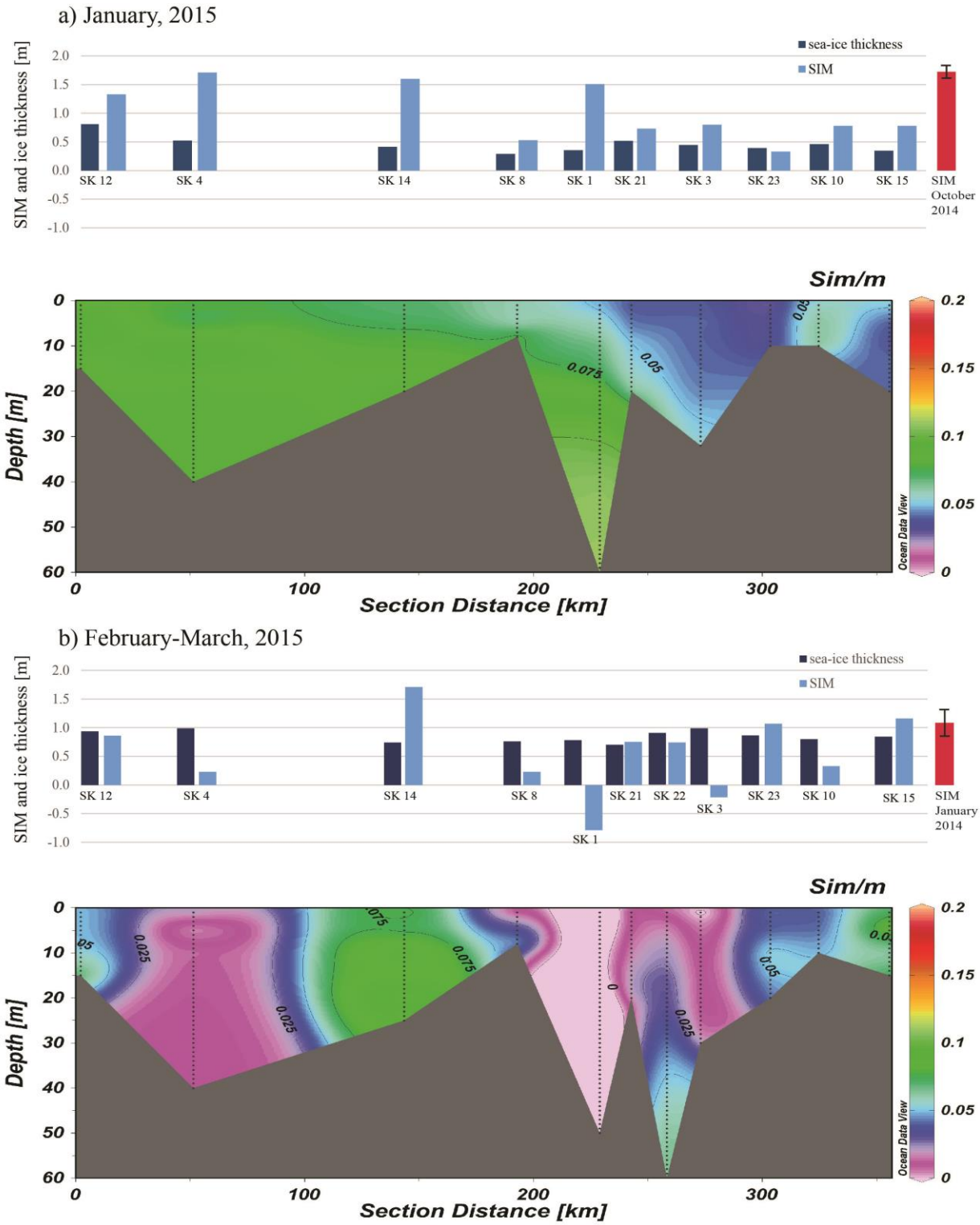

Figure 5.2. Fraction of sea-ice melt (Fsim) present in the water column along the sectional view (see map Figure 4.3) of the study area in January, 2015 (a) and February-March, 2015 (b), including sea-ice thicknesses [cm]. Above the sections, bars show the SIM inventories in the top 20 m of the water column, including the mean SIM present in the top 20 m in October, 2014 (a) and January, 2015 (b). Note that negative SIM inventories imply net brine

Table 5.4. mean applies salinity, MW [%] of surface waters and expected brine [m]

Station	Mean Implied Surface water Salinity (SD)	Mean Implied MW [%] in surface water (SD)	Expected brine[2] [m]
2015 Coastal Domain			
SK 1	28.7 (0.7)	10.9 (2.0)	0.70
SK 21	28.4 (1.2)	11.7 (3.8)	0.61
SK 3	28.4 (0.6)	11.7 (1.9)	0.85
SK 23	28.5 (0.5)	10.7 (1.6)	0.77
SK 2	28.9 (1.3)	10.1 (3.9)	0.72
SK 9	29.0 (1.0)	9.8 (3.1)	0.79
SK 22	27.7 (1.1)	13.9 (3.4)	0.74
T1C	26.9 (1.9)	16.5 (5.9)	0.60
T1B	29.0 (2.0)	10 (6.3)	0.89
T1A	26.2 (1.5)	18.5 (4.6)	0.65
SK 10	29.4 (1.0)	8.6 (3.2)	0.74
SK 15	30.0 (1.4)	6.7 (4.3)	0.81
2015 Interior Domain			
SK 4	31.1 (1.0)	3.9 (3.2)	0.96
SK 8	29.9 (1.3)	7.1 (4.0)	0.69
SK 14	30.9 (1.2)	3.9 (3.7)	0.72
Coastal Domain (CD)	28.4 (1.1)	11.6 (3.3)	0.7
Interior Domain (Int)	30.6 (0.6)	5.0 (1.8)	0.8
Overall Average	28.9 (1.3)	10.3 (4.1)	
p value: CD vs Int Anova test	0.01	0.01	
2014 Coastal Domain			
SK 1	30.0 (0.6)	6.7 (2.0)	0.44
SK 3	27.2 (1.2)	14.7 (3.7)	0.18
SK 2	28.2 (1.1)	12.5 (3.5)	0.38
SK 9	29.6 (0.7)	8.0 (2.3)	0.68
SK 10	29.1 (1.3)	9.6 (4.1)	0.57
2014 Interior Domain			
SK 8	27.9 (1.3)	13.3 (4.0)	0.45
SK 14	29.9 (1.0)	7.2 (3.0)	0.65
Coastal Domain	28.8 (1.1)	10.3 (3.3)	
Interior Domain	28.9 (1.1)	10.3 (4.3)	
Mean	28.8 (1.1)	10.3 (3.2)	
p value	>0.05	>0.05	

[1]Ice thickness in January, 2015 (Table 1), snow thickness was on average <4.5 cm
[2]Expected brine addition from ice (ice thickness(m) - (MW%) * ice thickness)

In the coastal domain between January, 2015, and March, 2015, the average amount of SIM in the top 20m further decreased by +0.61 m (Figure 5.2b; Table 5.2). Compared to October, 2014, inventory (+1.80 m), the March SIM inventory reflects the loss of 1.19 m of SIM through the winter. This loss would be equivalent to brine released by the formation of 1.32 m of sea-ice. Within the coastal domain, the average thickness of ice in March was 0.93± 0.09 m (Table 3.2). Correcting again for the RW content of the cores (Table 3.2), the average sea ice accumulation between October, 2014, and March, 2015, ~ 0.85 m, is not sufficient to explain the 1.19 m of SIM removed from the water. The discrepancy is even greater if we consider the SIM inventories in the total water column (Table 5.3). These data imply that, like RW, brine must also have been imported into the coastal domain around the Belchers during the winter of 2014-2015.

In the interior domain in January, 2015, the top 20 m of the water column contained on average +1.29 ± 0.5 m SIM (Fig. 5.2a, Table 5.1). By February-March, 2015 (Fig. 5.2b), the SIM inventory had decreased to +0.76 m, implying the removal of 0.53 m SIM. In January the ice thickness was 0.52 ± 0.23 m (Appendix A) and in March 0.87±0.14 m (Table 3.2), which is an average addition of 0.35 ± 0.27 m of sea ice. Applying a RW correction of 5% for ice growth in the interior domain (Table 3.2) yields ~ 0.33 m of sea-ice produced between January, 2015, and March, 2015. Although the amount of sea ice grown is about the same in both coastal and interior domains over this period of time, we have no data for water column SIM in October for the interior domain and therefore cannot compare ice growth water inventories. Nevertheless the sea-ice grown in the interior domain after January is, once again, not sufficient to fully account for the loss of SIM inventory in the water column.

Comparing SIM in the two domains, we find similar inventories (not statistically different) in both January, 2015, and February-March, 2015, but there is a fair amount of variation between stations with, for example, SK 14 holding 1.71 m of SIM inventory compared to SK 23 with 0.33 m of inventory in January (Fig. 5.2a,b; Table 5.1). This variability could be explained either by imported brine or by locally produced brine in the network of polynyas. Unlike the RW inventories, the SIM inventories do not show a statistically significant difference between the coastal and interior domains. However, it is worth noting that the stations with the low SIM inventories tend to be associated with the stations with high RW inventories (e.g., SK 1, SK 21, SK 22, SK 3).

In the coastal domain in February-March, 2015, are found some of the lowest SIM inventories, which indicates that these stations have accumulated brine between January and February-March. For this region, there has been an average loss of 0.5 m of SIM in the top 20 m of the water column between January and February-March, which is substantially greater than expected from the modest ice growth that occurred during this period (Table 5.4).

Along the offshore transect orthogonal to the coast of the Belcher Islands, distributions of RW and SIM were similar to those described above for the coastal domain during the same period (Feb-March, 2015). The fractional contribution of RW (Frw) exceeded 0.125 in surface waters along the offshore transect and the amount of RW present in the top 20m of the water column was consistently > 2.0 m. The fraction of SIM was very low (0.01-0.04), yielding inventories in the top 20 m of the water column of 0.7-1.4 m. Thus, the coastal domain waters are similarly rich in RW and brine within ~20 km of the southeast tip of the Belcher Islands.

5.3 The relation between river water and sea ice melt

The change in RW inventories at all stations between January, 2015, and March, 2015, are negatively correlated with the change in SIM inventories (R^2=0.88, p<0.001; n=10; Figure 5.3). This unanticipated relationship holds true for the top 20m inventories and for total-water column inventories but is stronger for the former. The direct implication of the correlation is that the RW imported into the region around the Belcher Islands during winter carries brine (negative SIM) with it, which would explain why the brine added to the water column during winter considerably exceeded the capacity of local ice formation to produce brine. Furthermore, the relationship between RW inventory and brine is not statistically different than 1:1 (Figure 5.3).

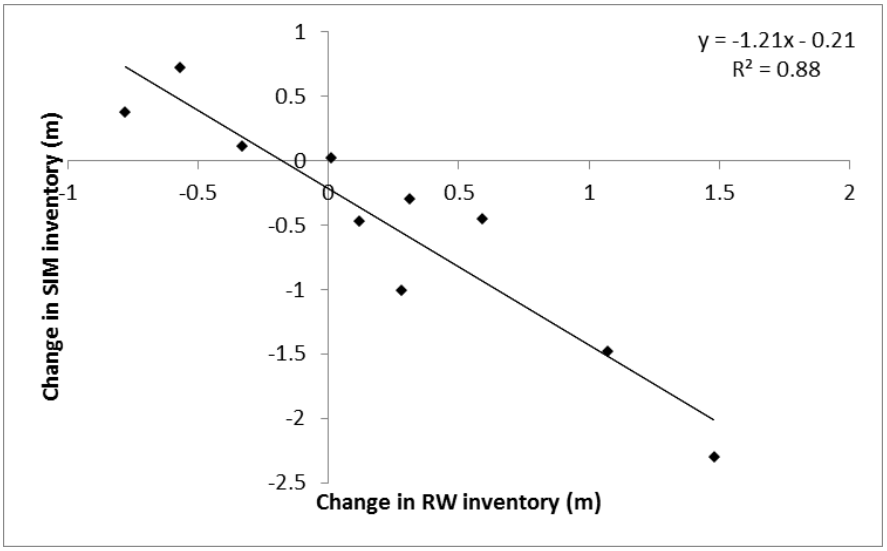

Figure 5.3. Change in the sea-ice melt (SIM) inventory compared to change in the river water (RW) inventory present in the top 20 m of the study area's water column (from January to February-March, 2015)

We infer from this that the inventory of RW in the surface water sets a limit to the capacity to hold brine. Once the brine component becomes equivalent to the RW component, further addition of brine will tend to mix and deepen the surface layer. As long as there is additional RW contributing to stratification beneath the mixed layer, the mixing process will continue to deepen the surface layer. If the brine eventually exceeds the capacity of RW to

stratify the surface layer, the water can then convect more deeply; thus, the 1:1 ratio sets a limit for brine transport within a river plume spreading in water where sea ice is forming.

5.4 The $\delta^{18}O$ record in the landfast ice

As shown by Macdonald et al. (1991; 1995), the landfast ice in a coastal zone may accumulate a record of the surface-water $\delta^{18}O$ properties as the ice thickens, but with an approximately +2‰ offset due to isotopic fractionation during freezing. A time frame can be approximated for landfast ice using a model for growth rate, and by knowing the start and end dates for the ice accumulation (see Methods for details). Using the same transect as previously (inset, Figure 4.3), the ice core record for the stations, corrected for fractionation and transformed to time, shows the evolution of $\delta^{18}O$ content in water just beneath the ice for the period from mid-December, 2014, to mid-March, 2015 (Figure 5.4).

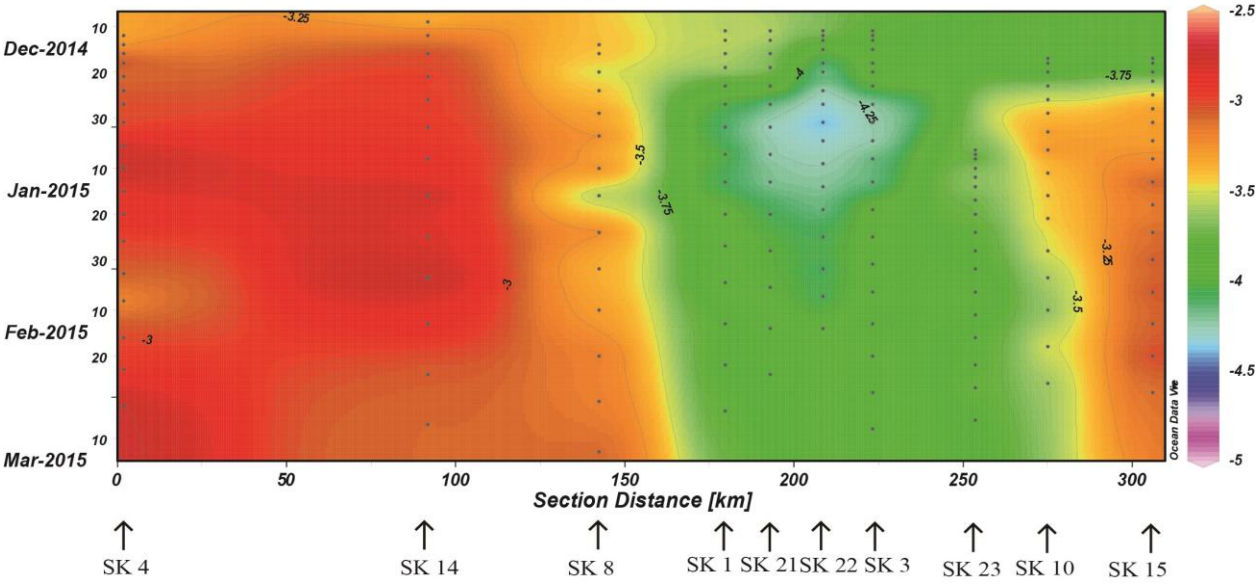

Fig 5.4. $\delta^{18}O$ record in the sea ice along the sectional view of the study area (see map in Figure 4.3), plotted as a function of time beginning at first freeze-up date (December 10, 2014) and ending last day of sample collection (March 14, 2015)

In contrast to the interior zone, the coastal-zone record is dominated by the invasion of isotopically light water, centered at stations SK-1, -21, -22 and -3. This invasion commenced

early in winter (~late December, 2014), two to three weeks before the water column observations revealed this plume in January, 2015 (compare with Figure 5.1a). According to the landfast ice record, this isotopically light water remained at the surface throughout the rest of winter at these stations, again agreeing with the observations in late February and March, 2015. According to the ice record, the isotopically lightest water (i.e., containing the greatest component of RW) occurred at SK 22 in late December to early January: the $\delta^{18}O$ estimated for surface water from the ice data (~ -4.25‰) implies an F_{rw} of ~ 0.15, in agreement with the water-mass distributions displayed in Figure 5.1.

5.5 The source of fresh water to the Belcher Island coast in winter

The data displayed in Figures 4.3 and 4.4 demonstrate that the Belcher Islands straddle two oceanographic domains in winter. Surface waters in the interior domain are saline and well mixed compared to the fresher, strongly-stratified waters of the coastal domain. These two domains have previously been described for the summer (Prinsenberg 1986, Wang et al. 1994; Saucier et al. 2004; Granskog et al. 2011; St-Laurent et al. 2011) and can be viewed as the result of a coastally-constrained surface current that transports collected river inflow as it transits around the Hudson Bay margin, and an interior ocean that is less affected by river inflow. Both domains are affected by sea-ice formation and melting, and the region generally gains extra sea-ice melt through southward drift of sea ice during spring and summer. The winter data presented here show that the oceanographic domains observed in summer remain in place throughout winter at the Belcher Islands, even though this is a time of year when freshwater inputs are normally at their least: throughout winter sea ice growth is removing fresh water by sea-ice distillation, and normal Arctic river inputs are at their lowest because drainage basins are mostly frozen.

Our isotopic data show definitively that the distinction between the two domains in winter rests almost entirely upon river inputs (i.e. RW), which are far more evident in the coastal domain. What is surprising, however, is not only the dominating influence of river water in the Belcher Island coastal zone during winter, a time of year when Arctic river inflows are normally very low, but that river water inventories *increase* throughout winter as shown by two field campaigns and a set of landfast ice cores. This brings us to two questions; what is the origin of the RW in the winter of 2014-15, and is the invasion of RW throughout winter a normal occurrence or something new? Answering these questions is rendered difficult due to the lack of oceanographic data for this region in winter, especially considering the hydrological developments that have occurred over the past several decades in the Hudson Bay watershed. In James Bay, ~ 120 km to the south of the Belcher Islands, the James Bay Project (Phase I; 1971-1984) included the diversion of ~1700 m^3/s (54 km^3/yr) of runoff from neighboring watersheds into the La Grande watershed, which supplies 81 km^3/yr to James Bay (Table 4.1), and the shifting of summer inflow to winter. Farther upstream (>1000 km), the Churchill River Diversion (1972-1977) shifted water from the Churchill River to the Nelson River (combined annual inflow of 122 km^3/yr ; Table 4.1) and summer inflow to winter.

The nearest source of RW for the Belcher Islands is James Bay (Figure 2.5), which receives an annual inflow of 270 km^3/yr (~ 45% of the total Hudson Bay river inflow (Granskog et al., 2011). Relatively persistent northwesterly background flow advects the La Grande plume northward (Freeman et al. 1982; Peck 1976), and mean summer surface currents at Cape Jones measured in the late 1970s (pre-development) exceeded 0.15 m/s (Prinsenberg 1984). Granskog et al. (2009) estimated current speeds of ~ 0.1 to 0.2 m/s in the coastal current. These speeds imply a transit time from the La Grande Complex to the Belchers (~220 km) of just over two

weeks. The post-1970 diversion of river water into the La Grande Riviere and the shifting of a portion of the river inflow from summer to winter would provide an ample supply of RW in winter to James Bay. The salinity-$\delta^{18}O$ data collected in our study show that RW impinging on the Belchers in winter brings with it an approximately equivalent amount of brine (Figure 5.3). As shown by the satellite image in Figure 2.7, there was a corridor of flaw leads along the edge of land fast ice in 2015 that extended from the mouth of the La Grande Riviere to the mouth of James Bay and then to the Belchers. This flaw lead zone would provide the setting to produce sea ice rapidly and thereby add brine to the river plume as it transited along the coast and out into Hudson Bay. Thus, James Bay inflow could account for the coincident arrival in winter of RW and brine at the Belcher Islands and, therefore, account for both the increase in RW during winter and the excess of brine over the supply from local sea-ice growth.

An implication of our data is that the buoyancy supplied by RW in the winter of 2015 was more than sufficient to capture the brine and transport it at the surface with the result that flaw leads along the outer edge of the landfast ice were not capable of producing deeply convecting water. The consequence of the buoyancy of the plume is that despite brine enhancement in the flaw leads, sufficient stratification remained to trap heat below ~20 m water depth (Figure 4.3). Furthermore, these flaw leads would not be capable of producing dense enough water to contribute to basin-water renewal (e.g., see Granskog et al. 2011).

The Churchill and Nelson Rivers also supply RW in winter, but they are over 1000 km away, which would require transit times in the boundary current of ~ 3 months, making them less likely to be the major source of the RW plume seen along the SE coast of the Belchers in January-March, 2015.

Is the strong stratification by RW observed in 2015 exceptional with respect to historical conditions? We have been able to find only one winter oceanographic dataset relevant to the Belcher Islands. In February, 1977, Prinsenberg (Canadian Hydrographic Service/Canadian Centre for Inland Waters (Burlington) unpublished) collected CTD data at four stations at the SE corner of the Belcher Islands from which it is possible to calculate freshwater inventories and compare these with data collected in February, 2015 (Figure 5.5).

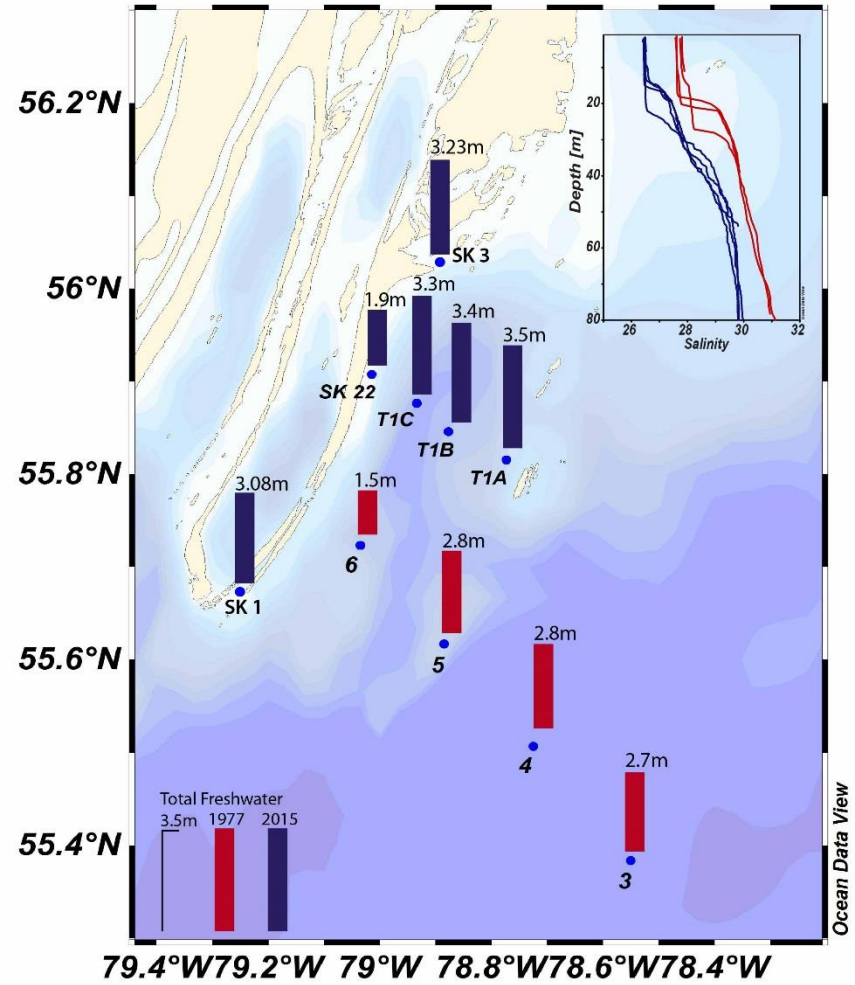

Figure 5.5. Comparison of total freshwater inventory in the top 20 m of the water column in the coastal domain between February, 1977 and February, 2015

Excluding the very shallow station from 1977, the average freshwater inventory for the top 20 m of the water column in February, 1977, was 2.8 ± 0.1 m compared to 3.4 ± 0.2 m in February, 2015. Similarly, the total water column inventories at stations of comparable depth were higher by ~ 0.5 m in 2015. While the higher freshwater inventory in 2015 is consistent with enhanced winter inflow from nearby and upstream rivers entering James Bay and Hudson Bay, the data do not provide definitive evidence of change partly because there is only the one historical year and partly because the CTD data do not permit discrimination between RW and SIM.

5.6 Implications for seasonal freshwater cycling in Hudson Bay

The seasonal evolution of freshwater distribution in the coastal domain described above presents a different view of freshwater cycling in SE coastal Hudson Bay than proposed by Granskog et al. (2011; their Fig 4.9). In their schematic, the brine produced in flaw leads and polynyas located at the outer boundary of landfast ice in Hudson Bay during winter (Figue 2.6) promotes convection through enhanced sea-ice formation and brine production, which contributes to a deeper mixed layer and, in extreme cases, could produce water dense enough to enter the basin. The emphasis in the Granskog et al. (2011) scheme was on the strength of the ice engine, while RW and residual SIM remaining from previous summer played a smaller role in maintaining the winter surface mixed layer (WSML). For the coastal domain of southeast Hudson Bay in winter, the results suggest that the local ice engine is relatively weak due to limited local sea-ice growth. The entire study area also has enhanced SIM inventory in late summer due the southward transport of sea-ice. The extensive flaw leads to the south of the Belcher Islands produce sea ice and brine, but the river water continually moving northward in

the coastal current prevents these polynyas from producing sufficient brine to mix the water deeply, or produce water that could sink into the basin.

The increased RW supply in the SE corner of Hudson Bay due to hydroelectric development after 1971 on James Bay Rivers, and possibly the Churchill/Nelson Rivers, would only enhance stratification. In 2015 the stratification was sufficient to trap heat below 20 m in the coastal zone (Figure 4.3c), but the data record is far too sparse to determine whether these circumstances are new, or whether this extra RW observed in the Belcher's coastal water is also causing winter stratification of the small polynyas within the Belcher System, permitting them to freeze.

In contrast to the coastal domain, the seasonal evolution of freshwater distribution in the interior domain complies with the Granskog et al. (2011) conceptual model. During our study, water in the interior domain became well-mixed to a depth of at least 40 m (the limit of our nearshore stations) and the SIM inventory of the water column progressively decreased through the winter, consistent with brine addition. Although there was significant freshwater present in the interior domain in winter, the major source was SIM remaining from the summertime, not RW. The results of this research have provided more detail to the structure of the winter water column within the coastal domain, off the shores of Hudson Bay (Figure 5.6).

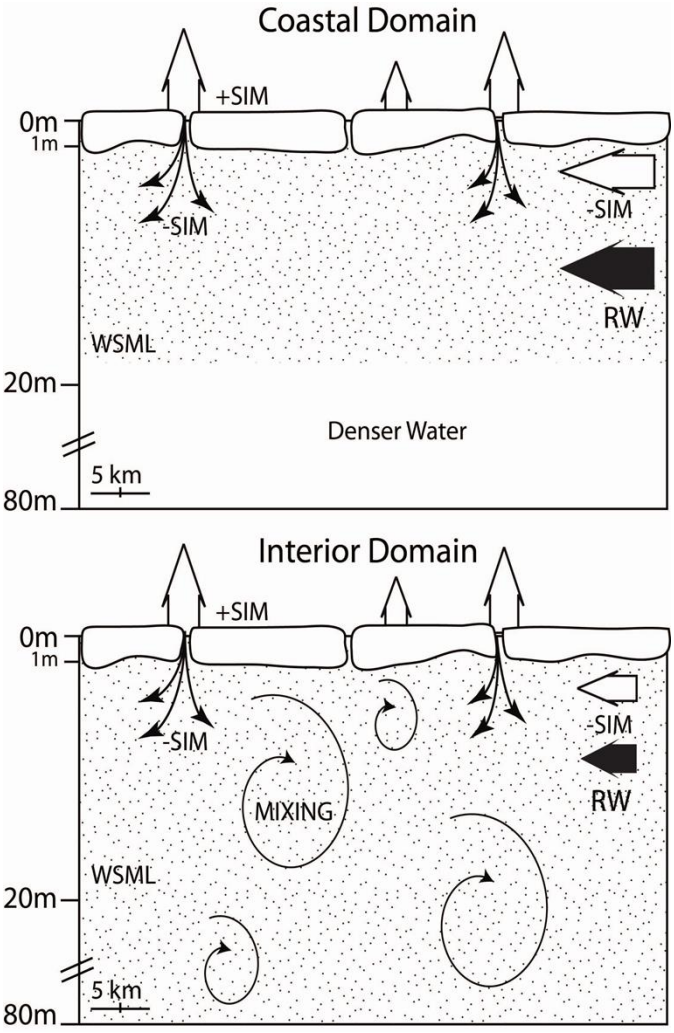

Figure 5.6. Schematic of freshwater cycling and water column structure present in the coastal domain and interior domain of study area during the winter season

The two years of winter data examined in this study (2014, 2015) indicate that inter-annual differences in RW and SIM in this region are substantial. Presumably some of the differences between years is due to fall conditioning (i.e., the SIM and RW balances at the start of winter), but there isn't the data to evaluate fall conditioning for the 2013-14 winter and hence we have focused our analysis here on the 2014-15 winter. Furthermore, river discharge data for the hydrologically-controlled rivers in James Bay are not publicly available to allow testing accurate assessment of the changes to winter inflow for this important region. The collective

evidence, however, is that the shift of runoff from summer to winter due to hydroelectric development has led to a significant positive temporal trend in winter river discharge to Hudson Bay between 1964 and 2008 (Dery et al. 2011).

Chapter 6. Conclusion

During the winter seasons of 2014 and 2015 (i.e. January-March) and in the intervening fall period (October, 2014), members of the Centre for Earth Observation Sciences (CEOS) from the University of Manitoba joined in collaboration with the Arctic Eider Society and community of Sanikiluaq to begin studying winter oceanographic conditions around the Belcher Islands. The original question posed by the community placed a focus on understanding the anomalies that caused the surrounding polynyas to rapidly freeze, and negatively affecting the local eider duck population. They wondered whether these anomalies were due to anthropogenic changes to northern Quebec river systems due to hydroelectric energy generation? Or were they due to climate variability or change causing inconsistent atmospheric temperatures and forcing unpredictable freezing of the surface waters manifest as change in when and how sea-ice forms? Or are the anomalies caused by a combination of these factors? Local hunters have commented that this anomaly hasn't recurred in the most recent winters, although the same hunters describe other observations of a continuously changing icescape. The hunters of Sanikiluaq heavily rely on the sea-ice as their hunting grounds. Their knowledge of the surrounding sea-ice has been passed down through many generations. In the last few decades in particular, the local hunters have expressed that the sea-ice has become increasingly difficult to navigate and is a danger in some circumstances due to unpredictable structural integrity. These men have commented that the timing of sea-ice formation has changed, affecting when and how the landfast sea-ice and sea-ice pack forms in the region.

Since there was little oceanographic data available for this region, especially related to the freshwater content and distribution during the winter, a baseline of the physical oceanography was a first step to investigating this anomaly. Thus, this thesis investigated the

freshwater content of the winter water column around the Belcher Islands, and the spatial and temporal variation of the surface water composition during the winter season. The objectives of this thesis research were to determine the freshwater content of the water column differentiating river runoff and sea-ice melt (brine), establish a freshwater inventory of the water column specific to the two freshwater types, describe the spatial variation in freshwater distribution around the Belcher Islands from early to late winter, and infer temporal changes of the surface waters using the composition of sea-ice. Based on the results, we were able to expand upon the currently accepted model of winter freshwater cycling and water mass evolution for the waters that surround the Belcher Islands.

It was concluded that two oceanic domains exist in the study region throughout the winter season. The coastal domain is continuously being inundated with river runoff that accumulates in the surface waters as the winter progresses from January to March, developing a lobe of freshwater particularly along the southeast corner of the Belcher Islands. The interior domain remains more saline, well mixed, and has less river runoff compared to the coastal domain. There is variability between seasons in the amount of river water, sea-ice melt, and brine, however the separation between the two domains remains present during the year (see Chapter 5, Table 5.2 and Table 5.3). The presence of freshwater in the coastal domain during the winter season is not a new phenomenon based on the previous observations (see Chapter 5). Keeping in mind that the CTD only provides total freshwater, the comparison between 1977 freshwater content and that of the present day showed an increased amount of freshwater present in the top 20 m of the water column during the winter seasons of 2014 and 2015 (See Chapter 5, Figure 5.5). One major drawback of this comparison is that it isn't possible to explain in detail why there was an increase in freshwater due to the lack of prior data appreciate to distinguish between river runoff

input and sea-ice melt. Since data collected before 1978 is considered the natural state of Hudson Bay (Messier 1986), the difference between the two snapshots in time is consistent with expectations for an altered river discharge regime in which winter discharges have been increased due to hydro-electric demand. The observed increase in river runoff in the study area from early to late winter is difficult to explain in the context of natural river discharge patterns that are minimal in winter and peak in spring. These results support previous findings that winter river plumes impinge on coastal waters on a larger scale than summer plumes (e.g. Ingram 1981; Ingram et al., 1996). Now knowing that river plumes move further offshore than anticipated, it is necessary to continue investigating the implications of this new finding and its relationship to the specifics of polynya and flaw lead behaviour in this area.

In order to fully understand whether the increased amount of river runoff into northeast James Bay and the seasonal shift of this discharge into winter has impacted regional freshwater dynamics in a way that affects sea-ice formation, an extensive time series is necessary to investigate the annual cycle of freshwater inventory (river water, sea-ice melt) in relation to ice-ocean properties in southeast Hudson Bay, and understand the causes of variability that occurs from year to year. To infer whether there is a link between specific regulated rivers and the river plumes present in southeast Hudson Bay during the winter, discharge data from Hydro companies would have to be examined in relation to the series of observations; additional tracers to identify specific river runoff contributions could also be employed; and modelling of the large James Bay plume under the sea-ice as it moves north along the southeast coast of Hudson Bay could be conducted. Specific to the Belcher Islands portion of the project, the geographical location is good for 1) sampling both the interior and coastal domain, 2) investigating the span (from shore) of the freshwater mass as it moves northward, and 3) assessing how changes in

freshwater content of the water column impact local sea-ice growth. Specific sampling stations that form a good basis for future study are SK 1, SK 3, SK 4, SK 14. Sampling locations in between the islands, while easier to assess, add additional complications in terms of looking at freshwater dynamics in the two regional domains.

Since the first winter field season in 2014, the project has expanded to include coastal studies near the communities of Inukjuaq, Umiujaq, Chisasibi and Kuujjuarapik, and sites distributed along the coastline of James Bay and southeast Hudson Bay. This expansion to the project will allow for further study of river runoff as it moves northward through Hudson Bay. Even though my thesis research project was not able to answer the question of why the polynyas froze differently during certain winters, there is now new information on the amount of freshwater present in the winter, the thickness of ice and how much brine it produces, the depth of the halocline and the different domains that are in the study region. This baseline data collection was a critical step. From this basis, an improved understanding of the ice-ocean interaction, and responsiveness to change may be developed through future work.

A project devoted to documenting the traditional knowledge of the changes to the frozen environment shared by community members, elders, and hunters, would be beneficial for providing historical context that hasn't been available through past oceanographic data. The book 'Voices of the Bay' does broadly describe the sea-ice changes that have been observed, however now is the time to add to the past documentation with more recent observations.

On a global scale, Arctic estuarine systems are important indicators of climate change. With the combination of the hydrological cycle (runoff) and sea-ice cycle, investigating changes to the freshwater budget of an estuarine system such as the Arctic Ocean estuary will not only

provide information on spatial and temporal distribution of river runoff and sea-ice melt, it provides an overall depiction of potential change to the terrestrial and atmospheric systems (i.e. more liquid freshwater available on land, and changes in sea-ice extent due to warmer temperatures). It has been proposed that Hudson Bay, a region of the Arctic Ocean estuary, is an important indicator for changes to come in the future in the high Arctic areas. Since several river systems that feed into Hudson Bay have altered discharge with increases in the winter, and because increases in winter discharge are projected for the entire Arctic, understanding the impacts of increased freshwater on winter processes is widely relevant. On a small scale, investigating change to the freshwater budget of an Arctic estuarine system in local regions such as the Belchers Islands, allows for larger scale budgets (i.e. Hudson Bay) to be tailored to reflect local processes that may alter the freshwater content of the water column. Investigating environmental changes to small scale regions, opens up the opportunity to answer more questions about the system we know today, and the local-scale ramifications of global scale climate variability and change.

References

Aagaard, K., & Carmack, E. C. (1989). The role of sea ice and other fresh water in the Arctic circulation. *Journal of Geophysical Research: Oceans, 94*(C10), 14485-14498. doi: 10.1029/JC094iC10p14485

Aagaard, K., & Carmack, E. C. (1994). The Arctic Ocean and Climate: A Perspective *The Polar Oceans and Their Role in Shaping the Global Environment* (pp. 5-20): American Geophysical Union.

Aagaard, K., Coachman, L. K., & Carmack, E. (1981). On the halocline of the Arctic Ocean. *Deep Sea Research Part A. Oceanographic Research Papers, 28*(6), 529-545. doi: https://doi.org/10.1016/0198-0149(81)90115-1

Alkire, M. B., Nilsen, F., Falck, E., Søreide, J., & Gabrielsen, T. M. (2015). Tracing sources of freshwater contributions to first-year sea ice in Svalbard fjords. *Continental Shelf Research, 101*(Supplement C), 85-97. doi: https://doi.org/10.1016/j.csr.2015.04.003

Alkire, M. B., & Trefry, J. H. (2006). Transport of spring floodwater from rivers under ice to the Alaskan Beaufort Sea. *Journal of Geophysical Research: Oceans, 111*(C12), n/a-n/a. doi: 10.1029/2005jc003446

AMAP. (2012). Arctic Climate Issues 2011: Changes in Arctic Snow, Water, Ice, and Permafrost. SWIPA 2011 Overview Report. Arctic and Assessment Programme (AMAP), Oslo. xi-97.

Anderson, J. T. (1961). Growth rate of sea-ice. *Journal of Glaciology*, 1170-1172.

Anderson, J. T., & Roff, J. C. (1980). Seston ecology of the surface waters of Hudson Bay, Can. *Fish. Aquat. Sci., 37*, 858-870. doi: 10.1139/f80-114

Andrews, J., Babb, D., & Barber, D. G. (2017). Climate change and sea ice: Shipping accessibility on the marine transportation corridor through Hudson Bay and Hudson Strait (1980–2014). *Elem Sci Anth*, 5-15. doi: http://doi.org/10.1525/elementa.130

Barber, D. G., & Massom, R. A. (2007). Chapter 1 The Role of Sea Ice in Arctic and Antarctic Polynyas. *Elsevier Oceanography Series, 74*, 1-54. doi: http://dx.doi.org/10.1016/S0422-9894(06)74001-6

Brown, R., Lemay, M., Allard, M., E Barrand, N., Barrette, C., Bégin, Y., Bell, T., Bernier, M., Bleau, S., Chaumont, D., Dibike, Y., Frigon, A., Leblanc, P., Paquin, D., Sharp, M., & Way, R. (2012). *Climate variability and change in the Canadian Eastern Subarctic IRIS region (Nunavik and Nunatsiavut)*. doi: 10.13140/RG.2.1.3745.0323

CARC. (1997). *Voices of the Bay; Traditional Ecological Knowledge of Inuit and Cree in the Hudson Bay Bioregion*. Ottawa, Ont.: Canadian Arctic Resources Comittee.

Carmack, E., Winsor, P., & Williams, W. (2015). The contiguous panarctic Riverine Coastal Domain: A unifying concept. *Progress in Oceanography, 139*(Supplement C), 13-23. doi: https://doi.org/10.1016/j.pocean.2015.07.014

Carmack, E. C. (2000). The Arctic Ocean's Freshwater Budget: Sources, Storage and Export. In E. L. Lewis, E. P. Jones, P. Lemke, T. D. Prowse & P. Wadhams (Eds.), *The Freshwater Budget of the Arctic Ocean* (pp. 91-126). Dordrecht: Springer Netherlands.

Carmack, E. C., Yamamoto-Kawai, M., Haine, T. W. N., Bacon, S., Bluhm, B. A., Lique, C., Melling, H., Polyakov, I. V., Straneo, F., Timmermans, M. L., & Williams, W. J. (2016). Freshwater and its role in the Arctic Marine System: Sources, disposition, storage, export, and physical and biogeochemical consequences in the Arctic and global oceans. *Journal of Geophysical Research: Biogeosciences, 121*(3), 675-717. doi: 10.1002/2015jg003140

Crabeck, O., Delille, B., Thomas, D., Geilfus, N., Rysgaard, S., & Tison, J. (2014). CO^2 and CH^4 in sea ice from a subarctic fjord. *Biogeosciences Discussions, 11*(3), 4047-4083.

Craig, H. (1961). Isotopic Variations in Meteoric Waters. *Science, 133*(3465), 1702-1703. doi: 10.1126/science.133.3465.1702

Defossez, M., Saucier, F. J., Myers, P. G., Caya, D., & Dumais, J. F. (2008). Multi-year observations of deep water renewal in Foxe Basin, Canada. *Atmosphere-Ocean, 46*(3), 377-390. doi: 10.3137/ao.460306

Defossez, M., Saucier, F. J., Myers, P. G., Caya, D., & Dumais, J. F. (2010). Analysis of a dense water pulse following mid-winter opening of polynyas in western Foxe Basin, Canada. *Dynamics of Atmospheres and Oceans, 49*(1), 54-74. doi: https://doi.org/10.1016/j.dynatmoce.2008.12.002

Delavau, C., Stadnyk, T., & Birks, S. (2011). *Model Based Spatial Distribution of Oxygen-18 Isotopes in Precipitation Across Canada* (Vol. 36). Canadian Water Resources.Journal, 36:4, 313-330, DOI: 10.4296/cwrj3604875

Déry, S. J., Mlynowski, T. J., Hernández-Henríquez, M. A., & Straneo, F. (2011). Interannual variability and interdecadal trends in Hudson Bay streamflow. *Journal of Marine Systems, 88*(3), 341-351. doi: http://dx.doi.org/10.1016/j.jmarsys.2010.12.002

Déry, S. J., & Wood, E. F. (2005). Decreasing river discharge in northern Canada. *Geophysical Research Letters, 32*(10), n/a-n/a. doi: 10.1029/2005gl022845

Deser, C., & Teng, H. (2008). Evolution of Arctic sea ice concentration trends and the role of atmospheric circulation forcing, 1979–2007. *Geophysical Research Letters, 35*(2), doi: 10.1029/2007gl032023

Dionne, J. C. (1980). An outline of the eastern James Bay coastal environments. In:S.B. McCann (ed.). *Geological Survey of Canada :* 331-338.

Dittmar, W. (1884). Report of researches into the composition of ocean water collected by HMS Challenger during the years 1873&76. Voyage of the H.M.S.Challenger. *Physics and chemistry, 1*.

Dmitrenko, I. A., Wegner, C., Kassens, H., Kirillov, S. A., Krumpen, T., Heinemann, G., Helbig, A., Schröder, D., Hölemann, J. A., & Klagge, T. (2010). Observations of supercooling and frazil ice formation in the Laptev Sea coastal polynya. *Journal of Geophysical Research: Oceans, 115*(C5).

Eicken, H. (2008). From the Microscopic, to the Macroscopic, to the Regional Scale: Growth, Microstructure and Properties of Sea Ice *Sea Ice* (pp. 22-81): Blackwell Science Ltd.

Eicken, H., Dmitrenko, I., Tyshko, K., Darovskikh, A., Dierking, W., Blahak, U., Groves, J., & Kassens, H. (2005). Zonation of the Laptev Sea landfast ice cover and its importance in a frozen estuary. *Global and Planetary Change, 48*(1), 55-83. doi: https://doi.org/10.1016/j.gloplacha.2004.12.005

Eicken, H., Weissenberger, J., Bussmann, I., Freitag, J., Schuster, W., Valero Delgado, F., Evers, K.-U., Jochmann, P., Krembs, C., Gradinger, R., Lindemann, F., Cottier, F., Hall, R., Wadhams, P., Reisemann, M., Kousa, H., Ikavalko, J., Leonard, G., Shen, H., & Smedsrud, L. (1998). *Ice-tank studies of physical and biological sea-ice processes*.

Ekwurzel, B., Schlosser, P., Mortlock, R. A., Fairbanks, R. G., & Swift, J. H. (2001). River runoff, sea ice meltwater, and Pacific water distribution and mean residence times in the Arctic Ocean. *Journal of Geophysical Research: Oceans, 106*(C5), 9075-9092. doi: 10.1029/1999jc000024

El-Sabh, M. I., & Koutitonsky, V. G. (1977). An Oceanographic Study of James Bay before the Completion of the La Grande Hydroelectric Complex. [Environmental impacts; Hydroelectric power; Ocean currents; Oceanography; Sea ice; Spatial distribution; Water resources; Hudson Bay; James Bay]. *1977, 30*(3), 18. doi: 10.14430/arctic2697

Environment Canada. (2017a). Canadian Ice Service Retrieved October-December, 2015, from http://ice-glaces.ec.gc.ca/.

Environment Canada. (2017b). Environment Canada weather forecast Retrieved January-March , 2015, from http://climate.weather.gc.ca/historical_data/.

Fisheries and Oceans Canada. (2017). Canadian Hydrographic Service/Canadian Centre for Inland Waters (Burlington) unpublished (oceanogrpahic) (Publication no. http://www.dfo-mpo.gc.ca/science/hydrography-hydrographie

Freeman, N. G., Roff, J. C., & Pett, R. J. (1982). Physical, chemical and biological features of river plumes under ice cover in James and Hudson Bays. *Nat. Can., 109*, 745-764.

Friedman, I., Redfield, A. C., Schoen, B., & Harris, J. (1964). The variation of the deuterium content of natural waters in the hydrologic cycle. *Reviews of Geophysics, 2*(1), 177-224. doi: 10.1029/RG002i001p00177

Gagnon, A. S., & Gough, W. A. (2005a). Trends in the dates of ice freeze-up and breakup over Hudson Bay, Canada. *Arctic, 58*(4), 370-382.

Galbraith, P. S., & Larouche, P. (2011). Reprint of "Sea-surface temperature in Hudson Bay and Hudson Strait in relation to air temperature and ice cover breakup, 1985–2009". *Journal of Marine Systems, 88*(3), 463-475. doi: https://doi.org/10.1016/j.jmarsys.2011.06.006

Gibson, J. J., Edwards, T. W. D., Birks, S. J., St Amour, N. A., Buhay, W. M., McEachern, P., Wolfe, B. B., & Peters, D. L. (2005). Progress in isotope tracer hydrology in Canada. *Hydrological Processes, 19*(1), 303-327. doi: 10.1002/hyp.5766

Gilchrist, H. G., & Robertson, G. J. (2000). Observations of Marine Birds and Mammals Wintering at Polynyas and Ice Edges in the Belcher Islands, Nunavut, Canada. *Arctic, 53*(1), 61-68.

Granskog, M. A., Kuzyk, Z. Z. A., Azetsu-Scott, K., & Macdonald, R. W. (2011). Distributions of runoff, sea-ice melt and brine using δ18O and salinity data — A new view on freshwater cycling in Hudson Bay. *Journal of Marine Systems, 88*(3), 362-374. doi: http://dx.doi.org/10.1016/j.jmarsys.2011.03.011

Granskog, M. A., Macdonald, R. W., Kuzyk, Z. Z. A., Senneville, S., Mundy, C.-J., Barber, D. G., Stern, G. A., & Saucier, F. (2009). Coastal conduit in southwestern Hudson Bay (Canada) in summer: Rapid transit of freshwater and significant loss of colored dissolved organic matter. *Journal of Geophysical Research: Oceans, 114*(C8), n/a-n/a. doi: 10.1029/2009jc005270

Granskog, M. A., Macdonald, R. W., Mundy, C. J., & Barber, D. G. (2007). Distribution, characteristics and potential impacts of chromophoric dissolved organic matter (CDOM) in Hudson Strait and Hudson Bay, Canada. *Continental Shelf Research, 27*(15), 2032-2050.

Hansen, B., Ketil, I., Rasmus, E. B., Jack, K., Åshild Ø, P., Leif, E. L., Stephen, J. C., Jan Otto, L., & Øystein, V. (2014). Warmer and wetter winters: characteristics and implications of an extreme weather event in the High Arctic. *Environmental Research Letters, 9*(11), 114021.

Heath, J., & Sanikiluaq, C. o. (2011). People of a Feather: A film about Survival in a Changing Canadian Arctic.

Hochheim, K. P., & Barber, D. G. (2010). Atmospheric forcing of sea ice in Hudson Bay during the fall period, 1980–2005. *Journal of Geophysical Research: Oceans, 115*(C5), doi: 10.1029/2009jc005334

Hochheim, K. P., & Barber, D. G. (2014). An Update on the Ice Climatology of the Hudson Bay System. *Arctic, Antarctic, and Alpine Research, 46*(1), 66-83. doi: 10.1657/1938-4246-46.1.66

Hochheim, K. P., Lukovich, J. V., & Barber, D. G. (2011). Atmospheric forcing of sea ice in Hudson Bay during the spring period, 1980–2005. *Journal of Marine Systems, 88*(3), 476-487. doi: http://dx.doi.org/10.1016/j.jmarsys.2011.05.003

Holmes, R. M., McClelland, J. W., Peterson, B. J., Tank, S. E., Bulygina, E., Eglinton, T. I., Gordeev, V. V., Gurtovaya, T. Y., Raymond, P. A., Repeta, D. J., Staples, R., Striegl, R. G., Zhulidov, A. V., & Zimov, S. A. (2011). Seasonal and Annual Fluxes of Nutrients and Organic Matter from Large Rivers to the Arctic Ocean and Surrounding Seas. [journal article]. *Estuaries and Coasts, 35*(2), 369-382. doi: 10.1007/s12237-011-9386-6

Ingram, R. G. (1981). Characteristics of the Great Whale River plume. *Journal of Geophysical Research: Oceans, 86*(C3), 2017-2023. doi: 10.1029/JC086iC03p02017

Ingram, R. G., & Larouche, P. (1987). Changes in the under-ice characteristics of La Grande Rivière plume due to discharge variations. *Atmosphere-Ocean, 25*(3), 242-250. doi: 10.1080/07055900.1987.9649273

Ingram, R. G., & Prinsenberg, S. (1998). Coastal Oceanography of Hudson Bay and surrounding eastern Canadian Arctic waters. *The Global Coastal Ocean, 11*(The Sea).

Ingram, R. G., Wang, J., Lin, C., Legendre, L., & Fortier, L. (1996). Impact of freshwater on a subarctic coastal ecosystem under seasonal sea ice (southeastern Hudson Bay, Canada). I. Interannual variability and predicted global warming influence on river plume dynamics and sea ice. *Journal of Marine Systems, 7*(2), 221-231. doi: https://doi.org/10.1016/0924-7963(95)00006-2

Johannessen, O. M., Bengtsson, L., Miles, M. W., Kuzmina, S. I., Semenov, V. A., Alekseev, G. V., Nagurnyi, A. P., Zakharov, V. F., Bobylev, L. P., Pettersson, L. H., Hasselmann, K., & Cattle, H. P. (2004). Arctic climate change: observed and modelled temperature and sea-ice variability. *Tellus A, 56*(4), 328-341. doi: 10.1111/j.1600-0870.2004.00060.x

Kuzyk, Z. A., Macdonald, R. W., Granskog, M. A., Scharien, R. K., Galley, R. J., Michel, C., Barber, D., & Stern, G. (2008). Sea ice, hydrological, and biological processes in the Churchill River estuary region, Hudson Bay. *Estuarine, Coastal and Shelf Science, 77*(3), 369-384. doi: https://doi.org/10.1016/j.ecss.2007.09.030

Kuzyk, Z. Z. A., Macdonald, R. W., Stern, G. A., & Gobeil, C. (2011). Inferences about the modern organic carbon cycle from diagenesis of redox-sensitive elements in Hudson Bay. *Journal of Marine Systems, 88*(3), 451-462.

Lammers, R. B., Shiklomanov, A. I., Vörösmarty, C. J., Fekete, B. M., & Peterson, B. J. (2001). Assessment of contemporary Arctic river runoff based on observational discharge records. *Journal of Geophysical Research: Atmospheres, 106*(D4), 3321-3334. doi: 10.1029/2000jd900444

Landy, J. C., Ehn, J. K., Babb, D. G., Thériault, N., & Barber, D. G. (2017). Sea ice thickness in the Eastern Canadian Arctic: Hudson Bay Complex & Baffin Bay. *Remote Sensing of Environment, 200*(Supplement C), 281-294. doi: https://doi.org/10.1016/j.rse.2017.08.019

Lapoussière, A., Michel, C., Gosselin, M., Poulin, M., Martin, J., & Tremblay, J.-É. (2013). Primary production and sinking export during fall in the Hudson Bay system, Canada. *Continental Shelf Research, 52*, 62-72. doi: https://doi.org/10.1016/j.csr.2012.10.013

Lawford, R. G. (1994). The hydroclimatology of north-flowing high latitude rivers, in P.Lemke, L. Anderson, R. Barry and V. Vuglinsky (eds.), ACSYS *Conference on the Dynamics of the Arctic climate System,* World Meteorological Organization , Goteborg, Sweden World 8-23.

Legendre, L., Robineau, B., Gosselin, M., Michel, C., Ingram, R. G., Fortier, L., Therriault, J. C., Demers, S., & Monti, D. (1996). Impact of freshwater on a subarctic coastal ecosystem under seasonal sea ice (southeastern Hudson Bay, Canada) II. Production and export of microalgae. *Journal of Marine Systems, 7*(2), 233-250. doi: https://doi.org/10.1016/0924-7963(95)00007-0

Leppäranta, M. (1993). A review of analytical models of sea-ice growth. *Atmosphere-Ocean, 31*(1), 123-138.

Macdonald, R. W. (2000). Arctic Estuaries and Ice: A Positive—Negative Estuarine Couple. In E. L. Lewis, E. P. Jones, P. Lemke, T. D. Prowse & P. Wadhams (Eds.), *The Freshwater Budget of the Arctic Ocean* (pp. 383-407). Dordrecht: Springer Netherlands.

Macdonald, R. W., & Carmack, E. C. (1991). The role of large-scale under-ice topography in separating estuary and ocean on an arctic shelf. *Atmosphere-Ocean, 29*(1), 37-53. doi: 10.1080/07055900.1991.9649391

Macdonald, R. W., Carmack, E. C., & Paton, D. W. (1999). Using the δ18O composition in landfast ice as a record of arctic estuarine processes. *Marine Chemistry, 65*(1), 3-24. doi: http://dx.doi.org/10.1016/S0304-4203(99)00007-9

Macdonald, R. W., & Kuzyk, Z. Z. A. (2011). The Hudson Bay system: A northern inland sea in transition. *Journal of Marine Systems, 88*(3), 337-340. doi: https://doi.org/10.1016/j.jmarsys.2011.06.003

Macdonald, R. W., McLaughlin, F. A., & Carmack, E. C. (2002). Fresh water and its sources during the SHEBA drift in the Canada Basin of the Arctic Ocean. *Deep Sea Research Part I: Oceanographic Research Papers, 49*(10), 1769-1785. doi: http://dx.doi.org/10.1016/S0967-0637(02)00097-3

Macdonald, R. W., Paton, D. W., Carmack, E. C., & Omstedt, A. (1995). The freshwater budget and under-ice spreading of Mackenzie River water in the Canadian Beaufort Sea based on salinity and 18O/16O measurements in water and ice. *Journal of Geophysical Research: Oceans, 100*(C1), 895-919. doi: 10.1029/94jc02700

Martini, I. P. (1986). Chapter 7 Coastal Features of Canadian Inland Seas. In I. P. Martini (Ed.), *Elsevier Oceanography Series* (Vol. Volume 44, pp. 117-142): Elsevier.

Maxwell, J. B. (1986). Chapter 5 A Climate Overview of the Canadian Inland Seas. In I. P. Martini (Ed.), *Elsevier Oceanography Series* (Vol. Volume 44, pp. 79-100): Elsevier.

McClelland, J. W., Holmes, R. M., Dunton, K. H., & Macdonald, R. W. (2012). The Arctic Ocean Estuary. [journal article]. *Estuaries and Coasts, 35*(2), 353-368. doi: 10.1007/s12237-010-9357-3

McGuire, K., & McDonnell, J. (2008). Stable Isotope Tracers in Watershed Hydrology *Stable Isotopes in Ecology and Environmental Science* (pp. 334-374): Blackwell Publishing Ltd.

Messier, D., Ingram, R. G., & Roy, D. (1986). Chapter 20 Physical and Biological Modifications in Response to LA Grande Hydroelectric Complex. In I. P. Martini (Ed.), *Elsevier Oceanography Series* (Vol. Volume 44, pp. 403-424): Elsevier.

Morales Maqueda, M. A., Willmott, A. J., & Biggs, N. R. T. (2004). Polynya Dynamics: a Review of Observations and Modeling. *Reviews of Geophysics, 42*(1),. doi: 10.1029/2002rg000116

Nakawo, M., & Sinha, N. K. (1981). Growth rate and salinity profile of first-year sea ice in the high Arctic. *Journal of Glaciology, 27*(96), 315-330.

NASA. (2017). EOSDIS Worldview, 2014-2017, from https://worldview.earthdata.nasa.gov

Östlund, H. G., & Hut, G. (1984). Arctic Ocean water mass balance from isotope data. *Journal of Geophysical Research: Oceans, 89*(C4), 6373-6381. doi: 10.1029/JC089iC04p06373

Peck, G. S. (1978). *James Bay océanographie data report; Winter 1975 and 1976*. Department of fisheries and Environment. Burlington, Ont.

Prinsenberg, S. (1977). Hudson Bay oceanographic data report 1975 (O. a. A. Sciences, Trans.) (Vol. 1,308). Burlington, Ont.

Prinsenberg, S. J. (1980). Man-Made Changes in the Freshwater Input Rates of Hudson and James Bays. *Canadian Journal of Fisheries and Aquatic Sciences, 37*(7), 1101-1110. doi: 10.1139/f80-143

Prinsenberg, S. J. (1983). Effects of the hydroelectric developments on the oceanographic surface parameters of Hudson Bay. *Atmosphere-Ocean, 21*(4), 418-430. doi: 10.1080/07055900.1983.9649177

Prinsenberg, S. J. (1984). Freshwater contents and heat budgets of James Bay and Hudson Bay. *Continental Shelf Research, 3*(2), 191-200. doi: https://doi.org/10.1016/0278-4343(84)90007-4

Prinsenberg, S. J. (1986). Chapter 10 The Circulation Pattern and Current Structure of Hudson Bay. In I. P. Martini (Ed.), *Elsevier Oceanography Series* (Vol. Volume 44, pp. 187-204): Elsevier.

Prinsenberg, S. J. (1987). Seasonal current variations observed in western Hudson Bay. *Journal of Geophysical Research: Oceans, 92*(C10), 10756-10766. doi: 10.1029/JC092iC10p10756

Prinsenberg, S. J. (1988). Ice-cover and ice-ridge contributions to the freshwater contents of Hudson Bay and Foxe Basin. *Arctic, 41*(1), 6-11.

Prinsenberg, S. J., & Freeman, N. G. (1986). Chapter 11 Tidal Heights and Currents in Hudson Bay and James Bay. In I. P. Martini (Ed.), *Elsevier Oceanography Series* (Vol. Volume 44, pp. 205-216): Elsevier.

Prinsenberg, S. J., & Programme, H. B. (1994). *Effects of Hydro-electric Projects on Hudson Bay's Marine and Ice Environments*: Hudson Bay Programme = Programme sur la Baie d'Hudson.

Roff, J., & Legendre, L. (1986). Physico-chemical and biological oceanography of Hudson Bay *Elsevier Oceanography Series* (Vol. 44, pp. 265-292): Elsevier.

Saucier, F. J., Senneville, S., Prinsenberg, S., Roy, F., Smith, G., Gachon, P., Caya, D., & Laprise, R. (2004). Modelling the sea ice-ocean seasonal cycle in Hudson Bay, Foxe Basin and Hudson Strait, Canada. [journal article]. *Climate Dynamics, 23*(3), 303-326. doi: 10.1007/s00382-004-0445-6

Serreze, M. C., Barrett, A. P., Slater, A. G., Woodgate, R. A., Aagaard, K., Lammers, R. B., Steele, M., Moritz, R., Meredith, M., & Lee, C. M. (2006). The large-scale freshwater

cycle of the Arctic. *Journal of Geophysical Research: Oceans, 111*(C11), n/a-n/a. doi: 10.1029/2005jc003424

Serreze, M. C., Walsh, J. E., Chapin, F. S., Osterkamp, T., Dyurgerov, M., Romanovsky, V., Oechel, W. C., Morison, J., Zhang, T., & Barry, R. G. (2000). Observational Evidence of Recent Change in the Northern High-Latitude Environment. [journal article]. *Climatic Change, 46*(1), 159-207. doi: 10.1023/a:1005504031923

Shiklomanov, I. A., Shiklomanov, A. I., Lammers, R. B., Peterson, B. J., & Vorosmarty, C. J. (2000). The Dynamics of River Water Inflow to the Arctic Ocean. In E. L. Lewis, E. P. Jones, P. Lemke, T. D. Prowse & P. Wadhams (Eds.), *The Freshwater Budget of the Arctic Ocean* (pp. 281-296). Dordrecht: Springer Netherlands.

Sibert, V., Zakardjian, B., Gosselin, M., Starr, M., Senneville, S., & LeClainche, Y. (2011). 3D bio-physical model of the sympagic and planktonic productions in the Hudson Bay system. *Journal of Marine Systems, 88*(3), 401-422. doi: https://doi.org/10.1016/j.jmarsys.2011.03.014

Smith, A., Delavau, C., & Stadnyk, T. (2015). Identification of geographical influences and flow regime characteristics using regional water isotope surveys in the lower Nelson River, Canada. *Canadian Water Resources Journal / Revue canadienne des ressources hydriques, 40*(1), 23-35. doi: 10.1080/07011784.2014.985512

Smith, S. D., Muench, R. D., & Pease, C. H. (1990). Polynyas and leads: An overview of physical processes and environment. *Journal of Geophysical Research: Oceans, 95*(C6), 9461-9479. doi: 10.1029/JC095iC06p09461

St-Laurent, P., Straneo, F., Dumais, J. F., & Barber, D. G. (2011). What is the fate of the river waters of Hudson Bay? *Journal of Marine Systems, 88*(3), 352-361. doi: https://doi.org/10.1016/j.jmarsys.2011.02.004

Stadnyk, T., Dery, S., Macdonald, M., & Koenig, K. (2017). *The freshwater system in: The Hudson Bay IRIS, ArcticNet, NCE. (in press).*

Stirling, I. (1997). The importance of polynyas, ice edges, and leads to marine mammals and birds. *Journal of Marine Systems, 10*(1), 9-21. doi: http://dx.doi.org/10.1016/S0924-7963(96)00054-1

Straneo, F., & Saucier, F. (2008). The outflow from Hudson Strait and its contribution to the Labrador Current. *Deep Sea Research Part I: Oceanographic Research Papers, 55*(8), 926-946. doi: https://doi.org/10.1016/j.dsr.2008.03.012

Stroeve, J., & Maslowski, W. (2008). Arctic Sea Ice Variability During the Last Half Century. In S. Brönnimann, J. Luterbacher, T. Ewen, H. F. Diaz, R. S. Stolarski & U. Neu (Eds.), *Climate Variability and Extremes during the Past 100 Years* (pp. 143-154). Dordrecht: Springer Netherlands.

Talley, L. D., Pickard, G. L., Emery, W. J., & Swift, J. H. (2011). Chapter 3 - Physical Properties of Seawater *Descriptive Physical Oceanography (Sixth Edition)* (pp. 29-65). Boston: Academic Press.

Tan, F. C., & Strain, P. M. (1996). Sea ice and oxygen isotopes in Foxe Basin, Hudson Bay, and Hudson Strait, Canada. *Journal of Geophysical Research: Oceans, 101*(C9), 20869-20876. doi: 10.1029/96jc01557

UNESCO. (1983). Algorithms for computation of fundamental properties of seawater. *Tech. Paper Mar., Sci, 44*, 53.

Walker, S. A., Azetsu-Scott, K., Normandeau, C., Kelley, D. E., Friedrich, R., Newton, R., Schlosser, P., McKay, J. L., Abdi, W., Kerrigan, E., Craig, S. E., & Wallace, D. W. R. (2016). Oxygen isotope measurements of seawater (H218O/ H216O): A comparison of cavity ring-down spectroscopy (CRDS) and isotope ratio mass spectrometry (IRMS). *Limnology and Oceanography: Methods, 14*(1), 31-38. doi: 10.1002/lom3.10067

Wang, J., Mysak, L. A., & Ingram, R. G. (1994). Three-dimensional numerical simulation of Hudson Bay summer ocean circulation: Topographic gyres, separations, and coastal jets. *Journal of physical Oceanography, 24*, 2496-2514.

Wang, R., McCullough, G. K., Gunn, G. G., Hochheim, K. P., Dorostkar, A., Sydor, K., & Barber, D. G. (2012). An observational study of ice effects on Nelson River estuarine variability, Hudson Bay, Canada. *Continental Shelf Research, 47*(Supplement C), 68-77. doi: https://doi.org/10.1016/j.csr.2012.06.014

White, D., Hinzman, L., Alessa, L., Cassano, J., Chambers, M., Falkner, K., Francis, J., Gutowski, W. J., Holland, M., Holmes, R. M., Huntington, H., Kane, D., Kliskey, A., Lee, C., McClelland, J., Peterson, B., Rupp, T. S., Straneo, F., Steele, M., Woodgate, R., Yang, D., Yoshikawa, K., & Zhang, T. (2007). The arctic freshwater system: Changes and impacts. *Journal of Geophysical Research: Biogeosciences, 112*(G4). doi: 10.1029/2006jg000353

World Meteorological Organization, W. (1970). sea-ice nomenclature, *WMO Rep. 259., T.P. Geneva*, 145-147.

Appendix A.

Table A-1. A summary of all water samples collected during the four campaigns of field work. Salinity and $\delta^{18}O$ values for each depth of the water at each site, including the calculated fraction of river wter (Frw) and fraction of sea-ice melt (Fsim).

Cruise	Station	Latitude	Longitude	Date collected	Bottom Depth [m]	Depth [m]	Salinity [psu]	$\delta^{18}O$ [‰]	Frw	Fsim [+/-]
Winter_2014	SK-1	55.681	-79.2401	01/21/2014	65	0	27.21	-5.01	0.21	-0.06
Winter_2014	SK-1	55.6810	-79.2401	01/21/2014	65	1	26.95	-4.88	0.20	-0.04
Winter_2014	SK-1	55.6810	-79.2401	01/21/2014	65	5	27.00	-4.98	0.21	-0.05
Winter_2014	SK-1	55.6810	-79.2401	01/21/2014	65	10	27.30	-4.73	0.19	-0.04
Winter_2014	SK-1	55.6810	-79.2401	01/21/2014	65	20	28.13	-4.44	0.16	-0.04
Winter_2014	SK-2	55.7022	-79.2752	01/21/2014	65	1	27.54	-4.77	0.19	-0.05
Winter_2014	SK-2	55.7022	-79.2752	01/21/2014	65	5	27.80	-4.50	0.16	-0.03
Winter_2014	SK-2	55.7022	-79.2752	01/21/2014	65	10	27.55	-4.58	0.17	-0.03
Winter_2014	SK-2	55.7022	-79.2752	01/21/2014	65	20	28.59	-3.76	0.10	0.01
Winter_2014	SK-2	55.7022	-79.2752	01/21/2014	65	60	29.08	-4.02	0.12	-0.03
Winter_2014	SK-3	56.0246	-78.9059	01/22/2014	32	1	26.74	-5.18	0.21	-0.05
Winter_2014	SK-3	56.0246	-78.9059	01/22/2014	32	2	26.74	-4.77	0.19	-0.02
Winter_2014	SK-3	56.0246	-78.9059	01/22/2014	32	5	26.99	-4.76	0.19	-0.03
Winter_2014	SK-3	56.0246	-78.9059	01/22/2014	32	10	27.74	-4.66	0.17	-0.04
Winter_2014	SK-3	56.0246	-78.9059	01/22/2014	32	20	28.88	-3.20	0.06	0.05
Winter_2014	SK-3	56.0246	-78.9059	01/22/2014	32	30	N/A	N/A		
Winter_2014	SK-4	56.9818	-79.7672	01/25/2014	52	1	29.66	-3.98	0.11	-0.04
Winter_2014	SK-4	56.9818	-79.7672	01/25/2014	52	2	29.65	-4.15	0.13	-0.06
Winter_2014	SK-4	56.9818	-79.7672	01/25/2014	52	5	29.65	-4.14	0.13	-0.06
Winter_2014	SK-4	56.9818	-79.7672	01/25/2014	52	10	29.66	-4.69	0.17	-0.11
Winter_2014	SK-4	56.9818	-79.7672	01/25/2014	52	20	29.68	-4.48	0.15	-0.09
Winter_2014	SK-4	56.9818	-79.7672	01/25/2014	52	50	29.92	-4.29	0.14	-0.08
Winter_2014	SK-8	55.7689	-79.7874	02/08/2014	13	0	29.28	-4.26	0.14	-0.06
Winter_2014	SK-8	55.7689	-79.7874	02/08/2014	13	5	29.18	-4.41	0.15	-0.07
Winter_2014	SK-8	55.7689	-79.7874	02/08/2014	13	10	29.36	-3.98	0.12	-0.03
Winter_2014	SK-8	55.7689	-79.7874	02/08/2014	13	13	29.72	-4.01	0.12	-0.05
Winter_2014	SK-9	55.8540	-79.2670	02/14/2014	67	0	N/A	N/A		
Winter_2014	SK-9	55.8540	-79.2670	02/14/2014	67	5	N/A	N/A		
Winter_2014	SK-9	55.8540	-79.2670	02/14/2014	67	10	N/A	N/A		
Winter_2014	SK-9	55.8540	-79.2670	02/14/2014	67	20	N/A	N/A		
Winter_2014	SK-9	55.8540	-79.2670	02/14/2014	67	60	N/A	N/A		

Winter_2014	SK-10	56.4150	-78.8246	02/14/2014	28	0	28.87	-4.52	0.16	-0.07
Winter_2014	SK-10	56.4150	-78.8246	02/14/2014	28	2	28.16	-4.28	0.15	-0.02
Winter_2014	SK-10	56.4150	-78.8246	02/14/2014	28	5	28.98	-3.81	0.10	-0.01
Winter_2014	SK-10	56.4150	-78.8246	02/14/2014	28	10	29.06	-4.34	0.14	-0.06
Winter_2014	SK-10	56.4150	-78.8246	02/14/2014	28	28	29.17	-3.78	0.10	-0.01
Winter_2014	SK-14	56.1815	-80.0943	02/19/2014	60	0	30.17	-3.49	0.07	-0.01
Winter_2014	SK-14	56.1815	-80.0943	02/19/2014	60	2	30.18	-3.09	0.04	0.03
Winter_2014	SK-14	56.1815	-80.0943	02/19/2014	60	5	30.18	-4.18	0.13	-0.08
Winter_2014	SK-14	56.1815	-80.0943	02/19/2014	60	10	30.18	-3.55	0.08	-0.02
Winter_2014	SK-14	56.1815	-80.0943	02/19/2014	60	20	30.17	-4.06	0.12	-0.07
Winter_2014	SK-14	56.1815	-80.0943	02/19/2014	60	60	30.24	-3.36	0.06	0.00
Fall_2014	SK-1	55.6810	-79.2400	10/27/2014	60	1	27.70	-3.32	0.07	0.08
Fall_2014	SK-1	55.6810	-79.2400	10/27/2014	60	5	27.75	-2.99	0.05	0.11
Fall_2014	SK-1	55.6810	-79.2400	10/27/2014	60	10	27.76	-3.40	0.08	0.07
Fall_2014	SK-1	55.6810	-79.2400	10/27/2014	60	20	27.95	-3.17	0.06	0.09
Fall_2014	SK-1	55.6810	-79.2400	10/27/2014	60	60	28.95	-2.75	0.02	0.10
Fall_2014	SK-9	55.8540	-79.2670	10/27/2014	60	0	27.03	-3.21	0.07	0.11
Fall_2014	SK-9	55.8540	-79.2670	10/27/2014	60	5	27.03	-3.41	0.09	0.09
Fall_2014	SK-9	55.8540	-79.2670	10/27/2014	60	10	27.08	-3.35	0.08	0.10
Fall_2014	SK-9	55.8540	-79.2670	10/27/2014	60	20	27.06	-3.03	0.06	0.13
Fall_2014	SK-9	55.8540	-79.2670	10/27/2014	60	60	29.20	-2.72	0.02	0.09
Fall_2014	SK-3	56.0250	-78.9060	10/27/2014	30	0	28.03	-3.25	0.07	0.07
Fall_2014	SK-3	56.0250	-78.9060	10/27/2014	30	5	28.02	-3.13	0.07	0.08
Fall_2014	SK-3	56.0250	-78.9060	10/27/2014	30	10	28.06	-3.07	0.06	0.08
Fall_2014	SK-3	56.0250	-78.9060	10/27/2014	30	30	28.08	-2.72	0.04	0.11
Fall_2014	SK-10	56.4150	-78.8237	10/27/2014	30	0	28.08	-3.24	0.07	0.08
Fall_2014	SK-10	56.4150	-78.8237	10/27/2014	30	5	28.02	-3.21	0.06	0.08
Fall_2014	SK-10	56.4150	-78.8237	10/27/2014	30	10	28.05	-3.22	0.06	0.08
Fall_2014	SK-10	56.4150	-78.8237	10/27/2014	30	30	28.06	-3.28	0.07	0.07
Winter_2015	Chisasibi	53.7833	-78.8958	01/26/2015	1	1	0.00	-13.36	1.01	-0.01
Winter_2015	SK 1	55.6808	-79.2426	01/14/2015	57.3	1	25.86	-4.26	0.16	0.05
Winter_2015	SK 1	55.6808	-79.2426	01/14/2015	57.3	5	25.95	-4.04	0.14	0.07
Winter_2015	SK 1	55.6808	-79.2426	01/14/2015	57.3	10	26.96	-3.58	0.10	0.08
Winter_2015	SK 1	55.6808	-79.2426	01/14/2015	57.3	20	27.44	-3.27	0.07	0.09
Winter_2015	SK 1	55.6808	-79.2426	01/15/2015	57.3	50	*29.63	-2.34	-0.01	0.11
Winter_2015	SK 2	55.7024	-79.2763	01/26/2015	60	1	27.48	-3.51	0.09	0.07
Winter_2015	SK 2	55.7024	-79.2763	01/26/2015	60	5	27.89	-3.44	0.08	0.06
Winter_2015	SK 2	55.7024	-79.2763	01/26/2015	60	10	28.22	-3.30	0.07	0.07
Winter_2015	SK 2	55.7024	-79.2763	01/26/2015	60	20	28.56	-3.35	0.07	0.05
Winter_2015	SK 2	55.7024	-79.2763	01/26/2015	60	60	29.08	-2.98	0.04	0.07
Winter_2015	SK 3	56.0231	-78.9010	01/15/2015	47.7	1	26.15	-4.24	0.15	0.04

Winter_2015	SK 3	56.0231	-78.9010	01/15/2015	47.7	5	26.23	-4.11	0.14	0.05
Winter_2015	SK 3	56.0231	-78.9010	01/15/2015	47.7	10	26.75	-4.04	0.14	0.04
Winter_2015	SK 3	56.0231	-78.9010	01/15/2015	47.7	20	27.20	-3.86	0.12	0.05
Winter_2015	SK 3	56.0231	-78.9010	01/15/2015	47.7	32	28.57	-3.24	0.06	0.06
Winter_2015	SK 4	56.9719	-79.7839	01/20/2015	41.6	1	28.96	-2.89	0.03	0.08
Winter_2015	SK 4	56.9719	-79.7839	01/20/2015	41.6	5	29.03	-3.04	0.04	0.07
Winter_2015	SK 4	56.9719	-79.7839	01/20/2015	41.6	10	29.09	-2.66	0.02	0.10
Winter_2015	SK 4	56.9719	-79.7839	01/20/2015	41.6	20	29.14	-2.84	0.03	0.08
Winter_2015	SK 4	56.9719	-79.7839	01/20/2015	41.6	40	29.21	-2.83	0.03	0.08
Winter_2015	SK 8	55.7690	-79.8276	01/17/2015	8.3	1	28.84	-3.12	0.05	0.06
Winter_2015	SK 8	55.7690	-79.8276	01/17/2015	8.3	5	28.84	-3.29	0.07	0.05
Winter_2015	SK 8	55.7690	-79.8276	01/17/2015	8.3	8	28.85	-2.85	0.03	0.09
Winter_2015	SK 9	55.8620	-79.2285	01/29/2015	60	1	27.44	-3.45	0.09	0.08
Winter_2015	SK 9	55.8620	-79.2285	01/29/2015	60	5	27.54	-3.37	0.08	0.08
Winter_2015	SK 9	55.8620	-79.2285	01/29/2015	60	10	27.70	-3.13	0.06	0.10
Winter_2015	SK 9	55.8620	-79.2285	01/29/2015	60	20	28.06	-3.22	0.06	0.08
Winter_2015	SK 9	55.8620	-79.2285	01/29/2015	60	60	29.88	-2.43	-0.01	0.10
Winter_2015	SK 10	56.4150	-78.8246	01/29/2015	12	1	29.04	-3.08	0.05	0.06
Winter_2015	SK 10	56.4150	-78.8246	01/29/2015	12	5	29.07	-2.85	0.03	0.08
Winter_2015	SK 10	56.4150	-78.8246	01/29/2015	12	10	29.03	-2.86	0.03	0.08
Winter_2015	SK 12	56.6260	-79.2870	01/24/2015	20	1	28.80	-2.95	0.04	0.08
Winter_2015	SK 12	56.6260	-79.2870	01/24/2015	20	5	28.80	-2.79	0.03	0.10
Winter_2015	SK 12	56.6260	-79.2870	01/24/2015	20	10	28.79	-2.84	0.03	0.09
Winter_2015	SK 12	56.6260	-79.2870	01/24/2015	20	15	28.79	-3.02	0.05	0.08
Winter_2015	SK 14	56.1847	-80.0881	01/21/2015	25.5	1	29.38	-2.87	0.03	0.07
Winter_2015	SK 14	56.1847	-80.0881	01/21/2015	25.5	5	29.39	-2.85	0.03	0.07
Winter_2015	SK 14	56.1847	-80.0881	01/21/2015	25.5	10	29.38	-2.77	0.02	0.08
Winter_2015	SK 14	56.1847	-80.0881	01/21/2015	25.5	20	29.41	-2.68	0.01	0.09
Winter_2015	SK 15	56.6420	-79.1110	01/25/2015	24.7	1	28.94	-3.14	0.05	0.06
Winter_2015	SK 15	56.6420	-79.1110	01/25/2015	24.7	5	28.92	-3.46	0.08	0.03
Winter_2015	SK 15	56.6420	-79.1110	01/25/2015	24.7	10	28.92	-3.55	0.09	0.02
Winter_2015	SK 15	56.6420	-79.1110	01/25/2015	24.7	20	28.92	-3.41	0.07	0.03
Winter_2015	SK 21	55.7815	-79.1249	01/26/2015	22.4	1	26.59	-4.22	0.15	0.03
Winter_2015	SK 21	55.7815	-79.1249	01/26/2015	22.4	5	26.81	-4.18	0.15	0.03
Winter_2015	SK 21	55.7815	-79.1249	01/26/2015	22.4	10	27.85	-3.69	0.10	0.04
Winter_2015	SK 21	55.7815	-79.1249	01/26/2015	22.4	20	28.53	-3.47	0.08	0.04
Winter_2015	SK 23	56.2585	-78.6547	01/23/2015	30	1	27.91	-3.97	0.12	0.01
Winter_2015	SK 23	56.2585	-78.6547	01/23/2015	30	5	27.96	-3.84	0.11	0.02
Winter_2015	SK 23	56.2585	-78.6547	01/23/2015	30	10	28.06	-3.90	0.12	0.01
Winter_2015a	SK 3	56.0231	-78.9010	02/17/2015	45	1	27.25	-4.54	0.17	-0.02
Winter_2015a	SK 3	56.0231	-78.9010	02/17/2015	45	5	27.25	-4.44	0.16	-0.01

Winter_2015a	SK 3	56.0231	-78.9010	02/17/2015	45	10	27.55	-4.32	0.15	-0.01
Winter_2015a	SK 3	56.0231	-78.9010	02/17/2015	45	20	27.81	-4.26	0.15	-0.01
Winter_2015a	SK 3	56.0231	-78.9010	02/17/2015	45	30	28.01	-4.14	0.14	-0.01
Winter_2015a	SK 21	55.7815	-79.1249	02/28/2015	78	1	27.04	-4.02	0.13	0.03
Winter_2015a	SK 21	55.7815	-79.1249	02/28/2015	78	5	27.26	-3.97	0.13	0.03
Winter_2015a	SK 21	55.7815	-79.1249	02/28/2015	78	10	27.47	-3.94	0.12	0.03
Winter_2015a	SK 21	55.7815	-79.1249	02/28/2015	78	20	28.31	-3.40	0.08	0.05
Winter_2015a	SK 22	55.9079	-79.0154	02/26/2015	85	1	27.65	-4.14	0.14	0.00
Winter_2015a	SK 22	55.9079	-79.0154	02/26/2015	85	5	26.88	-4.08	0.14	0.03
Winter_2015a	SK 22	55.9079	-79.0154	02/26/2015	85	10	27.03	-4.01	0.13	0.04
Winter_2015a	SK 22	55.9079	-79.0154	02/26/2015	85	20	27.78	-3.59	0.09	0.05
Winter_2015a	SK 22	55.9079	-79.0154	02/26/2015	85	60	30.19	-2.61	0.00	0.07
Winter_2015a	SK 23	56.2585	-78.6547	02/25/2015	30	1	27.70	-3.68	0.10	0.05
Winter_2015a	SK 23	56.2585	-78.6547	02/25/2015	30	5	27.72	-3.72	0.11	0.04
Winter_2015a	SK 23	56.2585	-78.6547	02/25/2015	30	10	27.70	-3.46	0.09	0.07
Winter_2015a	SK 23	56.2585	-78.6547	02/25/2015	30	20	27.71	-3.68	0.10	0.05
Winter_2015a	T1A	55.8155	-78.7728	02/20/2015	54	1	26.90	-3.75	0.11	0.06
Winter_2015a	T1A	55.8155	-78.7728	02/20/2015	54	5	26.90	-3.85	0.12	0.06
Winter_2015a	T1A	55.8155	-78.7728	02/20/2015	54	10	26.91	-3.66	0.10	0.07
Winter_2015a	T1A	55.8155	-78.7728	02/20/2015	54	20	26.95	-3.55	0.10	0.08
Winter_2015a	T1A	55.8155	-78.7728	02/20/2015	54	50	29.88	-2.53	0.00	0.09
Winter_2015a	T1B	55.8424	-78.8555	02/22/2015	85	1	26.82	-4.05	0.14	0.04
Winter_2015a	T1B	55.8424	-78.8555	02/22/2015	85	5	26.84	-4.20	0.15	0.02
Winter_2015a	T1B	55.8424	-78.8555	02/22/2015	85	10	26.85	-4.12	0.14	0.03
Winter_2015a	T1B	55.8424	-78.8555	02/22/2015	85	20	27.73	-3.55	0.09	0.06
Winter_2015a	T1B	55.8424	-78.8555	02/22/2015	85	60	30.03	-2.72	0.01	0.07
Winter_2015a	T1C	55.8775	-78.9359	02/22/2015	85	1	26.94	-3.99	0.13	0.04
Winter_2015a	T1C	55.8775	-78.9359	02/22/2015	85	5	26.94	-4.11	0.14	0.03
Winter_2015a	T1C	55.8775	-78.9359	02/22/2015	85	10	26.97	-3.91	0.12	0.05
Winter_2015a	T1C	55.8775	-78.9359	02/22/2015	85	20	27.72	-3.26	0.07	0.09
Winter_2015a	T1C	55.8775	-78.9359	02/22/2015	85	60	29.95	-2.51	0.00	0.09
Winter_2015a	SK 1	55.6808	-79.2426	03/14/2015	56	1	27.06	-4.91	0.20	-0.05
Winter_2015a	SK 1	55.6808	-79.2426	03/14/2015	56	5	27.25	-4.73	0.19	-0.04
Winter_2015a	SK 1	55.6808	-79.2426	03/14/2015	56	10	27.46	-4.59	0.17	-0.03
Winter_2015a	SK 1	55.6808	-79.2426	03/14/2015	56	20	27.08	-4.91	0.20	-0.05
Winter_2015a	SK 1	55.6808	-79.2426	03/14/2015	56	50	29.90	-3.49	0.07	0.00
Winter_2015a	SK 2	55.7024	-79.2763	03/12/2015	80	1	27.58	-4.56	0.17	-0.03
Winter_2015a	SK 2	55.7024	-79.2763	03/12/2015	80	5	27.65	-4.32	0.15	-0.01
Winter_2015a	SK 2	55.7024	-79.2763	03/12/2015	80	10	27.67	-4.08	0.13	0.01
Winter_2015a	SK 2	55.7024	-79.2763	03/12/2015	80	20	28.25	-3.84	0.11	0.01
Winter_2015a	SK 2	55.7024	-79.2763	03/12/2015	80	60	28.98	-3.61	0.09	0.01

Winter_2015a	SK 4	56.9719	-79.7839	03/06/2015	40	1	29.23	-3.32	0.07	0.03
Winter_2015a	SK 4	56.9719	-79.7839	03/06/2015	40	5	29.24	-3.72	0.10	-0.01
Winter_2015a	SK 4	56.9719	-79.7839	03/06/2015	40	10	29.27	-3.50	0.08	0.02
Winter_2015a	SK 4	56.9719	-79.7839	03/06/2015	40	20	29.37	-3.48	0.08	0.01
Winter_2015a	SK 4	56.9719	-79.7839	03/06/2015	40	40	29.78	-3.38	0.07	0.01
Winter_2015a	SK 8	55.7690	-79.8276	03/09/2015	8.4	1	28.33	-3.99	0.12	0.00
Winter_2015a	SK 8	55.7690	-79.8276	03/09/2015	8.4	5	28.42	-3.44	0.08	0.05
Winter_2015a	SK 8	55.7690	-79.8276	03/09/2015	8.4	8	28.27	-3.32	0.07	0.06
Winter_2015a	SK 9	55.8620	-79.2285	03/12/2015	80	1	27.62	-3.68	0.10	0.05
Winter_2015a	SK 9	55.8620	-79.2285	03/12/2015	80	5	28.21	-3.67	0.10	0.03
Winter_2015a	SK 9	55.8620	-79.2285	03/12/2015	80	10	27.86	-3.48	0.09	0.06
Winter_2015a	SK 9	55.8620	-79.2285	03/12/2015	80	20	28.06	-3.45	0.08	0.06
Winter_2015a	SK 9	55.8620	-79.2285	03/12/2015	80	60	30.09	-2.63	0.01	0.07
Winter_2015a	SK 10	56.4150	-78.8246	03/01/2015	13	1	28.26	-3.62	0.09	0.03
Winter_2015a	SK 10	56.4150	-78.8246	03/01/2015	13	5	28.26	-3.64	0.10	0.03
Winter_2015a	SK 10	56.4150	-78.8246	03/01/2015	13	10	28.34	-3.54	0.09	0.04
Winter_2015a	SK 12	56.6260	-79.2870	03/12/2015	27.5	1	29.35	-3.16	0.05	0.05
Winter_2015a	SK 12	56.6260	-79.2870	03/12/2015	27.5	5	29.35	-3.07	0.05	0.05
Winter_2015a	SK 12	56.6260	-79.2870	03/12/2015	27.5	10	29.37	-3.07	0.05	0.05
Winter_2015a	SK 12	56.6260	-79.2870	03/12/2015	27.5	15	29.36	-2.77	0.02	0.08
Winter_2015a	SK 14	56.1847	-80.0881	03/09/2014	25.3	1	29.72	-2.64	0.01	0.08
Winter_2015a	SK 14	56.1847	-80.0881	03/09/2014	25.3	5	29.84	-2.76	0.02	0.07
Winter_2015a	SK 14	56.1847	-80.0881	03/09/2014	25.3	10	29.74	-2.45	0.00	0.10
Winter_2015a	SK 14	56.1847	-80.0881	03/09/2014	25.3	15	29.76	-2.73	0.02	0.07
Winter_2015a	SK 14	56.1847	-80.0881	03/09/2014	25.3	20	29.77	-2.32	-0.02	0.11
Winter_2015a	SK 14	56.1847	-80.0881	03/09/2014	25.3	25	29.80	-2.69	0.01	0.08
Winter_2015a	SK 15	56.6420	-79.1110	03/01/2015	19	1	28.82	-3.25	0.06	0.05
Winter_2015a	SK 15	56.6420	-79.1110	03/01/2015	19	5	28.80	-2.69	0.02	0.11
Winter_2015a	SK 15	56.6420	-79.1110	03/01/2015	19	10	28.88	-3.24	0.06	0.05
Winter_2015a	SK 15	56.6420	-79.1110	03/01/2015	60	15	28.82	-2.93	0.04	0.08

Appendix B

Table B-1. Mean temperature, wind speed, visibility, and wind chill at Sanikiluaq Airport on the Belcher Islands , NU; Weather Forecast retrieved from Environment Canada.

	Historical Weather Forecast			
Date	Temperature [^{0}C]	Wind spd [km]	visibility [km]	Wind Chill [^{0}C]
December, 2013	-16.6 (7.3)	25 (10.8)	17.8 (7.3)	-26.7 (8.9)
January, 2014	-20.6 (4.9)	25.6 (13.7)	15 (8.8)	-31.7 (7.1)
December, 2014	-13.2 (-6.4)	29.1 (12.4)	N/A	-23.2 (8.6)
January, 2015	-25.2 (4.1)	22.6 (10.1)	N/A	-37.1 (4.7)